Russian Original Vol. 45, No. 6, December, 1978

June, 1979

SATEAZ 45(6) 1147-1256 (1978)

SOVIET ATOMIC ENERGY

АТОМНАЯ ЭНЕРГИЯ
(ATOMNAYA ÉNERGIYA)

TRANSLATED FROM RUSSIAN

CONSULTANTS BUREAU, NEW YORK

SOVIET ATOMIC ENERGY

Soviet Atomic Energy is a cover-to-cover translation of *Atomnaya Énergiya*, a publication of the Academy of Sciences of the USSR.

An agreement with the Copyright Agency of the USSR (VAAP) makes available both advance copies of the Russian journal and original glossy photographs and artwork. This serves to decrease the necessary time lag between publication of the original and publication of the translation and helps to improve the quality of the latter. The translation began with the first issue of the Russian journal.

Consultants Bureau journals appear about six months after the publication of the original Russian issue. For bibliographic accuracy, the English issue published by Consultants Bureau carries the same number and date as the original Russian from which it was translated. For example, a Russian issue published in December will appear in a Consultants Bureau English translation about the following June, but the translation issue will carry the December date. When ordering any volume or particular issue of a Consultants Bureau journal, please specify the date and, where applicable, the volume and issue numbers of the original Russian. The material you will receive will be a translation of that Russian volume or issue.

Subscription (2 volumes per year)
Vols. 44 & 45: $130 per volume (6 Issues)
Vols. 46 & 47: $147.50 per volume (6 Issues)

Single Issue: $50
Single Article: $7.50

Prices somewhat higher outside the United States.

CONSULTANTS BUREAU, NEW YORK AND LONDON

227 West 17th Street
New York, New York 10011

Published monthly. Second-class postage paid at Jamaica, New York 11431.

Soviet Atomic Energy is abstracted or indexed in *Applied Mechanics Reviews, Chemical Abstracts, Engineering Index, INSPEC—Physics Abstracts and Electrical and Electronics Abstracts, Current Contents,* and *Nuclear Science Abstracts.*

SOVIET ATOMIC ENERGY

A translation of *Atomnaya Énergiya*

June, 1979

Volume 45, Number 6 December, 1978

CONTENTS

CONTENTS

(continued)

Engl./Russ.

The Russian press date (podpisano k pechati) of this issue was 11/24/1978. Publication therefore did not occur prior to this date, but must be assumed to have taken place reasonably soon thereafter.

ARTICLES

PROSPECTS OF THE UTILIZATION AND THE BASIC PROBLEMS OF THE INTRODUCTION OF HTGR* IN TECHNOLOGICAL PROCESSES AND ELECTRIC POWER GENERATION

V. A. Legasev, N. N. Ponomarev-Stepnoi,
A. N. Protsenko, Yu. F. Chernilin,
V. N. Grebennik, and A. Ya. Stolyarevskii

UDC 621.038.52.034.3

An extensive and comprehensive discussion of the various problems of the future development of power generation has originated with the increasing difficulties for providing the Soviet Union with cheap power and energy resources, for which the level of demand has reached significant scales.

The difficulties of the development of power generation are due to the constant price increase of organic resources and, in the first place, of petroleum and gas, which are the most suitable and most widely used sources of power, and for which reserves are limited; the necessity for taking ecological factors into consideration, which make the production of power more expensive and carry additional limitations on the scale and disposition of power-generating stations; and also the large "inertia" of power generation – the most time-consuming and investment-capacious branch of the economy, in consequence of which it is necessary to construct prototype facilities long in advance of the widespread introduction of stations with new power-generating trends into the fuel–power balance (FPB).

All this requires an extension of the range of applicability of nuclear power generation in the fuel–power structure of the country and its maximum utilization efficiency [1, 2]. Most important in the development of power generation in the near future is the gradual replacement of liquid and gaseous organic fuels [1, 3, 4].

At the present time, nuclear power generation in practice is being used for the production of electric power and is replacing the organic fuel necessary for its generation. The development of nuclear power generation in the European part of the Soviet Union will allow the deficit of energy resources in this region to be reduced significantly. However, the functions of nuclear power stations in supplanting the deficient hydrocarbon fuel are limited. As the functional power reactors are intended for use mainly in the base section of the power-system loading, then their introduction will supplant the condensation power stations, operating on coal, in the energy balance.

It can be seen from the data of Table 1 that the greatest demand on the fuel–energy resources, including petroleum and gas, is for the generation of medium- and low-potential heat and steam, high-potential heat for technological processes (metallurgy, chemistry, etc.), and for the provision of motor fuel to the national economy. In addition, gas–petroleum residue fuel is used in the production of peak and semipeak power.

The demand for gas–liquid fuels in some of these fields can be partially reduced by the use of nuclear heat-supply stations (NHSS) in the production of low-potential heat in functional nuclear power stations in certain technological processes, for the complex provision of low-potential heat and electric power. The possibilities of using nuclear power based on functional reactors for the purpose of supplanting gas–liquid energy resources are limited. Wider prospects are being opened up by the construction and introduction of high-temperature gas-cooled reactors (HTGR).

The principal feature of HTGR is the production of heat at a temperature of ~1000°C and higher. This temperature allows the introduction of these reactors into various central-heating, power-technological and other processes, and will allow deficient hydrocarbon fuel to be supplanted. In Tables 2-4 the possible fields of application of HTGR are considered. The potential scales of development of HTGR are considered by the example of the use of high-temperature heat for the steam conversion of methane and are given in Table 2.

*High-temperature gas-cooled reactor.

Translated from Atomnaya Énergiya, Vol. 45, No. 6, pp. 411-418, December, 1978. Original article submitted April 17, 1978.

0038-531X/78/4506-1147$07.50

TABLE 1. Structure for the Requirement on Fuel-Energy Resources, % FEB

Field of requirement	Period 1970—1980		Long-term‡		Potential fraction of nuclear power	
	total*	fraction of petroleum and gas (at end of period)†	total	fraction of petroleum and gas	LWR**	HTGR
Generation of electric power	25	13	30—35	~10	Up to 20—25	Up to 25-28
Generation of heat and steam of medium and low potential	32	22	25—30	~20	Up to 8—10	Up to 25
Generation of high-potential heat	19	14	14—16	10	—	Up to 12-14
Mobile and fixed power facilities	18	14	16	15	—	Production of synthetic fuel
In the chemical and petrochemical industries as raw material	6	5	10	~8	—	—
Total	100	68	100	60		

*According to data of [5], average for the period.
†According to authors' estimates, effected by taking account of the structure of the demand for petroleum and gas according to data of [5], and the scales of demand for petroleum and gas in 1980 from the data of [6].
‡According to authors' estimates, taking account of the main trends of change of the FEB and forecasts, for example [3].
**Light-water reactors (VVÉR and RBMK) [Water-cooled/water-moderated power reactor, and high-powered water-cooled channel reactor, respectively].

About 20% of the total organic fuel which will be extracted in 1980 should be consumed by the high-temperature heat industry. Some 60-70% of the fuel consumed for this purpose comprises deficient hydrocarbon fuel, and this fraction will not change significantly during the next 15-20 years. High-temperature potential is essential for the production of ammonia and ammoniacal fertilizers, synthetic alcohol, hydrogen, etc., and also in metallurgy in the direct reduction of iron, blast-furnace processes, etc.

A key problem of the majority of high-temperature processes is the production of the various reducing agents, and particularly hydrogen, which can be obtained by means of HTGR. Hydrogen, as raw material, is obtained from organic fuel in the steam conversion of methane or the gasification of coal (see Table 2). In the long-term, the thermochemical or thermoelectrochemical decomposition of water can provide an inorganic source of hydrogen (Table 3). The production of reducing agents and, particularly hydrogen, by means of HTGR will allow all the organic fuel consumed to be supplanted in this field of power generation.

Thus, the use of HTGR in power-technological factories will open up a wide prospect for the development and use of nuclear power generation, which will have a positive effect on the solution of the problem of protection of the environment.

As mentioned earlier, the greatest portion of the extracted organic energy resources, including hydrocarbons, is consumed in the production of medium- and low-potential heat steam. Part of the concentrated consumers of low-potential heat can be provided by NHSS based on functional reactors. A high portion of gas—black oil fuel is necessary for decentralized and industrial heat supply with a small concentration of power requirement, the transmission of which by coal is made difficult in view of the technicoeconomic and ecological reasons. One of the possible routes for solving this problem is opened by nuclear long-distance heat-supply stations (NLDHSS). In this case, HTGR are used for the steam conversion of methane with the transmission of the cooled conversion products (CO and H_2) (Fig. 1) through gas pipelines to the sites of heat requirement, where the reverse methanization reaction with the release of heat is carried out. The temperature during methanization is ~450-650°C. As a result, CO and H_2 are converted almost completely into methane, which can be returned to the reactor through pipelines.

In all the schemes considered for the use of HTGR in power-technological processes, the use of part of the heat generated by the reactor is intended for the generation of electric power. Owing to the high temperature of the coolant in this case, steam turbines can be used with modern high-steamparameters (550°C and 170/240 bar) and net effective efficiencies of ~40%.

TABLE 2. Nuclear-Power-Technological Processes with HTGR as the Basis of Methane Conversion

Field of Application	Type of technological production	Production product	Replaced gas (black oil) by a nuclear power heat facility (NPHF) with a capacity of 300 MW (thermal)		Economic effectiveness	Potential volume of supplanted fuel by the introduction of nuclear power thermal stations (NPTS)* with HTGR, 10^6 ton fuel consumed/yr
			10^9 m^3/yr	10^6 ton fuel consumed/yr		
Reduction of natural gas requirement	Steam conversion of methane for the production of hydrogen	Ammonia, ammoniacal fertilizers, synthetic alcohol, hydrogen	1.7	2.1	10-15% cost reduction	30-50 (with NPTS, by (15-20) · 10^6 tons of ammoniacal fertilizers)
	Direct reduction of ore	Sponge iron	1.5	1.8	Not estimated	2-3 (20 · 10^6 tons sponge iron)
	Reduction of ore in blast furnaces	Cast (Pig) iron	1.4-1.6	1.7-2.0	Not estimated	5-6 (30-40 · 10^6 tons of cast iron)
Production of synthetic fuel	Gasification of coal	Synthetic gas	3-3.2	3.6-3.8	40-50 rubles/ton fuel consumed	60-70 (with gasification of 50 million tons coal)
Replacement of gas-liquid fuel	Chemothermal energy transmission	Decentralized domestic and industrial heat supply	1.3-1.6	1.6-1.8	More economical than nuclear heat-supply stations (NHSS) at distances of > 20-30 km	80-120 (50% decentralized heat supply of European part of the Soviet Union in long-term)
	Chemothermal storage of energy	Peak electric power	1.9-2.1	2.4-2.6	Not estimated	32-35 (installed capacity of shunted nuclear power stations ~20 GW)

* NPTS – Nuclear Power Technological Station.

TABLE 3. Nuclear Power-Technological Processes with HTGR Based on Different Methods of Decomposition of Water

Technological process	Efficiency, %	H_2 prod. by NPTS with capacity 3000 MW (thermal)		T_{max}, °C
		10^9 m^3/yr	10^6 ton fuel consumed/yr	
Thermochemical cycle	65—70	4—4,5	1,6—1,8	1225
	55—60	3,5—3,8	1,4—1,5	925
	35—40	2,2—2,5	0,9—1,0	800
Thermoelectrochemical cycle	45—50	2,9—3,2	1,2—1,3	800
High-temp. electrolysis	40—45	2,5—2,9	1,0—1,2	800—900

TABLE 4. Nuclear Stations with HTGR

Energy cycle	Efficiency, %	Special features
Steam turbine	38-40	Use of commercial-type steam-turbine units, operating, e.g., at 170 bar and 545°C. Reduction of waste heat by 30-35%
Closed gas-turbine	41-44	Possibility of achieving high efficiencies, including the use of binary cycles. Reduction of capital costs, increase of nuclear power station switching, possibility of use of "dry" water cooling towers and use of waste heat (up to 250-300°C) for central heating
Closed gas-turbine with thermosorption compression	50-55 (taking account of low-potential heat supply) 80-90 (without taking account of low-potential heat supply)	High efficiency, possibility of using "dry" water cooling towers Essentially, supply of low-potential (100-150°C) heat.

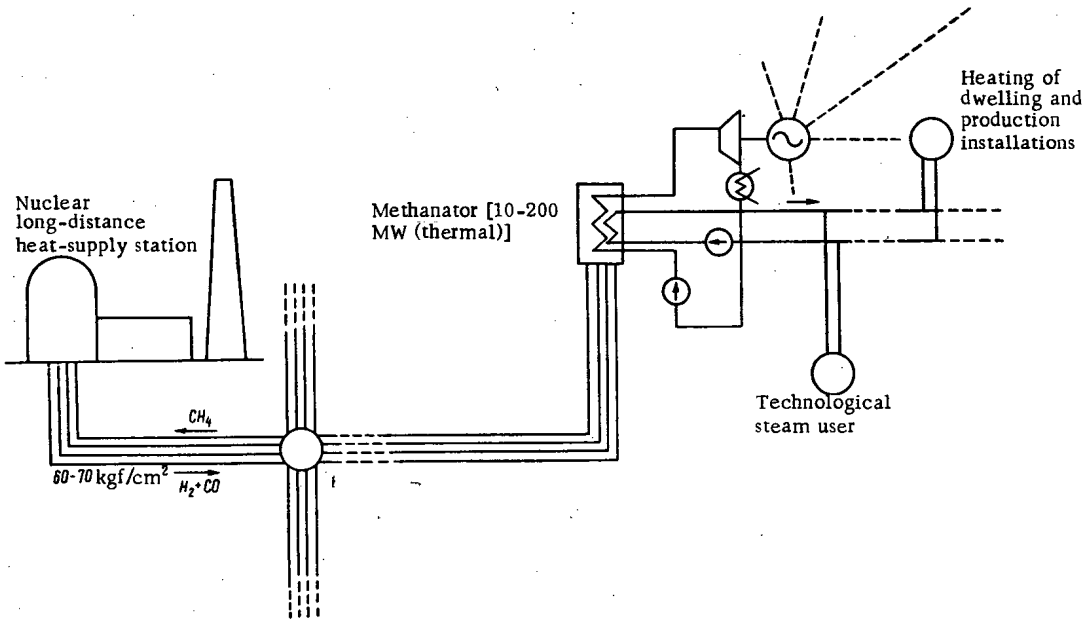

Fig. 1. Long-distance chemothermal heat-supply system.

The capability of HTGR to generate heat of higher parameters makes them promising also for the installation in power generation, of nuclear power stations with a direct gas-turbine cycle. Gas-turbines become economically profitable at 800°C and higher. In this case, the direct gas-turbine cycle will have the advantage over the steam turbine in both high efficiency and also a reduction of capital costs because of the reduction of the metal content of the plant. In addition, the advantages of a direct cycle nuclear power station are the significantly lower requirement on cooling water and the probability of conversion to air cooling, increase of adjustability of nuclear power stations, and the possibilities of its utilization in a controlled mode. Various alternatives for the use of HTGR in electric power generation are shown in Table 4.

The development of nuclear power generation should be based on a reliable solution of the problem of fuel provision. The development of helium technology for thermal HTGR will accelerate the solution of the problem of gas-cooled breeder-reactors [1].

As Academician A. P. Aleksandrov mentioned, "... obviously, it is precisely the development of high-temperature reactors on a par with breeder reactors, that will be the characteristic trend of change of the structure of nuclear power generation by the 90's of our century.

It may happen that the development of breeder reactors, cooled by sodium, with a doubling time of the fissile material of 4-6 years will be found to be complex and impracticable, as the marked softening of the neutron spectrum by sodium reduces the breeding ratio. In this case, the gas-cooled reactor may be found to be promising, although the necessity for a very high heat release rate of the fuel leads to high pressures and complex emergency cooling systems. Nevertheless, it seems that this trend merits development, especially if we take into consideration that a shortening of the fissile material doubling time in metal-cooled reactors will require transition from oxide fuel compositions to the denser carbides, nitrides or metal compositions, the resistance of which is more easily ensured in chemically inert helium than in sodium" [1].

One of the distinctive and important advantages of all concepts of HTGR is the generality and uniformity of the basic technical, technological and structural solutions for all the above-mentioned trends of development. This concerns the design of the fuel elements, the main plant, the design of the reactor vessels, structural and heat insulating materials, control system, etc. This generality and uniformity of the basic solution will allow the volumes of scientific-research and pilot-design work to be reduced, and also the times of their achievement. This advantage of HTGR undoubtedly is positively expressed also in the establishment of the production base.

To the most important scientific-technical problems of development of HTGR may be referred the development of the structure and manufacturing technology of the fuel, high-temperature radiation- and corrosion-resistant graphite, high-temperature materials for the plant, accessories, conduits, etc., heat-insulating materials and structures; the production of structures of the main technological equipment (heat-exchangers, gas-blowers, accessories, steam generators, etc.) and multicavity high-pressure vessels of prestressed ferroconcrete, and also the use of helium technology (monitoring, purification, mass transfer, etc.).

In almost all these problems, investigations are developing which are directed at the achievement of the characteristics to meet the requirements of HTGR for the production of high-potential heat. The highest demands are being imposed on reactors for this purpose, and their compliance simultaneously will solve problems also for other HTGR-type reactors.

At present, numerous trends for the use of HTGR are being investigated and developed. On the one hand, this defines the widespread interest in HTGR as a new source of energy and, in this way, promotes the development of this trend. On the other hand, the use of HTGR creates the problem of finding and developing an optimum scheme of reactor facility, designed for different branches of the national economy. The majority of existing studies of nuclear power technological stations (NPTS) with HTGR indicate a close relation between the spheres of application and construction, layout and parameters of NPTS. It follows from this that in principle for each field of application (see Tables 2-4), its own optimum design and layout of the facility can be developed. It is not yet possible to distinguish unambiguously from all this diversity of applications, the main trends, which are promising both from the point of view of the requirements of the national economy, and from the point of view of technical achievability and efficiency. This can be done only during further investigations, development, accumulation of operating experience, etc.

It should be stipulated that the individual units and parameters of HTGR for different trends – core, gas blowers, control and safety actuators, helium inlet and outlet parameters, etc. – can be and should be unified. However, depending on the field of application and the accepted technical and circuit solutions, such important units and parameters of a facility as the heat-exchangers, steam generators, the relations between

TABLE 5. Principal Thermotechnical Parameters of HTGR

Parameter	NPS with a steam power cycle	NPS with gas-turbine facility	NPTS*	NPS with fast helium reactor
t^{He}_{max}, °C	650—750	800—1000	900—1000	600—650 (Up to 800)
t^{He}_{min}, °C	300—350	300—350	300—350	250—300
p, bar	50	50—80	50	120—160

* Nuclear power technological station.

the capacities of these heat-exchangers and, consequently, the hydraulics of the primary circuit, design of the prestressed ferroconcrete pressure vessel, etc., may be significantly different. The parameters of different types of HTGR are shown in Table 5.

Another problem is to guarantee a high reliability, emergency arrangements, and the maximum reactor power utilization. For HTGR with globular fuel elements operating on the STC (Single Transit of Core) principle, there is hope for obtaining a high power utilization factor (PUF). For example, for the experimental high-temperature reactor AVR, operating for a long time at a helium outlet temperature of 950°C, this factor in the last few years has been equal to 0.85-0.90. Nevertheless, it cannot be expected that the PUF for HTGR will be significantly higher than for facilities with other reactors. Obviously, a PUF of 0.80-0.95 should be aimed at.

At the same time, the operating load factors in the metallurgical and chemical industries approach 0.95-0.98. Many specialists in these branches consider that the nuclear power used in technology also will have to have this load capacity. Although it is not obvious that the most economical solution for HTGR is to provide power for which the technological production load factor amounts to 0.95-0.98 (e.g., because of the increase of reliability of the individual reactor components, their supplementary emergency arrangements, etc.); nevertheless, there exists the problem of incompatibility between the load factors for nuclear reactors and certain technological factories.

The problem of reliability is quite closely linked with the problem being considered. Certain technological processes are carried out continuously. A forced accident to the facility may lead to damage which will require subsequent repair and restoration work (e.g., blast-furnace production), or after which a prolonged startup period will be necessary to bring it to a steady-state operating cycle. In this case, a demand will be imposed on the nuclear power source for guaranteeing a high power supply reliability, i.e., the operational readiness factor of the reactor must be close to 1.

In a number of fields of application, the problem of "heteroscalability" may arise. For example, when using NPTS for the direct reduction of iron ore, with an output of $5 \cdot 10^6$ tons/yr, the reactor thermal power required for technological heat amounts to ~1000 MW [7]. Thus, even for a factory with such large output, the required thermal power of a nuclear power facility does not fall within the range of economic reactor capacities. By means of a reactor with this thermal capacity, $\sim 2 \cdot 10^6$ tons of ammonia per year can be produced.

At the present time it is not possible to give well-defined formulas for the solution to the problem of development of HTGR. The development process of HTGR from experimental test-bench facilities and reactors to industrial pilot plants gives the answers to all the problems. Only the possible routes for research and the solutions requiring verification can be indicated, including: the design of maximally unified reactor facilities, suitable for use in different technological processes; facilities for the centralized production of hydrogen, with its distribution to the various users; storage cells for the intermediate products of NPTS (gases of different compositions for metallurgy and chemistry); nuclear power stations with several medium-capacity nuclear reactors; development of back-up regimes for technological facilities in the operating condition, by means of emergency power supply sources.

At the present time several types of HTGR are being developed. However, the most tenable is the design of the VG-400 facility (Fig. 2) [8, 9], the principal distinctive features of which are: combined production of heat and electric power, and also the use of an intermediate circuit for the removal of high-potential heat. What are the advantages of this scheme?

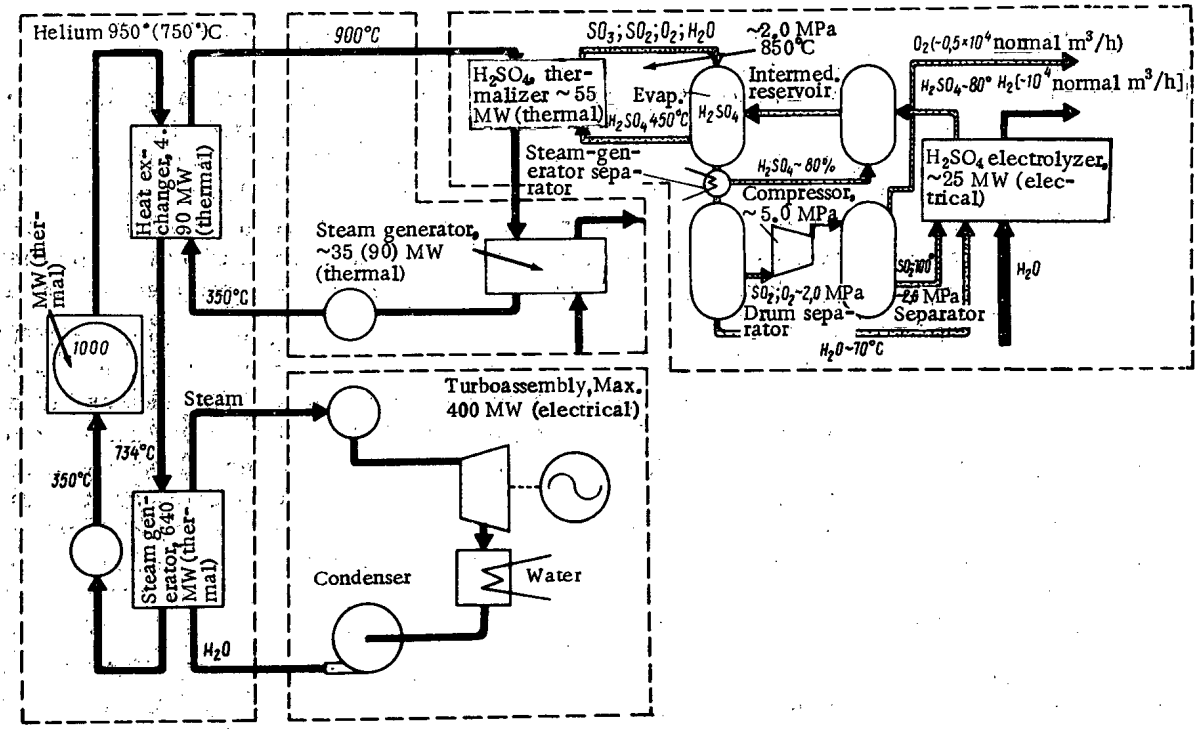

Fig. 2. VG-400 NPTS for the production of hydrogen and electric power. The parameters are: reactor capacity 1000 MW (thermal); helium temperature reactor outlet ~950°C; planned hydrogen production 100 tons/day; capacity of turboassembly 300 MW (electrical).

As already mentioned, by choosing HTGR in the Soviet Union as the primary course of development for technological processes, the construction of prototype facilities for the generation of electric power is eliminated as an independent stage of development. Nevertheless, it will be necessary in time to become familiar with temperatures of 660-750° and later 900-950°C [9]. The VG-400 scheme will provide this possibility: In the first stage, the facility can operate for the production of electric power with a maximum temperature in the primary circuit of up to 750°C. By means of special equipment installed instead of the intermediate circuit heat-exchanger, tests can be conducted at elevated temperatures without the obligatory introduction of an intermediate and technological circuits.

In case of necessity, technological processes on this facility can be transferred to subsequent stages with the assured operation strictly of the reactor equipment at elevated temperatures. A version is also possible, using an intermediate circuit and a special steam-generator in the technological section, with delivery of steam to the steam-turbine facility.

The use of an intermediate circuit in a prototype facility contributes several useful properties. The nuclear section, disregarding the explosion hazard, is isolated from the technological chain, the operation of which can be conducted almost without consideration of radiation hazard. The constant and dangerous penetration of products of the technological circuit, first and foremost hydrogen, into the primary circuit has almost been eliminated [10]. The replacement and servicing of experimental technological plant are unrelated with the decontamination measures. Installation of the technological heat-exchangers is possible after completion of the reactor proper; as a result of this, their replacement during operation is simplified.

The use in the VG-400 of several loops of the primary circuit, makes it possible to investigate various technological processes in them. If the capacities of industrial pilot installations of this type are in the range of 3000-5000 MW (thermal), then the capacity of the prototype facility of 1000 MW amounts to 20-30%, which can be assumed to be the optimum value. The VG-400 facility, as one of the first prototype NPTS, will allow the problems of a technological nature listed above to be studied and solved, as well as problems associated with the introduction of the concept of high-temperature nuclear power generation.

CONCLUSIONS

The development of nuclear power generation for more than 20 years in the Soviet Union has led to the widespread introduction of nuclear power stations into the electric power generation of the country, and their role will be increased even more. Based on VVÉR and RBMK reactors, high-capacity power-generating units

with high technicoeconomic indices are being brought into operation, which will allow the deficiency of energy resources in the European part of the Soviet Union to be reduced significantly. The currently organized structure of the energy balance of the country and the future prospects for its development, show that the existing and under-construction nuclear power stations, first and foremost will replace condensation electric power stations (CEPS) in the energy balance, designed for use in the base part of the power network loading. Coal is the main fuel of the CEPS. At the same time, because of the rise in costs of hydrocarbon types of fuel, it is necessary to search for a path to replace petroleum and gas by nuclear power in such fields as the production of medium- and low-potential heat and steam, the production of artificial types of fuel, the provision of power for large-scale technological factories, and the generation of peak and semipeak electric power.

This problem can be partially solved by the construction of nuclear heat-supply stations (NHSS) based on already operating reactors, and also by the optimum utilization of these reactors for the thermoelectric supply of technological factories. Wider possibilities for the replacement of petroleum and gas in the energy balance are given by the construction and widespread introduction of HTGR, able to utilize more efficiently the capabilities of nuclear energy. At the present time, the optimum fields have been planned and the possible scales of introduction of HTGR have been assessed, and also technical solutions are being worked out, which will permit their introduction to be ensured. It can be expected, that about two-thirds of the potential field of utilization of nuclear high-temperature heat sources can be coped with by HTGR, and with a significant national economic effect. Because of this, it is essential to accelerate work in this direction for the purpose of speeding up the construction of the first commercial HTGR.

The principal problem of the first stage is the construction of industrial pilot NPTS with HTGR with a capacity of 1000 MV (thermal) and with a helium temperature of ~950°C at the core outlet. In a pilot and, in certain cases, also in industrial NPTS, it is advantageous to use compositely the HTGR power for the combined production of high-potential heat and electric power. This solution will allow stations to operate stagewise in purely power-generating and also in power-technological conditions. As a result of this; it would be possible in an industrial pilot facility, to investigate by stages or simultaneously, power-technological processes based on high-temperature processes for the thermochemical or thermoelectrochemical decomposition of water, the high-temperature electrolysis of water, the high-temperature catalytic steam conversion of methane, and also on prospective power cycles, e.g., on a closed gas turbine.

The experience obtained by the operation of such systems for the production of power from HTGR will serve as the basis for the creation of nuclear-industrial complexes of different purpose based on HTGR.

LITERATURE CITED

1. A. P. Aleksandrov, Nuclear Power Generation and Scientific–Technical Progress [in Russian], Nauka, Moscow (1978).
2. A. P. Aleksandrov and N. N. Ponomarev-Stepnoi, in: Twenty Years of Nuclear Power Generation [in Russian], Atomizdat, Moscow (1974).
3. V. A. Legasov et al., in: Problems of Nuclear Science and Technology. Series Nuclear-Hydrogen Power Generation [in Russian], Institute of Atomic Energy, Moscow, Edition 1 (1976).
4. V. N. Grebennik et al., Prospects for the Utilization of HTGR in Power-Technological Processes [in Russian], Vienna, IAEA-TS-109/2 (1977).
5. L. A. Melent'ev, Teploenergetika, No. 11, 8 (1974).
6. A. M. Nekrasov and M. G. Pervukhina (editors), Power Generation in the Soviet Union in 1976-1980 [in Russian], Énergiya, Moscow (1977).
7. N. N. Ponomarev-Stepnoi et al., in: Problems of Nuclear Science and Technology. Series Nuclear-Hydrogen Power Generation [in Russian], No. 1, Institute of Atomic Energy, Moscow (1976).
8. State and Development Prospects of Work on HTGR in the Soviet Union [in Russian], Vienna, IAEA-TC-109/3 (1977).
9. F. M. Mitenkov et al., in: Problems of Nuclear Science and Technology. Series Nuclear-Hydrogen Power Generation [in Russian], No. 2 (3), Institute of Atomic Energy, Moscow (1977).
10. A. N. Protsenko and A. Ya. Stolyarevskii, in: Problems of Nuclear Science and Technology. Series Nuclear-Hydrogen Power Generation [in Russian], No. 1 (2), Institute of Atomic Energy, Moscow (1977).

COMPARISON OF CALCULATIONS FOR A STANDARD FAST REACTOR (BAKER MODEL)

A. I. Voropaev, A. A. Van'kov, and A. M. Tsybulya

UDC 621.039.51

Calculation Model. The one-dimensional calculation model of a "standard" reactor was developed on the basis of the IAEA proposal for comparing the calculations of parameters determining the criticality and reproduction of fast reactors designed in different countries [1]. The publication of the results of this comparison in 1971 (17 laboratories in 10 countries) facilitated international cooperation in fast-reactor physics. In 1975 the Physics and Electronics Institute (FÉI) proposed to a number of laboratories that these calculations should be repeated, retaining the specifications of [1]. The composition and dimensions of the model are shown in Table 1. In the calculations we considered three types of fuel composition:

A. ^{239}Pu and ^{238}U.

B. ^{239}Pu, ^{238}U, and fission products (FP), whose concentration was $\rho_{FP} = 0.0_372 \times 10^{24}$ nuclei/cm^3.

C. ^{239}Pu, ^{240}Pu, ^{238}U, and fission products [$\rho_{FP} = 0.0_372 \cdot 10^{24}$ nuclei/cm^3; $\rho(^{239}\text{Pu}) : \rho(^{240}\text{Pu}) = 1 : 0.5$]. The temperature of the medium was 300°K. The calculation was carried on in the diffusion approximation. Criticality within the limits of $0.999 \geq K_{eff} \leq 1.001$ was ensured by varying the enrichment. The external boundary conditions correspond to a vacuum beyond the conversion zone.

Characteristics of the Calculations

FÉI, Obninsk, USSR. The results of three calculations are given.

1. Calculations based on the BNAB-70 system of constants, which is a modification of the well-known system of Bondarenko [2]. The constants for ^{238}U, ^{235}U, and ^{239}Pu correspond to 1970 estimates. The data on other nuclides correspond to 1964 estimates. The BNAB-70 system of constants has been widely used in the USSR in the design of reactors with uranium fuel (BOR-60, BN-350, BN-600). As was shown by the experience of the physical startup and the initial state of operation of the BN-350 reactor, its fundamental characteristics were predicted with satisfactory accuracy. This is largely due to the fact that the aforementioned system of constants was optimized on the basis of the results of many experiments on critical assemblies with uranium charge. However, it is expected that the prediction of the parameters of large fast plutonium reactors on the basis of the BNAB-70 constants will be substantially poorer [3-5].

The calculation results given in this article are taken from [6]. They were obtained by means of the M-26 one-dimensional complex, which in the preparation of the constants carries out the formalism of Bondarenko et al., [2]. In finding the correction to the slowing-down cross section, we used parabolic interpolation

TABLE 1. Composition (10^{24} nuclei/cm^3) and Dimensions of Spherical Reactor Model

Nuclide	Active zone (R = 84.196 cm)	Blanket (d = 45.72 cm)
Pu+U+FP	0,0072	—
^{239}Pu	—	0,00012
^{238}U	—	0,012
Ni	0,00088	0,00088
Fe	0,00814	0,00814
Cr	0,00198	0,00198
Na	0,0123	0,0069
O	0,0144	0,024
Recommended No. of calc. nodes	14	8

Translated from Atomnaya Énergiya, Vol. 45, No. 6, pp. 419-426, December, 1978. Original article submitted March 6, 1978.

0038-531X/78/4506-1155$07.50

of the integral fluxes in the active zone and the shield. The fission spectrum corresponded to $\nu = 2.9$. The resonance structure of the cross sections was taken into account by means of the self-shielding factors.

2. The results of the calculations made on the basis of the OSKAR-75 system of constants are given in [7]. This system was obtained by fitting constants to the results of 48 integral experiments [8]. In the initial system of constants the σ_f and σ_c for ^{235}U, ^{238}U, and ^{239}Pu correspond to the data from the UKNDL library, and the Fe capture cross section to the estimate made by the Nuclear Data Center of the FÉI. The other cross sections and the resonance self-shielding factors were taken to be the same as in the BNAB-70. We adjusted the cross sections σ_c, σ_f, and $\bar{\nu}$ of ^{235}U, ^{238}U and ^{239}Pu in three broad groups. The calculation of a standard reactor was carried out according to the 9M-26 program. The fission spectrum corresponded to $\bar{\nu} = 3.0$. In finding the correction to the slowing-down cross section, we used linear interpolation of integral fluxes on log–log paper.

3. Calculations based on the BNAB-M system of constants. At present the FÉI, taking account of the latest (early 1977) data from microscopic experiments, has been carrying out a review of nuclear data for ^{235}U, ^{238}U, ^{239}Pu, ^{240}Pu, and ^{10}B. On the basis of these estimates, an experimental version of the BNAB-M constants was prepared.* The data for O and Na in this version correspond to the BNAB-70 estimates; those for Fe, Ni, Cr, ^{241}Pu, and ^{242}Pu correspond to the preliminary estimates. The results given here for the calculation of a standard reactor were carried out with the aid of the ARAMAKO complex [9]. A subgroup representation of the cross sections was used. The correction to the slowing-down cross section was found in the Gruhling–Gertzel approximation on the assumption of constant cross sections in the broad groups.

Cadarache, France [10]. The calculations were carried out on the basis of the CARNAVAL-IV [11] system, which dates from 1976. There were considerable changes from the previous version in the constants for Fe, Ni, Cr, and Na. The changes in the constants for ^{240}Pu, ^{241}Pu, ^{242}Pu, and the fission products agreed with the results of the fission-rate measurements made on the MASURCA and ERMINE assemblies and reaction rates in irradiated specimens on the PHENIX and RHAPSODIE reactors. The authors of [11] believe that the CARNAVAL-IV system yields an error in the prediction of criticality and reproduction factor of a 1200-MW (electrical) reactor in the average stationary state of $\pm 0.4\%$ ΔK_{eff} and ± 0.04 in absolute units (a.u.).

Winfrith, Great Britain [12]. The calculations were carried out on the basis of the FD-5 system of constants [13], which is used for design calculations of the PFR and CFR reactors. As in the CARNAVAL-IV system, the role of the integral data in the FD-5 system is very pronounced. The error in the prediction of criticality and reproduction factor for a large reactor is estimated at $\pm 0.5\%$ ΔK_{eff} and ± 0.03 a.u. (68% confidence interval [13]).

Karlsruhe, Federal Republic of Germany [14]. We used the KFK-INR system of constants [15], which dates from 1972. The estimates of the constants were essentially based on the data of microscopic experiments from the KEDAK library, which were adjusted for agreement with the criticality of the set of uranium and plutonium assemblies. The error in the prediction of criticality and reproduction factor for the initial state of the SNR reactor is estimated in [16] at $\pm 0.8\%$ K_{eff} and ± 0.06 a.u. (90% confidence interval), respectively. The values given in [17] for the discrepancy between experiment and calculation for the ZPR-6-7 large plutonium assembly, in our view, confirm this estimate: $K_{eff} = 0.997$, $c_8/f_9 = 0.152$, $f_8/f_9 = 0.0248$ (calculation); $K_{eff} = 1.000 \pm 0.006$, $c_8/f_9 = 0.143 \pm 0.006$, $f_8/f_9 = 0.0239 \pm 0.011$ (experiment). The experimental reaction rates are given here for the conditions of a homogeneous calculation. The error in the experiment was increased as a result of the factors discussed in [4].

Argonne National Laboratory (ANL), U.S.A. [18]. The ANL calculation was carried on the basis of ENDF/B IV. The preparation of the constants for a 26-group calculation was carried out on the basis of the MC²-2 complex in the P_1 approximation for $\varkappa^2_{a.z} = 9.34 \cdot 10^{-4}$ and $\varkappa^2_{sh} = 0$. Results were obtained only for variant A. An idea of the reliability of plutonium systems of this type is given by the discrepancy between the experiment on the ZPR-6-7 (values given above) and the calculation in [19]: $K_{eff} = 0.984$, $c_8/f_9 = 0.156$; $f_8/f_9 = 0.0232$.

Comparison Results

In Table 2 we give the nuclear concentrations corresponding to the critical state, the critical charge with respect to ^{239}Pu, ^{240}Pu, and the equivalent critical charge (M_{eq}). In Table 3 we give the reproduction

*A more complete version of these constants, now being prepared by M. I. Nikolaev and his coworkers, has been given the designation BNAB-MIKRO.

TABLE 2. Concentration of Fuel (10^{22} nuclei/cm^3), Critical Mass, and K_{eff}

Lab., system of constants	Variant	ρ_{239Pu}	ρ_{240Pu}	ρ_{238U}	M_9, kg	M_0, kg	M_{eq}, kg	K_{eff}
FÉI, BNAB-7	A	0,0999	0	0,6201	991	0	991	1,0005
	B	0,1060	0	0,5420	1052	0	1052	0,9988
	B	0,1010	0,0507	0,4960	1002	505	1036	0,9981
FÉI, OSKAR-75	A	0,0963	0	0,6237	956	0	956	0,9998
	B	0,1033	0	0,5447	1025	0	1025	1,0000
	B	0,0983	0,0491	0,5006	975	490	1008	0,9995
FÉI, BNAB-M	A	0,0975	0	0,6225	968	0	968	0,9996
	B	0,1054	0	0,5426	1046	0	1046	1,0018
	B	0,0970	0,0485	0,5025	963	483	1038	1,0010
Cadarache, CARNAVAL-IV	A	0,0957	0	0,6243	946	0	946	0,9992
	B	0.1026	0	0,5454	1018	0	1018	1,0008
	B	0,0956	0,0476	0,5043	948	476	1013	1,0008
Winfrith, FD-5	A	0,0936	0	0,6264	929	0	929	0,9996
	B	0,1004	0	0,5476	997	0	997	1,0003
	B	0,0938	0,0469	0,5073	931	467	990	0,9998
Karlsruhe, KFK-INR	A	0,0952	0	0,6248	945	0	945	1,0000
	B	0,1024	0	0,5456	1016	0	1016	1,0000
	B	0,0940	0,0470	0,5070	933	468	1018	1,0000
Argonne, ENDF/B IV	A	0.0982 (0,0999)	0 0	0,6218 (0,6201)	973 (991)	0 0	973 (991)	1,0000 (1,0102)

TABLE 3. Reproduction Characteristics

Lab., system of constants	Variant	$G_{a,z}$	G_{bl}	G	$B_{a,z}$	B_{bl}	B
FÉI, BNAB-70	A	—0,194	0,601	0,407	0,764	0,609	1,373
	B	—0,327	0,537	0,260	0,643	0,589	1,232
	B	—0,065	0,570	0,505	0,766	0,623	1,389
FÉI, OSKAR-75	A	—0,296	0,547	0,251	0,675	0,553	1,228
	B	—0,416	0,532	0,116	0,566	0,534	1,100
	B	—0,156	0,521	0,366	0,678	0,566	1,244
FÉI, BNAB-M	A	—0,224	0,576	0,352	0,716	0,580	1,296
	B	—0,361	0,557	0,196	0,593	0,557	1,150
	B	—0,183	0,552	0,369	0,705	0,604	1,309
Cadarache, CARNAVAL-IV	A	—0,238	0,613	0,375	0,702	0,610	1,312
	B	—0,368	0,594	0,226	0,587	0,586	1,173
	B	—0,199	0,587	0,389	0,686	0,629	1,316
Winfrith, FD-5	A	—0,229	0,598	0,369	0,707	0,613	1,320
	B	—0,358	0,576	0,218	0,593	0,582	1,175
	B	—0,176	0,567	0,391	0,705	0,624	1,329
Karlsruhe, KFK-INR	A	—0,195	0,584	0,390	0,730	0,588	1,319
	B	—0,329	0,566	0,237	0,610	0,566	1,176
	B	—0,196	0,563	0,366	0,701	0,610	1,311
Argonne, ENDF/B IV	A	—0,273 (—0,277)	0,568 (0,557)	0,295 (0,280)	0,713 (0,697)	0,567 (0,557)	1,280 (1,253)

characteristics. Since in the ANL calculations criticality of the system was not ensured (K_{eff} = 1.0102), we made appropriate corrections on the basis of the calculation using the BNAB-M constants. The values in parentheses in Tables 2 and 3 are the initial ANL data (K_{eff} = 1.01). In calculating the parameters indicated in Tables 2 and 3, we used the following definitions.

Equivalent critical mass:

$$M_{eq} = M_9 + \omega_0 M_0\ (239.052/240.054). \tag{1}$$

Physical reproduction factor

$$B_{a,z\text{ or }bl} = (C_8 + C_0)_{a,z\text{ or }bl}/(F_9 + C_9)_{a,z+bl} \tag{2}$$

Excess reproduction factor

$$G_{a,z\text{ or }bl} = \frac{[C_8 + C_9(\omega_0 - 1) + C_0(\omega_1 - \omega_0) - F_9]_{a,z\text{ or }bl}}{[F_8 + F_0 + F_0]_{a,z\text{ or }bl}}. \tag{3}$$

TABLE 4. Active-Zone Average Cross Sections

Nuclide	FÉI, BNAB-70			FÉI, OSKAR-75			FÉI, BNAB-M			Karlsruhe,
	$\langle\nu\sigma_f\rangle$	$\langle\sigma_c\rangle$	$\langle\sigma_f\rangle$	$\langle\nu\sigma_f\rangle$	$\langle\sigma_c\rangle$	$\langle\sigma_f\rangle$	$\langle\nu\sigma_f\rangle$	$\langle\sigma_c\rangle$	$\langle\sigma_f\rangle$	$\langle\nu\sigma_f\rangle$
										Variant
^{239}Pu	5,281	0,519	1,798	5,423	0,601	1,857	5,499	0,577	1,883	5,593
^{240}Pu	—	0,809	0,337	1,060	0,824	0,358	1,220	0,668	0,390	—
^{238}U	0,1275	0,301	0,0454	0,124	0,271	0,0450	0,1285	0,292	0,0464	0,1261
FP		—			0,577			—		
Ni		0,0239			0,0239			0,0307		
Fe		0,0068			0,0106			0,0095		
Cr		0,0088			0,0089			0,0166		
Na		0,0016			0,0016			0,0017		
O		0,0012			0,0013			0,0012		
										Variant
^{239}Pu	5,170	0,479	1,759	5,285	0,545	1,808	5,339	0,520	1,828	5,451
^{240}Pu	—	0,759	0,339	1,072	0,765	0,362	1,229	0,601	0,393	—
^{238}U	0,1287	0,296	0,0458	0,1251	0,266	0,0456	0,1302	0,285	0,0471	0,1278
FP		0,524			0,528			0,565		
Ni		0,0238			0,0238			0,0305		
Fe		0,0066			0,0102			0,0092		
Cr		0,0086			0,0086			0,0160		
Na		0,0015			0,0016			0,0017		
O		0,0012			0,0013			0,0013		
										Variant
^{239}Pu	5,135	0,461	1,746	5,242	0,522	1,792	5,325	0,513	1,822	5,451
^{240}Pu	1,041	0,694	0,346	1,093	0,697	0,368	1,232	0,542	0,393	1,180
^{238}U	1,325	0,292	0,0472	0,1290	0,262	0,0469	0,1323	0,285	0,0478	0,1282
FP		0,504			0,507			0,556		
Ni		0,0240			0,0240			0,0306		
Fe		0,0065			0,0099			0,0091		
Cr		0,0084			0,0084			0,0159		
Na		0,0015			0,0015			0,0017		
O		0,0013			0,0013			0,0013		

"Equivalent weights" of isotopes:

$$\omega_i = (x_i - x_8)/(x_9 - x), \tag{4}$$

where $x_i = \langle\nu\sigma_f\rangle - \langle\sigma_f\rangle - \langle\sigma_c\rangle$.

(The subscripts 8, 9, 0, 1 refer to ^{238}U, ^{239}Pu, ^{240}Pu, and ^{241}Pu, a.z to the active zone, bl to the blanket; C and F are the integral rates of the capture and fission reactions.)

Taking account of the data of Tables 2 and 3, we can draw a number of conclusions.

1. The critical charge of ^{239}Pu in the calculation based on the BNAB-70 constants is higher than in all the other calculations. On the average, the difference is 37 kg (~2.1% ΔK_{eff}) in variant A, 31 kg (~1.8% ΔK_{eff}) and 52 kg (~3.2% ΔK_{eff}) in variants B and C. The increased discrepancy in variant C (high ^{240}Pu content) is essentially due to the 20–25% overestimate of the ^{240}Pu capture cross section in the BNAB-70 estimates in comparison with present-day microscopic data. This also explains the unduly high critical charge (~31 kg) for variant C in the calculation based on OSKAR-75 constants, since the estimates of the ^{240}Pu constants in the OSKAR-75 correspond to the BNAB-70 data. The results of the excessive value for the ^{240}Pu cross section can be clearly seen both in the components of the neutron balance and in the active-zone average cross sections (Table 4).

2. The critical charge values for ^{239}Pu calculated on the basis of OSKAR-75, CARNAVAL-IV, and KFK-INR are practically identical (956, 946, and 945 kg in variant A and 1025, 1020, and 1016 kg in variant B). As noted earlier, the KFK-INR constants satisfactorily predict the criticality of the ZPR-6-7 plutonium assembly, whose composition is close to that of variant A of the standard reactor. The integral experiments on the ZPR-6-7 were used in adjusting the constants of the OSKAR-75 system [8]. The adjustment yielded a criticality prediction within the limits of 0.5% ΔK_{eff}. It is not surprising, therefore, that the calculations for OSKAR-75 agree with those for KFK-INR. It may also be assumed that combined calculation-and-experiment investigations on SNEAK plutonium assemblies made for better agreement between the Cadarache and Karlsruhe results [20].

KFK-INR		Argonne, ENDF/B IV			Cadarache, CARNAVAL-IV			Winfrith, FD-5		
$\langle\sigma_c\rangle$	$\langle\sigma_f\rangle$	$\langle\nu\sigma_f\rangle$	$\langle\sigma_c\rangle$	$\langle\sigma_f\rangle$	$\langle\nu\sigma_f\rangle$	$\langle\sigma_c\rangle$	$\langle\sigma_f\rangle$	$\langle\nu\sigma_f\rangle$	$\langle\sigma_c\rangle$	$\langle\sigma_f\rangle$
A										
0,567	1,901	5,454	0,566	1,864	5,388	0,587	1,843	5,501	0,564	1,870
—	—	—	—	—	—	—	—	—	—	—
0,291	0,0448	0,1233	0,283	0,0445	0,1263	0,278	0,0440	0,132	0,274	0,0477
—			—		—	—	—	—	—	—
0,0285			0,0320			0,0265			0,0256	
0,0148			0,0116			0,0075			0,0116	
0,0084			0,0187			0,0090			0,0077	
0,0015			0,0021			0,0016			0,0014	
0,00074			0,0010			0,00092			0,00079	
B										
0,5145	1,851				5,252	0,543	1,795	5,375	0,520	1,826
—	—				—	—	—	—	—	—
0,2864	0,0455				0,1290	0,274	0,0450	0,132	0,271	0,0477
0,559		Results not shown				0,496			0,511	
0,0283						0,0265			0,0254	
0,0143						0,0072			0,0113	
0,0082						0,0087			0,0073	
0,0014						0,0015			0,0014	
0,00075						0,00093			0,00079	
C										
0,516	1,851				5,233	0,535	1,788	5,350	0,511	1,817
0,410	0,375				1,098	0,511	0,353	1,167	0,576	0,369
0,289	0,0456				0,1313	0,274	0,0458	0,134	0,270	0,0485
0,558		Results not shown				0,489			0,501	
0,0284						0,0266			0,0256	
0,0144						0,0071			0,0111	
0,0081						0,0086			0,0073	
0,0014						0,0014			0,0013	
0,00075						0,00095			0,00080	

3. The deviation of the critical-charge calculations for BNAB-M and ENDF/B IV from the average calculated values for KFK-INR and CARNAVAL-IV is 27 kg ($\sim 1.4\%\ \Delta K_{eff}$) in all variants. These values are close to the difference between the BNAB-M and ENDF/B IV calculated values and the experimental values for the ZPR-6-7 assembly.

4. We observe a lower critical charge in the calculation based on FD-5 in variants A and B. For example, the difference between the ENDF/B IV and the FD-5 calculated values is 44 kg ($\sim 2.4\%\ \Delta K_{eff}$). However, in variant C, with high ^{240}Pu content, the data for FD-5, CARNAVAL-IV, and KFK-INR are close to one another. As Table 4 suggests, this is due to the high ^{240}Pu capture cross section in the FD-5 system in comparison with the other systems of constants.

5. It follows from Table 3 that the dispersion of the excess reproduction factor and the physical reproduction factor in the BNAB-M, CARNAVAL-IV, KFK-INR, FD-5, and ENDF/B IV calculations is fairly small ($\sim \pm 0.02$), and the relation $G \approx (B-1)+0.06$ holds. The excess reproduction in the BNAB-70 calculations, as could be expected [4, 5], is ~ 0.06. The main contribution to the discrepancy comes from the difference in the reproduction in the active zone.

6. The adjustment of the OSKAR-75 constants assumed what we consider an unduly high accuracy in the reaction rates determining the neutron balance (primarily c_8/f_9 ($\pm 2\%$)) found in the experiment conducted on the ZPR-6-7 large plutonium assembly. This probably is one of the reasons for the low reproduction in the OSKAR-75 calculations. It has already been noted that the discrepancy between experiment and calculation on the basis of the KFK-INR, ENDF/B IV, and BNAB-M constants amounts to 6-8%. It is also possible that there was a systematic error in the experiment [21].

Table 5 shows the blocked group cross sections for ^{239}Pu and ^{238}U and the value of ν. We observe a considerable dispersion of σ_f (^{239}Pu) ($\sim 15\%$ in groups 14 and 15) and σ_c (^{238}U) ($\sim 25\%$ in groups 14 and 16). The dispersion in σ_c (^{239}Pu), in our view, is less than might have been expected, taking account of the accuracy of the microscopic data.

We do not have any analogous data from France and Great Britain. Therefore, it is useful to compare the active-zone averages of the cross section, which are easily obtained from the neutron balance (see Table 4). A comparison shows that the calculations of the integral spectra in the active zone are close to each other,

TABLE 5. Blocked Group Cross Sections of the Active Zone (variant A)*

No. of group	ν (^{239}Pu)				σ_f (^{239}Pu)				σ_c (^{239}Pu)				σ_c (^{238}U)			
	1	2	3	4	1	2	3	4	1	2	3	4	1	2	3	4
1	3,86	4,03	4,09	4,01	2,21	2,23	2,09	2,22	0,01	0,0244	0,0210	0,0360	0,0260	0,0256	0,0250	0,0236
2	3,51	3,63	3,62	3,59	1,72	1,79	1,72	1,73	0,02	0,0266	0,0223	0,0215	0,012	0,011	0,0290	0,0292
3	3,27	3,33	3,32	3,32	3,32	1,86	1,87	1,85	0,03	0,011	0,0250	0,0232	0,024	0,021	0,021	0,024
4	3,12	3,14	3,14	3,14	1,97	1,93	1,95	1,93	0,04	0,022	0,011	0,0294	0,060	0,049	0,055	0,059
5	3,01	3,01	3,03	3,02	1,76	1,78	1,74	1,75	0,04	0,052	0,022	0,025	0,13	0,11	0,13	0,11
6	2,95	2,93	2,96	2,95	1,59	1,65	1,61	1,61	0,10	0,112	0,065	0,091	0,13	0,12	0,13	0,11
7	2,91	2,89	2,92	2,91	1,53	1,51	1,55	1,51	0,16	0,154	0,16	0,18	0,14	0,13	0,13	0,12
8	2,89	2,88	2,94	2,89	1,50	1,50	1,53	1,53	0,23	0,20	0,22	0,22	0,18	0,16	0,18	0,16
9	2,88	2,87	2,90	2,88	1,47	1,61	1,58	1,60	0,26	0,30	0,25	0,35	0,26	0,26	0,28	0,26
10	2,87	2,87	2,89	2,87	1,59	1,61	1,69	1,62	0,48	0,49	0,51	0,50	0,44	0,45	0,44	0,41
11	2,87	2,86	2,89	2,87	1,74	1,74	1,84	1,74	0,83	0,84	0,83	0,86	0,62	0,61	0,54	0,55
12	2,87	2,86	2,89	2,87	2,16	2,12	2,31	2,08	1,67	1,51	1,60	1,46	0,80	0,78	0,70	0,72
13	2,87	2,86	2,89	2,87	2,88	2,99	3,25	2,73	2,88	2,70	2,93	2,49	1,14	0,98	1,09	0,95
14	2,87	2,86	2,89	2,87	4,01	4,04	4,44	4,26	3,72	3,58	3,97	3,50	1,12	0,78	0,91	0,98
15	2,87	2,86	2,89	2,87	6,85	7,44	6,49	6,78	5,28	5,81	5,51	5,36	1,07	0,96	0,92	1,09
16	2,87	2,86	2,89	2,87	10,7	10,4	10,6	9,59	8,52	8,82	8,10	8,00	1,22	1,14	0,95	1,12
17	2,87	2,86	2,89	2,87	15,8	13,0	14,1	14,6	12,8	9,63	9,19	10,2	2,04	1,78	1,60	1,67
18	2,87	2,86	2,89	2,87	38,7	38,5	39,7	38,3	31,2	17,9	16,2	15,8	1,79	1,26	1,62	1,35
19	2,87	2,86	2,89	2,87	14,8	13,5	8,72	6,22	21,1	12,9	15,6	20,4	3,32	3,26	3,22	3,90
20	2,87	2,86	2,89	2,87	70,2	53,4	41,4	26,8	42,8	29,9	28,2	16,1	4,50	3,39	5,73	20,8

*1) BNAB-70; 2) BNAB-M; 3) KFK-INR; 4) ENDF/B IV.

TABLE 6. Comparison of Calculation Results

Physical parameter	FÉI		Cadarache		Winfrith		Karlsruhe		Argonne	
	1970	1976	1970	1976	1970	1976	1970	1976	1970	1976
Variant A										
M (^{239}Pu), kg	975	968	952	946	939	929	961	945	978	973
B	1,34	1,30	1,25	1,31	1,26	1,32	1,31	1,32	1,41	1,28
$B_{a.z}$	0,74	0,72	0,67	0,70	0,69	0,71	0,74	0,73	0,79	0,71
G	0,37	0,35	0,30	0,38	0,34	0,37	0,38	0,39	0,46	0,30
c_8/f_9	0,161	0,155	0,147	0,151	0,146	0,147	0,160	0,153	0,164	0,152
α_9	0,301	0,306	0,334	0,319	0,306	0,302	0,312	0,298	0,253	0,304
f_8/f_9	0,0247	0,0246	0,0224	0,0239	0,0221	0,0255	0,0226	0,0236	0,0239	0,0239
f_9	1,82	1,89	1,89	1,84	1,92	1,87	1,87	1,90	1,89	1,86
Variant C										
M (^{239}Pu), kg	1006	963	956	948	929	990	965	933	951	—
B	1,36	1,31	1,26	1,31	1,25	1,33	1,28	1,31	1,42	—
$B_{a.z}$	0,74	0,71	0,67	0,68	0,66	0,71	0,70	0,70	0,75	—
G	0,44	0,37	0,39	0,38	0,31	0,39	0,36	0,37	0,46	—
c_8/f_9	0,162	0,156	0,149	0,153	0,148	0,149	0,162	0,156	0,162	—
α_9	0,270	0,282	0,310	0,299	0,281	0,282	0,290	0,279	0,237	—
c_{40}/f_9	0,414	0,298	0,316	0,286	0,198	0,317	0,240	0,222	0,238	—
f_8/f_9	0,0268	0,0262	0,0236	0,0256	0,0236	0,0267	0,0242	0,0246	0,0264	—
f_9	1,75	1,82	1,83	1,79	1,83	1,82	1,81	1,85	1,84	—

and therefore we may expect the discrepancy between the average cross sections to be mainly associated with the difference in the group constants. Noting the data of Table 4, we can observe the following:

the active-zone average capture cross sections for ^{238}U in the systems fitted under integral data (OSKAR-75, CARNAVAL-IV, FD-5) is ≈ 6% lower than in the BNAB-M, KFK-INR, and ENDF/B IV systems, which are based primarily on microscopic data;

α for ^{239}Pu in the OSKAR-75 calculations is ≈8% higher than the data;

the dispersion of the average capture cross sections for Fe, Ni, Cr, and Na is ~50%;

the average cross section for the fission products in the CARNAVAL-IV calculations differ considerably from the other data. It may be noted that the values shown in Table 4 (0.496 for variant B and 0.489 for variant C) also differ considerably from the analogous values and the calculation based on the previous version, CARNAVAL-III [22] (0.522 and 0.519). These changes are mainly due to the change in the fission-product constants, since the neutron spectrum did not change much in the transition from the third to the fourth version.

In Table 6 we compare the results of the calculation of the main parameters for the standard reactor (variants A and C) shown in this article with the data obtained in 1970 [1]. We can see that the critical charge in variant A has changed little; there is a substantial reduction in the average dispersion in the reproduction

parameters [$\bar{B} = 1.32 \pm 0.07$ (1970); $\bar{B} = 1.31 \pm 0.02$ (1976), variant A]. From this, of course, it does not follow that the real accuracy of the calculation of the physical reproduction factor is this high. Because of the unquestionable correlation between the principal nuclear data used in different laboratories, the estimate of the accuracy (± 0.02) should rather be considered a lower bound. It should also be noted that the considerable dispersion in critical charge (973 kg for the ENDF/B IV, 929 kg for the FD-5) in itself signifies an indefiniteness in the physical reproduction factor (± 0.05); the average dispersion of the data on the critical charge in variant C remains large ($M = 961 \pm 20$, 1970; $M = 959 \pm 18$, 1976); the change in the ratios of the active-zone averages of the reaction rates is the following: $\bar{c}_8/\bar{f}_9 = 0.156 \pm 0.07$, $\bar{\alpha}_9 = 0.301 \pm 0.020$ (variant A, 1970); $\bar{c}_8/\bar{f}_9 = 0.152 \pm 0.02$, $\bar{\alpha}_9 = 0.306 \pm 0.010$ (variant A, 1976).

The observed closeness in the results of the calculations of different laboratories objectively indicates an increased reliability in the calculation of fast reactors in different countries. There remains a considerable degree of indefiniteness in the prediction of the main physical characteristic, namely, the critical charge. It is desirable to make a representative international comparison of the results of the calculation of a two-dimensional model, which is closer to a real reactor than the one-dimensional model considered here.

The authors are deeply grateful to the staff of the laboratories in the various countries who were good enough to send the results of their calculations, and also to M. F. Troyanov for his support and his comments at every stage of the work.

LITERATURE CITED

1. A. Baker and A. Hammond, Calculations for a Large Fast Reactor. Risley, TRG Report 2133 (A) (1971).
2. L. P. Abagyan et al., Group Constants for the Calculation of Atomic Reactors [in Russian], Atomizdat, Moscow (1964).
3. A. A. Van'kov, A. I. Voropaev and L. N. Yurova, Analysis of a Reactor-Physics Experiment [in Russian], Atomizdat, Moscow (1977).
4. A. I. Voropaev et al., in: Problems of Atomic Science and Technology. Nuclear Constants Series [in Russian], Vol. 2, No. 20, Atomizdat, Moscow (1975), p. 112
5. A. I. Voropaev et al., in: Problems of Atomic Science and Technology. Nuclear Constants Series, No. 25, Izd. TsNIIatominform, Moscow (1977), p. 69.
6. L. P. Abagyan et al., "Calculations of the characteristics of a "standard" fast reactor," Preprint FÉI-525 Obninsk (1974).
7. Yu. G. Bobkov and L. N. Usachev, "Results of the calculation of a standard reactor by the OSKAR-75 system," Preprint FÉI-659 (1976).
8. B. G. Bobkov et al., in: Proceedings of the "Neutron Physics" Conference, Part I [in Russian], Izd. TsNIIatominform, Moscow (1976), p. 64.
9. V. F. Khokhlov, M. M. Savos'kin, and M. N. Nikolaev, in: Nuclear Constants. No. 8, Part 3 [in Russian], Atomizdat, Moscow (1972), p. 3.
10. J. Chaudat and J. Courchinoux, Charactéristiques d'un Réacteur Rapide "Etalon" Calculé avec le Formulaire CARNAVAL-IV. Note Technique, Cadarache (1977).
11. I. Barre, I. Bouchard, and I. Chadar, in: Proceedings of the Fourth Conference on Nuclear Cross Sections and Technology, Washington, March 3-7, 1975, Vol. 1, p. 51.
12. W. Barron and J. Mann, A Comparison of FD-5 and FD-4 Data for a Spherical Reactor Model. Technical Note. Risley (1975); J. Rowlands, Calculations for the Standard Fast Reactor. Technical Note. Winfrith (1975).
13. J. Rowlands et al., in: Proceedings of the IAEA Symposium on Physics of Fast Reactors, Tokyo, 1973, Vol. 3, p. 1133.
14. E. Kiefhaber and D. Thiem, Institut für Neutronenphysik und Reaktortechnik. Technical Note. Karlsruhe (1976).
15. E. Kiefhaber, KFK-1572. Karlsruhe (1972).
16. H. Küsters, KFK-1632, Karlsruhe (1973).
17. W. Oesterkamp, Trans. Am. Nucl. Soc., 16, 262 (1973).
18. R. Bucher et al., Calculation of the Breeding Properties of a Standard Fast Reactor. Technical Note. ANL (1975).
19. R. McKnight, Nucl. Sci. Eng., 62, No. 2, 309 (1977).
20. P. Hammer and F. Plum, Physics Investigations of Sodium-Cooled Fast Reactors Core Z1 Masurca in SNEAK Assembly, 6D, CEA-N-1561, KFK-1581 (1972).
21. P. Collins and M. Lineberry, Trans. Am. Nucl. Soc., 24, 481 (1976).

22. J. Chaudat, J. Courchinoux, and J. Barre, Caractéristiques d'un Réacteur Rapide Etalon Calculé avec le Formulaire CARNAVAL-III, Note Technique. Cadarache (1975).

POWER-REACTOR FUEL-PRODUCTION PROBLEMS*

F. G. Reshetnikov, Yu. K. Bibilashvili, and V. I. Kushakovskii

UDC 621.039.54:621.311.2:621.039

The quality of fuel-pin cores largely determines the viability and reliability of any nuclear-power system. Particular attention is therefore needed in the technology of pin production in order to ensure high and consistent quality. Although there are now closely defined specifications for UO_2, and these ensure high viability, improvements to the specifications should not only provide higher reliability but also should indicate where specifications are too stringent on particular parameters, which might assist in cheapening the process.

Fluorine and Water

It has previously been pointed out [1] that one of the major specifications for a uranium oxide fuel (the acceptable fluorine content) has been formulated without due allowance for the relationship to the water content in the pin. The acceptable fluorine content limit has been set as 0.006%. Dry fluorine at that level cannot produce any substantial pitting corrosion in the sheath, whereas water will convert such fluorine to a highly corrosive form. Therefore, a particular need is to reduce the water content, the more so since water is a basic source of hydrogen. The manufacture of UO_2 tablets is now highly advanced, and the water levels do not usually exceed 0.003-0.0005%. On the other hand, the specifications for fluorine have been tightened, which has given the impression that the specifications do not have a proper experimental basis. There is therefore some substantial practical interest in demonstrating the relationship between the standards for acceptable fluorine and water levels in fuel pins.

Specifications for Mechanical Parameters

Some specifications for UO_2 concern the mechanical features; the failure force is an inadequate characteristic for any tablet, and other criteria must be used to evaluate the fracture resistance during the various manufacturing and transport operations. For example, appropriate vibrational tests must be performed. Then it would be possible, e.g., to use a relatively small number of tablets and detect ones with latent flaws such as microcracks, which would mean that not so many expensive assembled pins might be rejected. These cracks are particularly hazardous when the pins have been assembled, because the damage in the cores may increase on irradiation, which can result in increased forces on the sheath and ultimately in premature failure of the pin. Therefore, preliminary careful testing of the material may be economically justified.

Plasticity in Fuel Pins

The absence of cracks does not necessarily mean that the sheath will not be affected, e.g., by thermal expansion or swelling in the fuel. Although the effects may be of very different types, the loads on the sheath may become very considerable. Of course, the loading can be adjusted to a certain extent via the density of the tablets, the volume of the end recesses, and the diameter of the holes. There may also be other effects on the interaction from the ratio of height to diameter, which should be within the range 1.1-1.2.

However, any adjustment to the above parameters is restricted by the specifications for a fairly high mean or effective density of the fuel in a pin. It has therefore been suggested that fuel should be made reasonably plastic at the irradiation temperature in order to eliminate substantial forces on the sheath.

The plasticity of sintered UO_2 can be increased by special technologies and by the addition of other substances, e.g., other oxides that form low-melting eutectics. The choice of such substances is not an easy matter, since the amounts must be small; also, they must not form solid solutions with UO_2, while the low-temperature eutectics must lie along the grain boundaries. Finally, these additives must not have any marked effects on the physical characteristics of the reactor itself. Nevertheless, the suggestion is valuable, and it should be given appropriate attention.

*Journal form of a paper read at the Reactor Materials Science Conference, Alushta, 1978.

Translated from Atomnaya Énergiya, Vol. 45, No. 6, pp. 426-429, December, 1978.

 0038-531X/78/4506-1162 $07.50

The production of cores with improved plasticity is particularly important for any power reactor that is to work with highly variable or peaky loads.

Fuel-Pin Design for Power Stations Working Under Variable-Load Conditions

The power-control problem becomes more important as the output power of a nuclear station increases, as there is more difficulty in matching the load curve. The specifications for control characteristics of nuclear power station units are presently formulated mainly from user requirements. The control specifications lay down that the power levels of the units should be adjustable at rates of up to 4-6% per minute. These specifications envisage power stations with thermal reactors, because the economic performance of a fast reactor is adversely affected by operation with peaky loads, and this relates particularly to the entire fuel cycle, not least because of the direct effect on the rate of accumulation of plutonium.

The development plans for nuclear power in the USSR and other countries envisage preferential construction of reactors using rod systems with cores composed of compact UO_2 sheathed in zirconium alloy. The loads on such sheaths under steady conditions are closely known. The forces arise from the external pressure of the coolant, the internal pressure from the gaseous fission products and filling gases, the swelling in the fuel proper, and thermal expansion. The physicomechanical characteristics of the material are affected by the radiation damage occurring during operation, in addition to any effects from mechanical fatigue, interaction with the coolant and the fission products, and so on.

All of these factors reduce the reliability of the fuel rods considerably. Any new effects superimposed on the long-term processes, such as ones arising from sharp changes in the temperature and heat production, naturally reduce the fuel-rod viability.

It is now considered firmly established that the main mechanism responsible for fuel-rod failure on account of power-level variation is the mechanical force exerted on the sheath by the fuel consequent on the thermal expansion. This interaction occurs in part because the temperature of the core is different from that of the sheath, while the thermal-expansion coefficient of zirconium alloy is less by a factor 1.5-2 than that of UO_2. The danger of sheath failure under thermal cycling is made worse by the tendency of the zirconium sheaths to show corrosion cracking under stress in the presence of corrosive fission products, in particular iodine.

Reliable operation under variable conditions has been researched as follows.

1. The limiting permissible thermal loads have been determined for rates of change of power level up to 4-6% per minute. Preliminary estimates show that the linear thermal load in that case should not exceed 400 W/cm.

2. The optimum rates or runup have been determined for systems with rods operating at 550-600 W/cm. In this connection, it has been necessary to consider the scope for increasing the threshold failure power when the reactor is run up to nominal power by stages. This suggestion involves maintaining the rods at two or three intermediate power levels for times sufficient to allow 40-60% relaxation in the stresses in the sheaths consequent on relaxation in the fuel.

3. Cores are being developed showing high creep rates or low temperatures of brittle-plastic transition, which should reduce the relaxation times and also the stress levels in the sheath. This implies the addition of minor components to the UO_2, which have almost no effect on the melting point but which do increase the creep rate of UO_2 in the range 700-1000°C. There are also other possibilities for increasing the plasticity of the cores.

4. Detailed studies are being made on the corrosion cracking of zirconium sheaths; in particular, one needs to establish the main factor responsible for such cracking, namely whether the limiting tensile stress or the threshold plastic-strain rate is the more important factor. In the first case, alloys with low yield points would be better, whereas stronger alloys would be preferable in the second. However, this is not the only possible criterion, because other factors influence the corrosion cracking: The composition and structural state of the alloy, the working temperature, the general quality of the sheath, etc.

Mixed Oxide Fuel

The above arguments apply equally to mixed uranium–plutonium oxide fuel, but here there is also another very important specification, viz., that the uranium and plutonium should be uniformly distributed. There

are two essentially different methods of producing mixed oxide fuel: Coprecipitation and mechanical mixing. The first is used with high-temperature sintering, which gives an ideal solid solution of the two oxides.

In the second method, the uniformity of the distribution is less perfect and is dependent on the grain size of the initial powders, the care taken in the mixing, and to some extent on the mode of sintering, since high temperatures and fairly long times are required to homogenize mechanically mixed oxides.

However, the advantages of the coprecipitation method involve considerable expense, since the reprocessing of large amounts of fuel containing plutonium is made more complicated. Also, the coprecipitated oxides cannot be stored for long periods. The mixture must be used almost immediately, since the accumulation of ^{241}Am hinders the subsequent handling and may require fresh purification.

In practice, it is often difficult to organize the production cycle for immediate use of prepared materials, particularly if the cycle involves a plant concerned with reprocessing uranium–plutonium fuel from spent rods, i.e., the plutonium may be repeatedly purified from ^{241}Am. In that case, the cost of repeated fuel purification will be much less if the PuO_2 is not mixed with UO_2.

All of these difficulties are much reduced if one uses mechanically mixed UO_2 and PuO_2, with preparation directly before manufacture. Research has shown that the specifications previously laid down for the homogeneity of mixed fuel are too stringent. Comparative tests have shown that identical degrees of viability are obtained by coprecipitation and mechanical mixing [2, 3]. There is a certain amount of redistribution of the plutonium that has no appreciable effect on the physics of the reactor during the irradiation, no matter how the fuel pins are produced. Therefore, mechanical mixing is considered as the technique of preference for making uranium–plutonium fuel.

Granulated Fuel

So far we have discussed fuel pins in which the cores are composed of sets of tablets of average density 10.5-10.6 g/cm^3, i.e., about 96% of the theoretical value. The effective fuel density in the pins for a thermal reactor is then about 9.55 g/cm^3 when allowance is made for all the permissible gaps, viz., about 87% of the theoretical value for the VVÉR-1000 reactors, or correspondingly 10 g/cm^3 or 91% of the theoretical value for the RBMK reactors.

The effective fuel density is somewhat lower at 8.8 g/cm^3, or about 80% of the theoretical value, for fast reactors; such densities are readily attained by the usual techniques for loading tablets with central holes or recesses. On the other hand, there are also other loading techniques based on vibrational consolidation of granulated fuel, and some experience is already available with such rods.

Granulated fuel has certain advantages over tablets; the sol–gel method of producing such fuel eliminates the dust hazards of powder techniques, as well as tablet grinding, and it also reduces the mechanical interaction between the fuel and the sheath and improves the heat transfer.

However, the published evidence indicates that vibrational consolidation of granulated fuel has not yet been widely used, although the technique is attractive in certain respects. One reason for this appears to be that good results have been obtained in making cores from sets of sintered tablets. Also, there are the following major aspects to be examined in any proper evaluation of the desirability of transferring to vibrational consolidation of granulated fuel.

1. An efficient and economical technique has to be developed for producing the granulated fuel, in particular densities close to the theoretical value. Such a technique should provide granules of closely controlled size, and it is necessary to have a set of sizes, including a fine fraction of grain size about 20 μ. Unless these conditions are met, the necessary effective fuel density cannot be attained, particularly for thermal-reactor rods. However, it appears difficult to attain even 90% of the theoretical density even if optimal characteristics are attained in the granulated fuel.

2. It is necessary to define a mode of vibrational consolidation such as to ensure a reasonably uniform distribution of the fuel throughout the length of a rod. The length of the active zone of a rod in a BN-350 reactor is about 1100 mm, while it is about 3500 mm for thermal reactors (RBMK and VVÉR-1000). The deviations from the specified density should not exceed 3-5%. It will not be an easy matter to attain this over such large lengths.

3. Research is required on the response of sheaths, particularly of zirconium alloys, during vibrational consolidation of such long rods, since dense sintered UO_2 is very abrasive.

Some researchers consider that most of these problems can be solved fairly readily, and they assume that rods containing vibrationally consolidated fuel, particularly of mixed uranium–plutonium type, may replace the tablet type [4]. However, major researches must be undertaken before any serious comparative evaluation of the techniques can be performed.

LITERATURE CITED

1. F. G. Reshetnikov et al., At. Energ., 43, No. 5, 408 (1977).
2. G. Karsten, Trans. Am. Nucl. Soc., 19, No. 1, 19 (1974).
3. R. Hilbertetol, Am. Nucl. Soc., 19, No. 1, 135 (1974).
4. W. Helfrid, Lahr. Nucl. Tech., 31, No. 2, 183 (1976).

ZIRCONIUM ALLOYS IN NUCLEAR POWER*

A. S. Zaimovskii

UDC 546.831+621.039.5

Presently there is a tendency for the unit power to increase in water-cooled reactors; this has meant more stringent specifications for the corrosion resistance and mechanical parameters of zirconium sheaths and tubes. Further, there has been an increase in the interest in the behavior of zirconium alloys under emergency conditions (LOCA). Finally, there is a tendency to operate reactors with more peaky loading. The development program for the RBMK reactors in particular envisages the need for alloys of high corrosion resistance capable of working in superheated steam at 400-500°C.

For this reason, the Soviet Union has researched zirconium alloys since 1950, in particular the phase diagrams and structures of about 50 ternary systems. Transmission electron microscopy and x-ray analysis have been employed to define the solubility of niobium in α-Zr, which is about 0.7 at. %, and studies have been made on the formation of metastable phases and the sequence of transitions in Zr–Nb alloys quenched from the β-phase region [1].

Niobium as an Alloying Element for Zirconium Alloys. Niobium is used in alloying zirconium for several reasons.

The oxide film on zirconium is usually considered as a semiconductor with anion vacancies, which indicates that cations of valency 5 or 6 will enter lattice nodes and reduce the number of anion vacancies, which will reduce the scope for oxygen ions to penetrate and thus tend to inhibit corrosion. Niobium is far better than tin as a hardening agent, and is inferior only to aluminum and molybdenum, which adversely affect the corrosion resistance. Niobium also has a relatively small thermal-neutron capture cross section.

Niobium also offsets the adverse effects of N, C, Al, Ti and other impurities (Fig. 1), and also substantially reduces the absorption of hydrogen; it is highly soluble in β-Zr and has reasonable solubility in α-Zr, which makes it favorable to mechanical treatment and means that the parameters of the alloys can be varied widely by heat treatment. The high melting point facilitates casting zirconium alloys, the more so since there is only one alloying element, in contrast to the four elements used in zircalloy, for example.

Properties of N-1 Alloy. Classical data on the corrosion of N-1 and N-2.5 alloys outside reactors [2, 3] indicate that alloys containing 1 or 2.5% Nb differ from zircalloy in showing no stepout in the oxidation kinetics on testing in water and steam–water mixtures for times up to 20,000 h. The oxide films adhere firmly to these alloys, while microcracks tend to heal up.

Numerous studies have been made on the effects of irradiation on the corrosion resistance of N-1, and it is clear that irradiation of itself has little tendency to accentuate corrosion, provided that there is no oxygen in the water or steam–water mixture, or any other oxidizing agent arising from radiolysis of water, as Fig. 2 shows [4, 5].

It has been concluded [6] from tests lasting up to 20,000 h under boiling conditions free from deposition in the RBMK reactors that N-1 and N-2.5 are corrosion-resistant and retain their plasticity; e.g., the total residual strain in N-1 was not less than 10%. Local signs of nodular corrosion were seen on tubes of this alloy, which were similar to those seen in zircalloy.

* Journal form of a paper read at the Reactor Materials Science Conference, Alushta, 1978.

Translated from Atomnaya Énergiya, Vol. 45, No. 6, pp. 430-433, December, 1978.

0038-531X/78/4506-

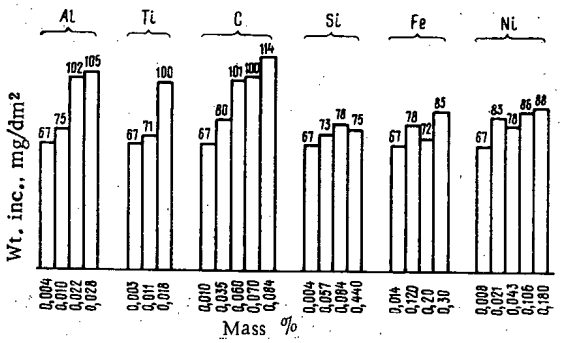

Fig. 1

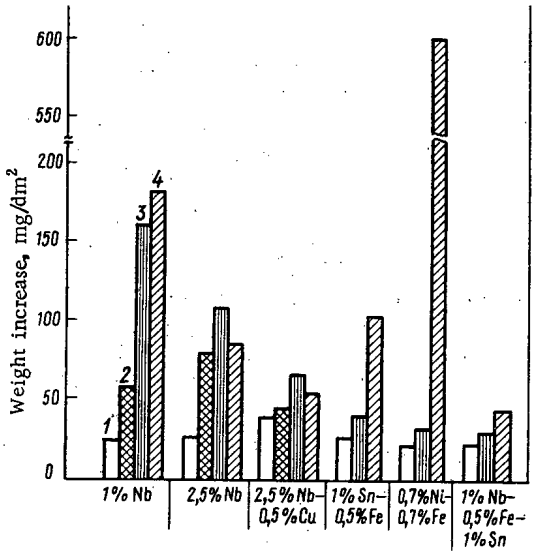

Fig. 2

Fig. 1. Effects of trace components on the corrosion resistance of N-1 alloy in water at 350°C for 7000 h.

Fig. 2. Corrosion resistance of zirconium alloys in water and steam–water mixtures in an autoclave and in a reactor loop (280°C, 3500 h): tests outside reactors: 1) autoclave, water under pressure, 0.3-0.6 mg/kg of O_2; reactor tests: 2) boiling water containing 0.5-0.6 mg/kg of O_2, outside core; 3) the same, but with 12-17 mg/kg of O_2; 4) boiling water with 12-17 mg/kg of O_2, irradiated by a fluence of $3.7 \cdot 10^{20}$ neutrons/cm^2 (E > 1 MeV).

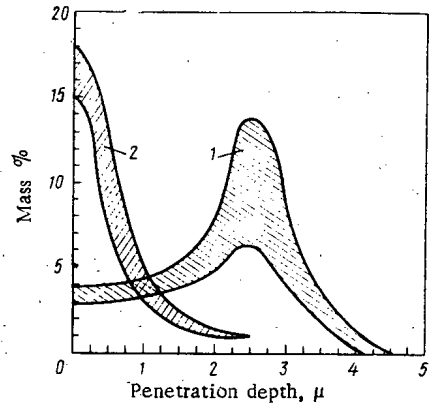

Fig. 3. Distributions of ^{18}O in oxide films on: 1) zirconium, which indicates diffusion over short paths; and 2) on N-1, which is characteric of diffusion by a bulk-vacancy mechanism.

N-2.5 Alloy and Improvement of Zirconium–Niobium Alloys. This alloy is used widely throughout the world because of its good mechanical parameters and good corrosion resistance in reactors. Canada has been particularly prominent in research on this alloy.

Figure 2 shows the weight changes for six alloys under various conditions, including ones that cause the highest corrosion rates; the gain in weight of an alloy of zircalloy type (1% Sn–0.5% Fe) under irradiation is three times that found in tests outside reactors, while an experimental alloy (0.7% Fe–0.7% Ni) showed catastrophic corrosion on account of rapid uptake of hydrogen consequent on the high nickel content. The best results were obtained with TsZhNo alloy (1% Nb–0.5% Fe–1% Sn), whose weight gain was minimal in all cases, whether in an autoclave outside a reactor or in boiling water emerging from the core and containing 12-17 mg/kg of oxygen, as well as on exposure to a fluence of $3.7 \cdot 10^{20}$ neutrons/cm^2 in boiling water with the same oxygen content.

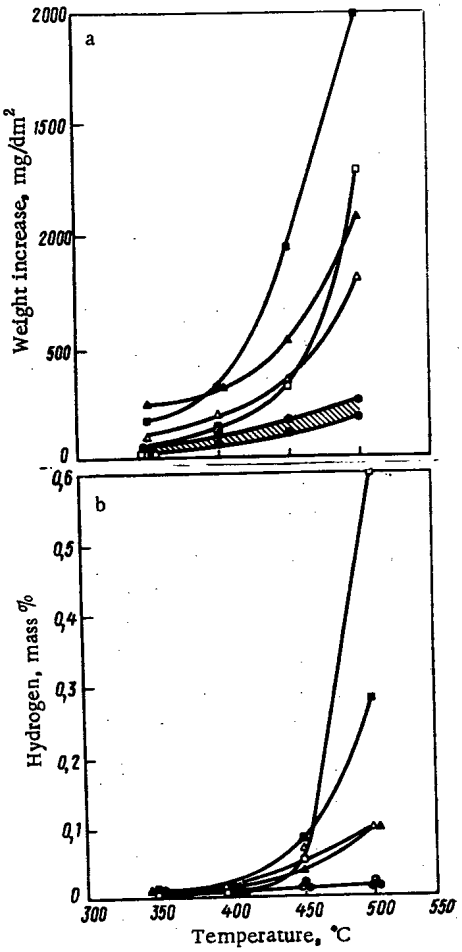

Fig. 4. Corrosion (a) and hydrogen absorption (b) during tests on zirconium alloys in a steam–water mixture at 350°C or in superheated steam at 400–500°C for 3000 h for the following alloys: ■) TsZhNO; □) Zr – 1% Sn – 0.5% Fe; ▲) N-2.5; △) N-1; ●) Zr–(Fe, Cr, W, Mo).

Oxygen Diffusion and Phase Composition for Oxide Films on Zirconium Alloys. Researches have been performed in the Soviet Union in recent years on the corrosion of zirconium alloys in order to provide alloys with good corrosion resistance in superheated steam.

Mössbauer techniques were used to determine the phase compositions of oxide films of alloys containing iron and tin when these elements enter the films during corrosion; this defines a relationship between the phase composition of the film and details of the corrosion in media containing oxygen [7]. The main result from the Mössbauer studies was that there are various phases in an oxide film, viz.: α-Fe, β-Sn, FeO, Fe_2O_3, Fe_3O_4, SnO, SnO_2, as well as solid solutions of various ions in ZrO_2 and ZrH_2, while the proportions of these phases vary during the corrosion. Therefore, the oxide film is substantially heterogeneous. The plastic metal phases (α-Fe, β-Sn) probably are advantageous to the protection provided by the film, whereas the oxide and hydride phases make the film brittle. The volume ratio between the metallic and nonmetallic phases is clearly one of the major factors governing the corrosion resistance.

The mode of oxygen transport in the oxide films was examined by treating the oxidized alloys with H_2O^{18} followed by evaluation of the oxygen concentration gradient by microanalysis [8]. The oxygen distribution (Fig. 3) shows that unalloyed iodide zirconium produces one type of diffusion mechanism, whereas N-1 alloy under the same conditions (500°C and about 100 kPa in steam) has another: In the first, the diffusion is along short paths (grain boundaries, cracks, etc.), whereas the diffusion occurs throughout the lattice (via vacancies) for N-1. However, the overall results from the two processes are fairly similar and the corrosion rates are roughly the same. Also, marked differences in corrosion resistance under these conditions were observed for most of the alloys of zirconium containing 1 at. % Al, Cu, Fe, Mo, or W, but the oxygen diffusion mechanism in the films was always the same: preferentially along short paths. This is a difference from alloys containing niobium and tin, where the vacancy mechanism predominates.

Therefore, the oxygen transport by the bulk-vacancy mechanism characteristic of zirconium alloys containing tin and niobium indicates that these alloys have comparatively little corrosion resistance in steam at 400–500°C; on the other hand, alloys containing iron, copper, tungsten and probably also chromium have good corrosion resistance in superheated steam.

Alloys for Reactors with Nuclear Steam Superheating. The Soviet Union has been a pioneer in reactors with nuclear steam superheating [9]. Replacement of steel tubes by zirconium ones not only increases the efficiency of the system considerably but also provides a reduction in the temperature of the superheated steam. A zirconium tube must be of bimetallic type: The side facing the superheated steam must be made of a corrosion-resistant alloy containing no tin or niobium, while the other side must be made of a strong and heat-resistant alloy containing tin, niobium, and other strengthening elements.

Figure 4 shows corrosion-resistance and hydrogenation curves for 350-500°C for the above alloys containing tin and niobium on the one hand and for alloys containing Cr, Fe, Cu, W, and Mo in various combinations on the other. The oxidation and hydrogen uptake are most pronounced for alloys containing tin, TsZhNO, and Zr–1.5% Sn–0.5% Fe. Somewhat lower weight gains due to corrosion occur for N-1 and N-2.5. The exceptionally large weight gain for TsZhNO is due to the simultaneous presence of tin and niobium. The largest hydrogen uptake occurs in Zr–1.5% Sn–0.5% Fe, whose composition is similar to that of zircalloy, and this is due to the lack of niobium. The hydrogenation of TsZhNO alloy, which contains 1% Nb, was less by a factor of 2.5, while even higher hydrogenation resistance occurred in the pure niobium alloys N-1 and N-2.5.

Alloys with several alloying elements show corrosion factors smaller by 5-10 times, and these are clearly promising for fuel-rod sheaths and tubes for reactors with nuclear steam superheating.

LITERATURE CITED

1. O. S. Ivanov (editor), Physical Chemistry of Zirconium Alloys [in Russian], Nauka, Moscow (1968); Structure and Properties of Alloys for Nuclear Power [in Russian], Nauka, Moscow (1973).
2. R. S. Ambartsumyan et al., "Mechanical parameters and corrosion resistance of zirconium alloys in water, steam, and gases at elevated temperatures," Proceedings of the Second Geneva Conference, 1958, USSR Paper No. 2044.
3. A. A. Kiselev et al., "A study of the corrosion of zirconium alloys in water and steam at high temperatures and pressures," Paper at the IAEA Conference on Corrosion of Reactor Materials, Salzburg (1962).
4. A. D. Amaev et al., "Principles for the choice of zirconium alloys for fuel-rod sheaths in routine-production VVÉR-440 power reactors," Proceedings of the Conference on Nuclear Power, Fuel Cycles, and Radiation Materials Science, Ul'yanovsk, 1970 [in Russian], Izd. SÉV, Moscow, No. 3 (1971), p. 503.
5. A. D. Amaev et al., "Corrosion of zirconium alloys in boiling water under irradiation," Proceedings of the Fourth Geneva Conference, 1971, USSR Paper No. 428.
6. A. D. Amaev, E. G. Ivanov, and G. P. Saenko, "Mechanical and corrosion parameters of zirconium alloys for fuel-rod sheaths and tubes in RBMK reactors." Paper at the British–Soviet Seminar on Reactor Channels and Fuel Rods [in Russian], Moscow (1977).
7. Yu. F. Babikov, A. A. Khaikovskii, et al., "Mössbauer studies of the effects of oxidation on the distribution of Fe-57 and tin-119 in zirconium alloys," in: Metallurgy and Metallography of Pure Metals [in Russian], No. 12, Atomizdat, Moscow (1976), p. 16.
8. V. N. Abramtsev and A. A. Khaikovskii, Diffusion of Oxygen in Oxide Films Formed on Zirconium and Zirconium Alloy Containing 1% Niobium [in Russian], Preprint VNIINM, Moscow (1973).
9. N. A. Dollezhal' et al., "Design of uranium–graphite channel reactors with tubular fuel rods and nuclear steam superheating," Proceedings of the Conference on Nuclear Power, Fuel Cycles, and Radiation Materials Science, Ul'yanovsk, 1970 [in Russian], Izd. SÉV, Moscow, No. 1 (1971), p. 368.

SWELLING OF STEELS AND ALLOYS IRRADIATED IN THE BOR-60 REACTOR TO A FLUENCE OF $1.1 \cdot 10^{23}$ NEUTRONS/CM^2*

N. P. Agapova, V. S. Ageev, I. N. Afrikanov, N. I. Budylkin, V. A. Krasnoselov, E. G. Mironova, V. D. Onufriev, Z. E. Ostrovskii, V. I. Prokhorov, and Yu. N. Sokurskii

UDC 621.039.53.531

A serious difficulty in the construction of fast power reactors is the radiation-induced swelling of the materials of the fuel-element jackets and the fuel-assembly (FA) sheaths. At a fluence of $(2-3) \cdot 10^{23}$ neutrons/cm^2, the expected swelling of the stainless steels and alloys now in use considerably exceeds 10%, which is clearly unacceptable for the fast reactors now being designed and makes it necessary to find ways of reducing the swelling of jacket and sheath materials to reasonable limits.

Because the chemical composition and the prior thermomechanical working is a major factor in the radiation-induced swelling of stainless steels and alloys, this swelling must be evaluated for each variant of chemical composition and working.

Materials and Methods of the Experiment

The investigation was conducted on specimens of 0Kh16N15M3B austenitic stainless steel, after various types of working, on the nickel alloys 0Kh17N40B, 0Kh20N60B, and KhN77TYu, on specimens of some alloys of Kh16N15 steel, and also on specimens of nickel and iron with purity values of 99.99% and 99.98%, respectively (Table 1).

In order to determine the swelling by hydrostatic weighing, we used cylinders 6 mm in diameter and 30 mm in height. Specimens of melts of Kh16N15 steel and 0Kh17N40B alloy were subjected to heat treatment in a vacuum at 1050°C for 0.5 h, specimens of KhN77TYu alloy at 1050°C for 0.5 h and at 720°C for 2 h, and specimens of iron and nickel at 850°C for 0.5 h. Some specimens were deformed by tension by values of 5, 10, and 20% (0Kh16N15M3B steel) or 10% (iron, nickel). A number of specimens of 0Kh16N15M3B steel, after austenizing annealing, were subjected to various types of working: a) aging at 650°C for 100 h; b) mechanical-thermal working (MTW) and cold deformation (CD) by 10%, with subsequent annealing at 800°C for 3 h; c) thermomechanical working (TMW), which was deformed by 10% at 650°C with subsequent annealing at 650°C for 100 h; d) cold deformation by 80% with subsequent annealing at 800°C for 1 h in order to produce a fine grain (3-5 μ). At least three specimens of each material were irradiated.

The specimens for investigation by the method of electron microscopy were cut from the appropriate cylinders and were reduced to a thickness of 0.1-0.2 mm by mechanical grinding and electrolytic polishing. From these blanks we cut out disks with a diameter of 3 mm, which were sealed into special vacuum cassettes before irradiation.

The irradiation was carried out in materials-study ampuls in the BOR-60. The specimens for hydrostatic weighing were irradiated to a fluence of $1.1 \cdot 10^{23}$ neutrons/cm^2 at a calculated temperature of 450 to 550°C, and the cassettes with the specimens for electron microscopy were irradiated to a fluence of $7.5 \cdot 10^{22}$ neutrons/cm^2 ($E > 0$) at a calculated temperature of ~520°C.

After irradiation, the specimens for electron microscopy were electrolytically thinned and investigated on the EM-300 electron microscope. The hydrostatic weighing was carried out on a remote-controlled balance in CCl_4 with an accuracy of 0.2% or better.

*Journal version of a report delivered at the Conference on the Study of Reactor Materials (Alushta, 1978).

Translated from Atomnaya Énergiya, Vol. 45, No. 6, pp. 433-439, December, 1978.

0038-531X/78/4506-1169$07.50

TABLE 1. Chemical Composition of Steels and Alloys, % by Weight

Material	C	Mn	Si	Cr	Ni	Nb	Mo	Ti	Al	Fe
0Kh16N15M3B	0,042	0,72	0,40	16,05	15,20	0,45	3,00	—	—	Remainder
0Kh16N15	0,052	0,45	0,25	14,90	15,96	—	—	—	—	Same
0Kh16N15M3	0,055	0,43	0,25	15,34	15,56	—	2,91	—	—	»
00Kh16N15M3	0,005	0,52	0,32	15,75	15,34	—	2,91	—	—	»
0Kh17N40B	0,030	1,59	0,05	16,70	41,05	0,64	—	—	—	39,8
0Kh20N60B	0,020	1,85	0,11	20,30	57,94	0,57	—	—	—	19,1
KhN77TYu	0,050	0,25	0,37	20,83	74,60	—	—	2,73	0,78	0,39

TABLE 2. Swelling of Materials According to the Hydrostatic Weighing Data

Material	Treatment	Irradiation parameters			Change in density, %
		F, neutrons/cm² (E > 0)	F, 10^{22} neutrons/cm² (E > 0.1 MeV)	T_{calc}, °C	
0Kh16N15M3B steel	Austenization (A) at 1050°C, 30 min	$1,1 \cdot 10^{23}$	9,0	550	13,7
	A+10% CD	$1,1 \cdot 10^{23}$	9,0	550	0,4—7,0
	A+20% CD	$1,1 \cdot 10^{23}$	9,0	550	0
	MTW (A+10% CD +800 °C, 3 h)	$1,12 \cdot 10^{23}$	9,2	550	7,4—13,5
	A+650 °C, 100 h	$1,12 \cdot 10^{23}$	9,2	550	12,3
	TMW (A+10% CD at 650 °C+ +650 °C, 100 h)	$1,12 \cdot 10^{23}$	9,2	550	3,8
		$1,1 \cdot 10^{23}$	9,2	550	3,3
Nickel	Anneal. 850 °C, 1h	$9,7 \cdot 10^{22}$	8,5	450	4,0
	Anneal. 850 °C, 1h +10% CD	$8,7 \cdot 10^{22}$	7,5	450	3,8
Iron	Anneal. 850 °C, 1h	$8,7 \cdot 10^{22}$	7,5	460	1,5
	Anneal. 850 °C, 1h +10% CD	$8,7 \cdot 10^{22}$	7,5	460	1,0

TABLE 3. Parameters of the Radiation Porosity in Irradiated Materials

Material	Treatment	$\Delta V/V$, %	$\bar{d}$, Å	$\bar{\rho}$, 10^{14} cm^{-3}
0Kh16N15M3B steel	A at 1050 °C 30 min	1,8	265	16,5
	A+5% CD	0,2	160	5,4
	A+10% CD	0,2	100	29,4
	A+20% CD	0,1	75	34,0
	MTW (A+10% CD +800 °C, 3h)	1,5	350	4,0
	TMW (A+10% CD at 650 °C+ +650 °C, 100 h)	1,5	230	14,0
	A+80% CD + +800 °C 30 min	5,4	365	17,0
0Kh16N15	A at 1050 °C, 30 min	2,1	340	6,6
0Kh16N15M3	Same	2,0	320	6,6
00Kh16N15M3	»	1,3	250	4,6
0Kh17N40B	»	1,3	385	17,0
0Kh20N60B	»	1,6	425	4,0
KhN77TYu	A at 1050 °C, 30 min+720 °C, 2 h	0,01	75	5,5

Experimental Results and Their Evaluation

Hydrostatic Weighing. The results of the density measurements on the materials (Table 2) show that the maximum swelling of the 0Kh16N15M3B austenized steel at a fluence of $1.1 \cdot 10^{23}$ neutrons/cm² (E > 0) and a temperature of ~550°C was 13.7%; at 10% CD the swelling was reduced to 0.4-7.0% (dispersion of the results for four specimens), and at 20% CD it was practically absent. MTW and prior aging at a temperature of 650°C had little effect on the swelling of the steel, while TMW reduced the swelling considerably (see Table 2).

The swelling of the nickel after irradiation to a fluence of $1.1 \cdot 10^{23}$ neutrons/cm² (E > 0) at a calculated temperature of ~450° and 550°C did not exceed 4%, and the swelling at ~460°C and a fluence of $8.7 \cdot 10^{22}$ neutrons/cm² was only 1.5%. A 10% cold deformation reduced the swelling of the nickel and iron to some extent, but its effect was considerably less than the effect on 0Kh16N15M3B steel.

Electron Microscopy. Table 3 shows the values of the average concentration ρ, the pore dimension d, and the swelling $\Delta V/V$, determined by the electron-microscopy method for materials irradiated to a fluence of $7.5 \cdot 10^{22}$ neutrons/cm² (E > 0) or $5.9 \cdot 10^{22}$ neutrons/cm² (E > 0.1 MeV) at a calculated temperature of ~520°C.

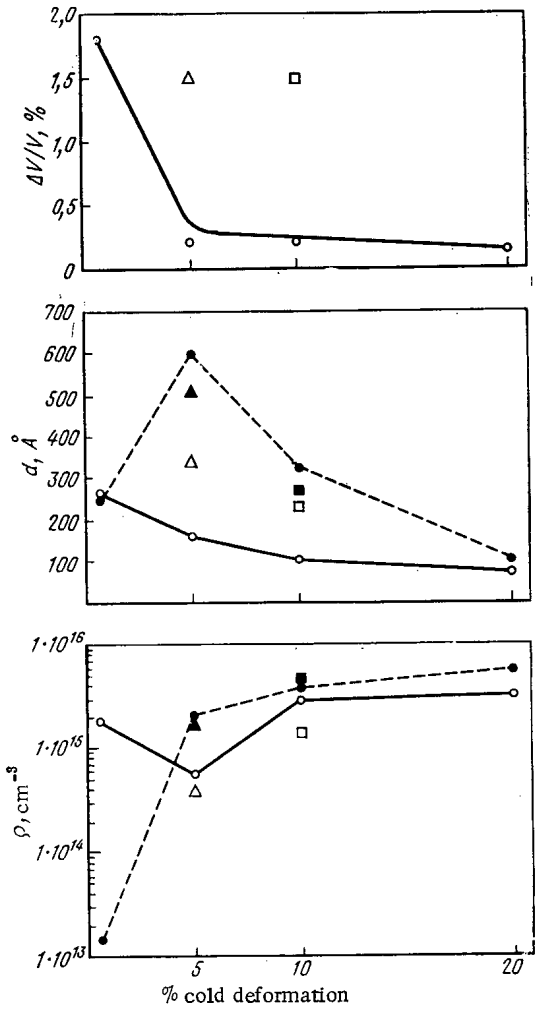

Fig. 1

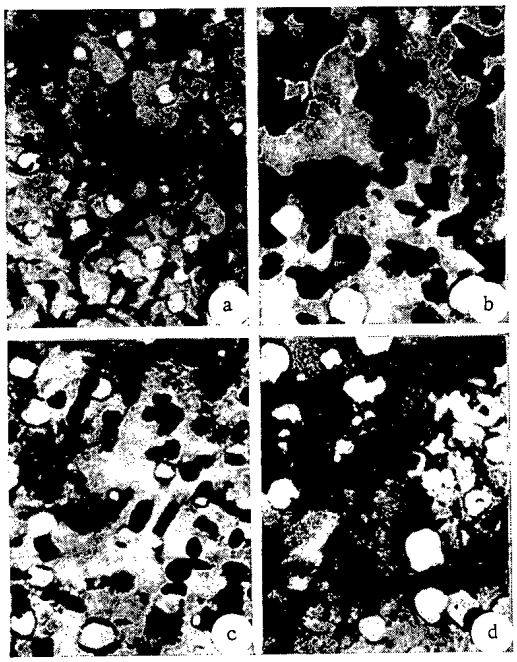

Fig. 2

Fig. 1. Swelling, pore dimension and pore concentration (○, △, □), and of lamellar precipitations (●, ▲, ■) as functions of the equivalent cold deformation at A+20% CD (○, ●), MTW (△, ▲), and TMW (□, ■).

Fig. 2. Structure of 0Kh16N15M3B steel subjected to various kinds of treatment and irradiated to a fluence of $7.5 \cdot 10^{22}$ neutrons/cm^2 at 520°C (× 130,000): a) austenization; b) MTW; c) TMW; d) fine grain.

0Kh16N15M3B Steel in Various Structural States. The results of the electron-microscopic investigation of the irradiated 0Kh16N15M3B steel in various structural states are shown in Fig. 1. In plotting the experimental points, we took account of the fact that the original density of the dislocations in these specimens corresponded to the density of dislocations in specimens with 5 and 10% cold deformation.

In the irradiated austenized steel we observed pores, prismatic dislocation loops measuring 200-700 Å, dispersed precipitations (to 100 Å) of Nb (C, N) and lamellar precipitations (Fig. 2a). The swelling amounted to 1.8%. The pores were essentially unrelated to the precipitations.

In steel with 5% deformation, the pore dimension and concentration and the swelling were reduced (see Fig. 1 and Table 3). In addition to the pores, we observed prismatic dislocation loops measuring ~500 Å, individual dislocations, and large lamellar precipitations, whose dimension and concentration increased in comparison with the austenized steel (Fig. 3a). The pores are essentially connected with the lamellar precipitations.

The lamellar precipitations in the irradiated specimens of 0Kh16N15M3B steel deformed by 5 and 10%, as well as in the specimens subjected to MTW and TMW, were investigated by the microfraction method. The results obtained give reason to assume that the lamellar precipitations are Laves phases of Fe_2 (Mo, Nb) with a basis plane parallel to the plane of the plates. In 10% deformed steel the dimensions of the pores and the

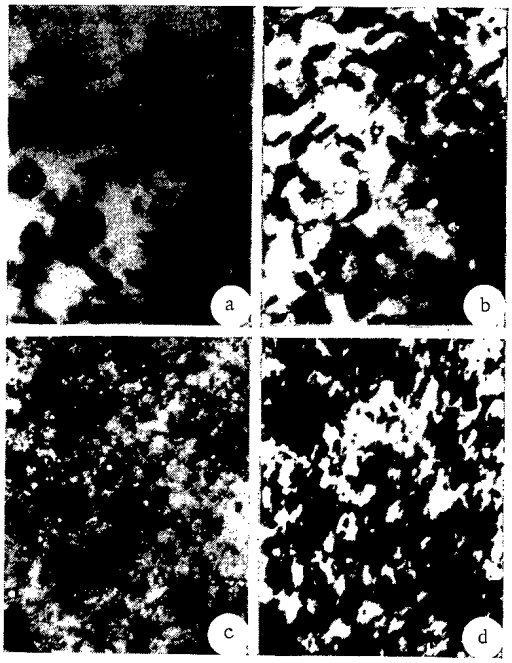

Fig. 3

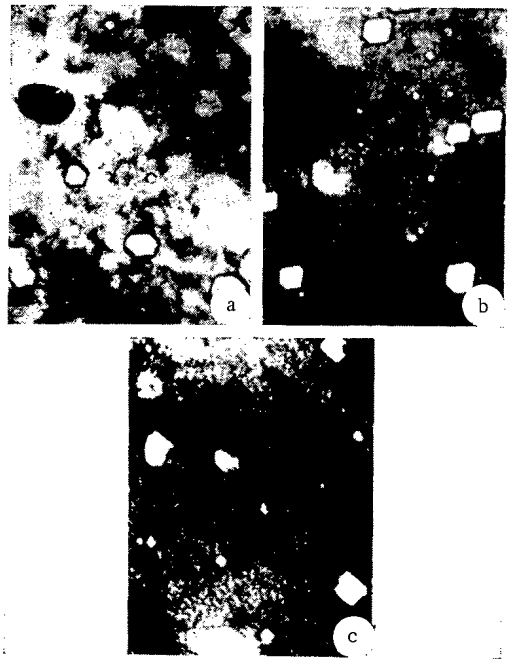

Fig. 4

Fig. 3. Effect of prior cold deformation on structure of 0Kh16N15M3B steel after irradiation to a fluence of $7.5 \cdot 10^{22}$ neutrons/cm^2 at ~520°C: a, b, c) 5, 10, and 20% CD. respectively: d) 20% CD, same segment, but with more clearly marked dislocations (× 130,000).

Fig. 4. Structure of Kh16N15 type steel with various kinds of alloying after irradiation to a fluence of $7.5 \cdot 10^{22}$ neutrons/cm^2 at ~520°C: a) 0Kh16N15; b) 0Kh16N15M3; c) 00Kh16N15M3 (× 130,000).

connected lamellar deformations (presumably Laves phases) were reduced, while the concentration increased (see Fig. 1 and Fig. 3b). It was impossible to estimate the dislocation structure in this case, apparently because of the high specific volume of the lamellar precipitations.

In 20% deformed steel we observed a further reduction of the dimensions of the lamellar precipitations and the connected pores and an increase in their concentration (see Fig. 1 and Fig. 3c). We observed a high density of linear dislocations and loops measuring up to 300 Å (see Fig. 3d).

Before irradiation, in the specimens subjected to MTW we observed small-angle boundaries and dislocation lattices decorated with dispersed precipitations (30-100 Å) of Nb (C, N) whose concentration was $2.5 \cdot 10^{15}$ cm^{-3}. After irradiation we observed large lamellar precipitations and large pores connected with them (see Fig. 2b). Along the grain boundaries, as in the unirradiated specimens, we observed $M_{23}C_6$ carbides measuring ~0.3 μ.

In the specimens which had been thermomechanically worked, before the irradiation we observed in the grain bodies dislocation lattices decorated with dispersed precipitations (up to 100 Å) of Nb (C, N), and along the grain boundaries $M_{23}C_6$ carbides measuring ~0.3 μ. After irradiation, we also observed $M_{23}C_6$ carbides along the grain boundaries, while in the grain bodies we observed lamellar precipitations and pores connected with them (see Fig. 2c), the concentration of which was larger than in the irradiated specimens subjected to MTW (Fig. 2b). The swelling of the irradiated specimens after MTW and TMW was the same, and in both cases we were unable to detect any precipitations of NB (C, N) or any dislocation lattice.

In fine-grained (3-5 μ) 0Kh16N15M3B steel we observed pores whose dimension was considerably larger than in the irradiated specimens with ordinary-sized grains (30-50 μ) and many precipitations of excess phases, which, for the most part, were there before the irradiation as well (see Fig. 2d). In Fig. 2d we can see a pore-deficient zone ~0.1 μ in width along the grain boundaries.

Steels with a Kh16N15 Base and Various Kinds of Alloying. After irradiation, 0Kh16N15 and 0Kh16N15M3 steels revealed large precipitations (0.2-0.5 μ) of $M_{23}C_6$ carbides along the grain boundaries. In the grain bodies in 0Kh16N15 steel there were individual precipitations of $M_{23}C_6$ carbides measuring up to 500 Å and

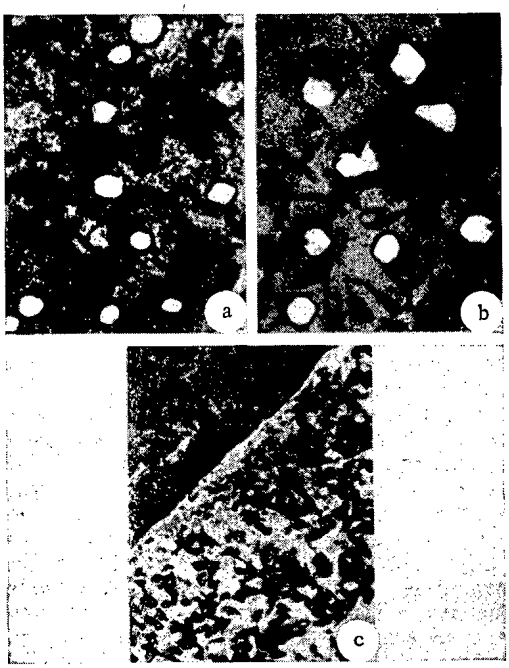

Fig. 5. Structure of high-nickel alloys irradiated to a fluence of $7.5 \cdot 10^{22}$ neutrons/cm^2 at ~520°C: a) 0Kh17N40B; b) 0Kh20N60B; c) KhN77TYu (× 130,000).

pores (Fig. 4a) whose concentration was considerably higher than that of the precipitations; in contrast, the 0Kh16N15M3 steel reveals only two systems of pores: large pores (450 ± 50 Å) and small pores (100 ± 20 Å) Fig. 4b).

In irradiated steel with reduced carbon content we observed a large number ($4.5 \cdot 10^{14}$ cm^{-3}) of large (~20,000 Å) lamellar precipitations (presumably Laves phases), to which were connected a number of large pores (450 ± 50 Å), while the small pores (100 ± 20 Å) were distributed homogeneously throughout the body of the grains (Fig. 4c).

High-Nickel Alloys. In the 0Kh17N40B alloy, the irradiation caused the formation in the body of the grains of some comparatively large pores (see Table 3), dispersed particles (50-100 Å) of Nb (C, N), and large (~900 Å) lamellar precipitations, and along the grain boundaries there was an elongated form of $M_{23}C_6$ carbide measuring ~1 μ (Fig. 5a). In addition to the precipitations and the pores, we observed prismatic dislocation loops whose dimension and concentration were 270 Å and $1.8 \cdot 10^{15}$ cm^{-3}, respectively. We did not identify the lamellar precipitations in the irradiated 0Kh17N40B alloy and the 0Kh20N60B alloy.

The phase composition of the irradiated 0Kh20N60B alloy is the same as in the 0Kh17N40B alloy, but the concentration of the lamellar precipitations is considerably higher ($5 \cdot 10^{14}$ cm^{-3}), while the dimension is somewhat smaller (~560 Å) (Fig. 5b). The pores, whose average dimension and concentration were 425 Å and $4.0 \cdot 10^{14}$ cm^{-3}, respectively, are essentially connected with the lamellar precipitations. The concentration and dimension of the dislocation loops are equal to $8.3 \cdot 10^{14}$ cm^{-3} and 350 Å, respectively.

After irradiation, in the dispersion-hardened KhN77TYu alloy, along the grain boundaries, we observed solid walls of $M_{23}C_6$ carbides, pores with small dimension and low concentration, and a large number of dislocation loops with $\rho = 6.4 \cdot 10^{15}$ cm^{-3}, $\alpha = 180$ Å (Fig. 5c).

We were unable to detect the presence of pre-precipitations of a γ' phase; probably, owing to the high concentration of loops, to judge by the electronograms, there were no γ'-phase precipitations.

Evaluation

An analysis of the results of the hydrostatic weighing of cylindrical specimens of 0Kh16N15M3B steel in the austenized, cold-deformed state and after MTW and TMW showed that under irradiation to a fluence of $1.1 \cdot 10^{23}$ neutrons/cm^2 ($E > 0$) at a temperature of ~550°C the swelling is reduced proportionately to the degree of cold deformation, i.e., the dislocation density in the specimens before irradiation. MTW led to the appearance of dislocations decorated with Nb (C, N) particles in the specimens, with a dislocation density equivalent to 5% cold deformation, but it did not bring any substantial reduction in swelling. After TMW the density

of dislocations decorated with NB (C, N) particles was equivalent to 10% cold deformation, and here we observed a substantial positive effect: The swelling was reduced by a factor of about 3.5 in comparison with steel in the austenized state.

Electron-microscopic investigation of the specimens irradiated to a fluence of $7.5 \cdot 10^{22}$ neutrons/cm^2 ($E > 0$) at a temperature of ~520°C showed that under the indicated conditions even 5 and 10% cold deformation is sufficient to reduce the swelling by a factor of about 10. However, account must be taken of the fact that such cold deformation does not yield a uniform distribution of the density of dislocations over the grains of the specimen, a fact confirmed by the dispersion in the swelling values for the cylindrical specimens with 10% cold deformation (see Table 2). The results of the electron-microscopic investigation relate to deformed grains. Since the total density of dislocations in the irradiated specimens increases with increased degree of prior deformation, the reduction in swelling of the deformed specimens may be connected with the increase in the migration of point defects to the dislocations.

In austenized 0Kh16N15M3B steel, pores are generated and grow under irradiation without any visible connection with precipitations of excess phases, whereas in cold-deformed steel and after MTW and TMW we observed a connection between the pores and the lamellar precipitations (presumably Laves phases). The nature of the variation of the dimension and concentration of pores coincides with the nature of the variation in the dimension and concentration of lamellar precipitations, i.e., the refinement of lamellar precipitations that is observed in the deformed specimens corresponded to the refinement of the pores connected with them and the reduction in swelling.

In the specimens subjected to MTW and TMW, before irradiation there were Nb (C, N) precipitations connecting the dislocations, thus preventing the migration of point defects. Earlier [1] it was shown that such precipitations serve as centers for the generation of lamellar precipitations. Therefore, after MTW and TMW we should expect the generation of vacancy pores and lamellar precipitations and their growth during the irradiation process to be more rapid than in deformed specimens. We did in fact find that after irradiation to a fluence of $7.5 \cdot 10^{22}$ neutrons/cm^2 ($E > 0$) the swelling in 0Kh16N15M3B steel in the austenized state and after MTW and TMW was about the same (see Table 3), and after irradiation to a fluence of $1.1 \cdot 10^{23}$ neutrons/cm^2 ($E > 0$) the specimens were found after TMW to swell much less than the austenized specimens (see Table 2), as a result of the high initial density of dislocations.

The swelling of 0Kh16N15M3B steel with fine (3-5 μ) grains is almost 3 times as high as the swelling in steel with ordinary (30-50 μ) grains. The dimension of the depleted zones (see Fig. 2d) was ~0.1 μ, i.e., not commensurable with the dimension of the grain. At such dimensions (3-5 μ), apparently, the conditions for the annihilation of vacancies and displaced atoms are violated. It may be assumed that the displaced atoms, possessing high mobility, move out to the grain boundaries and create a supersaturation with respect to vacancies, thereby increasing the swelling.

We should also take account of the depletion of the solid solution in alloying elements and interstitial impurities as a result of the precipitation of a large number of excess phases after treatment on the fine grains, which can also increase the swelling [2].

In the 0Kh16N15 and 0Kh16N15M3 steels we observed relatively few precipitations in the body of the grains, and the pores were not connected with them. This again confirmed the viewpoint that in unstabilized steels the generation of lamellar precipitations is difficult [3]. The concentration of pores in these is less by a factor of about 3, and their dimension is larger, than in the 0Kh16N15M3B steel. The reduction in the carbon content of the 00Kh16M15M3 steel led to the appearance of large lamellar precipitations (presumably Laves phases) and the generation and growth of pores on them. The large pores are connected with the lamellar particles, while the system of small pores is generated homogeneously.

An analysis of the effect of the chemical composition of steels of the KhN16N15 type showed that slower or faster precipitation of lamellar phases does not always determine the nature of the generation and growth of vacancy pores and the amount of swelling. However, since a change in the chemical composition of the steels may shift the maximum-swelling temperature, it is impossible to draw any firm conclusions about the effect of the lamellar precipitations on the swelling of steels.

The model metals – nickel, and especially iron – swelled much less than steels of the 16-15 type under irradiation to a fluence of $1.1 \cdot 10^{23}$ neutrons/cm^2 ($E > 0$). There are practically no published data concerning the swelling of these metals under neutron irradiation to high fluences. After irradiation with 5-MeV nickel ions in an accelerator at 625°C with a dose of 140 displacements per atom, the swelling of nickel was 12%, and the swelling of 316 steel was ~30% [4]. If we compare these data with those obtained in our investigations, we

are led to suppose that nickel and α iron, as well as alloys in which these metals predominate, have less of a tendency to swell than austenitic steels of the 16-15 type. Unlike the case of steels, cold deformation did not have a marked effect on the swelling of nickel and α iron, possibly because of the more rapid annealing of the dislocations under irradiation.

The swelling of alloys with 40 and 60% nickel (0Kh17N40B and 0Kh20N60B) after irradiation to a fluence of $7.5 \cdot 10^{22}$ neutrons/cm^2 ($E > 0$) at 520°C is about the same (1.3% and 1.6%), despite the fact that in the 0Kh20N60B alloy the concentration of lamellar precipitations is 10 times as high and there is a heterogeneous generation of pores. The addition of titanium and aluminum to the KhN77TYu alloy led to the appearance of γ'-phase pre-precipitations after heat treatment. The dimension of the pores in this alloy after irradiation was less by a factor of 5-6, and the swelling was less by a factor of 100, then in alloys with 40% and 60% nickel. Comparing these results with the data for austenitic steels, which swell slightly more than alloys with 40 and 60% nickel, we can assume that for such alloys one of the most important factors determining the tendency to swelling is the phase composition, especially the presence of γ'-phase pre-precipitations.

The favorable effect of finely dispersed particles of γ'-phase on the swelling of alloys of the PE-16 type has been noted in the past [5, 6]. However, some data [7, 8] indicate that the separation of a γ'-phase either during the irradiation or after aging leads to an increase in the swelling because of the depletion of titanium and aluminum atoms in the solid solution.

CONCLUSIONS

The structure created by preliminary treatment has a strong influence on the swelling, the nature of pore generation, the dislocation density, and the phase composition of 0Kh16N15M3B steel. The greatest reduction in swelling was produced by 20% cold deformation, which at a high dislocation density led to a sharp refinement of the pores and lamellar precipitations.

The lamellar phases precipitated in steels of the Kh16N15 type during the irradiation after special alloying or preliminary treatment do not always determine the nature of the generation and growth of vacancy pores.

At a temperature of 460 and 550°C the swelling of nickel is less by a factor of about 3, and the swelling of α iron is less by a factor of about 10, than the swelling of austenized 0Kh16N15M3B steel.

The least swelling was found in the Kh77TYu alloy (with 77% nickel), which before irradiation contained γ'-phase pre-precipitations, whereas the swelling of alloys with 40 and 60% nickel is 100 times as great. From this it is clear that the nickel content is not the only factor determining the swelling.

LITERATURE CITED

1. N. P. Agapova et al., Izv. Akad. Nauk SSSR, Ser. Fiz., 38, No. 11, 2351 (1974).
2. J. Leitnaker, E. Blom, and J. Stiegler, J. Nucl. Mater, 49, 57 (1973/74).
3. B. Wiess and R. Stickler, Metall. Trans., 3, 851 (1972).
4. W. Johnston et al., J. Nucl. Mater, 54, 24 (1974).
5. R. Bullough and R. Perrin, in: Proc. Reading Conf. on Void Formed by Irradiation of Reactor Materials, Harwell, BNES, (1971), p. 79.
6. J. Buswell et al., in: Proc. Intern. Conf. "Physical Metallurgy of Reactor Fuel Elements," E. Sykes (editor), London (1975), p. 170.
7. J. Gittus, J. Watkin, and I. Standring, in: Progr. with Abstracts of Intern. Conf. "Radiation Effects in Breeder Reactor Structural Materials," Scottsdale (1974), p. 22.
8. W. Johnston and J. Bates, ibid., p. 35.

MEASUREMENT OF THE $^{237}Np/^{239}Pu$ AND $^{241}Am/^{239}Pu$ FISSION CROSS SECTION RATIOS FOR 0.13-7.0 MeV NEUTRONS

V. M. Kupriyanov, B. I. Fursov,
V. I. Ivanov, and G. N. Smirenkin

UDC 539.173.84

The method of measuring fission cross section ratios is described in detail in [1-3]. The measurements were performed at electrostatic accelerators. Neutrons from the $^{7}Li(p, n)^{7}Be$, $T(p, n)^{3}He$, and $D(d, n)^{3}He$ reactions bombarded solid targets consisting of layers of ^{239}Pu, ^{237}Np, and ^{241}Am oxides of practically 100% isotopic purity 0.2-0.4 mg/cm^2 thick deposited on thin aluminum or platinum backings.

The energy dependence of the fission cross section ratios was studied in detail by the ionization method, and the components of the neutron background were measured as described in [2, 3]. Then, using the glass detector method [3], which permits an accurate determination of the ratios of the efficiencies of counting fission fragments, the absolute values of the fission cross section ratios were measured for $E_n = 2.0$, 2.5, and 3.0 MeV. The final results were obtained by normalizing the data on the energy dependence to the absolute values.

The $^{237}Np/^{239}Pu$ and $^{241}Am/^{239}Pu$ fission cross section ratios were measured simultaneously by using two back-to-back fission chambers [2]. The ratios of the numbers of fissionable nuclei were determined by comparing the alpha activities of the layers. The use of ^{239}Pu instead of ^{235}U, whose cross section is the standard, was dictated by the shortcomings of ^{235}U as an alpha emitter: The low specific activity, particularly in comparison with ^{241}Am, the complex α-particle spectrum, and the considerable partial activity of the admixture of ^{234}U, whose content in highly enriched ^{235}U is difficult to determine with acceptable accuracy. At the same time the $^{237}Np/^{239}Pu$ and $^{241}Am/^{239}Pu$ fission cross section ratios can be converted to $^{237}Np/^{235}U$ and $^{241}Am/^{235}U$ fission cross section ratios without appreciable loss of accuracy by multiplying by the $^{239}Pu/^{235}U$ fission cross section ratio measured by the authors with an error of ~1.5% [3] by using the same procedure.

The α activities of the fissionable layers were compared in good geometry by using a semiconductor detector. The measurements performed at the beginning and end of the whole cycle of experiments agreed within the limits of error, and were averaged. The total error in determining the number of fissionable nuclei was 0.9% for $^{237}Np/^{239}Pu$ and 1.3% for $^{241}Am/^{239}Pu$, taking account of the uncertainties of the half-lives $(2.41 \pm 0.01) \cdot 10^4$ yr for ^{239}Pu [4], $(2.14 \pm 0.1) \cdot 10^6$ yr for ^{237}Np [5], and 432 ± 4 yr for ^{241}Am [4].

The ratio of efficiencies of counting fragments was easily found by using glasses, since the geometric factors were kept very closely the same, and the small correction to take account of the dependence of the efficiency on the angular anisotropy of fission was calculated by using the values of the anisotropy measured in the same experiment.

Since the ionization detector was used only to study the energy dependence of the fission cross section rations, it was not necessary to determine the efficiencies of the fission chambers. The dependence of the efficiency ratio on neutron energy was taken into account by a small correction ($\leq 2.3\%$) calculated by allowing for the momentum introduced by a neutron, and the angular distributions of the fragments.

The correction to take account of neutron scattering by the target structure was greatest near the fission threshold, and at $E_n = 0.13$ MeV it reached 12.0 and 4.2% for $\sigma_f^{237}Np/\sigma_f^{239}Pu$ and $\sigma_f^{241}Am/\sigma_f^{239}Pu$, respectively. In the 1.5-7.0-MeV range this value varied from 2.2 to 0.2%.

The background of accompanying (d, n) reactions reached 30% at $E_n = 7.0$ MeV. The correction to the fission cross section ratios resulting from this background was 0.2-8.1% for $E_n = 3.6$-7.0 MeV. The analogous correction for (p, n) reactions did not exceed 1.2% for $E_n \leq 3$ MeV. The correction for the background in the laboratory did not exceed 0.3-0.4% over the whole energy range studied.

In measuring absolute values, the glass detectors were irradiated alternately from both sides to average the neutron flux and eliminate the necessity of introducing a correction for the elastic scattering of neu-

Translated from Atomnaya Énergiya, Vol. 45, No. 6, pp. 440-442, December, 1978. Original article submitted April 17, 1978.

0038-531X/78/4506-1176$07.50

TABLE 1. $^{237}Np/^{239}Pu$ and $^{241}Am/^{239}Pu$ Fission Cross Section Ratios Measured by Glass Method

E_n, MeV	ΔE_n, keV	σ_f^7/σ_f^9	$\Delta(\sigma_f^7/\sigma_f^9)$, %	σ_f^{41}/σ_f^9	$\Delta(\sigma_f^{41}/\sigma_f^9)$, %
2,0	60	0,832	1,4	0,935	2,0
2,5	72	0,860	1,5	0,970	2,0
3,0	78	0,873	1,5	0,997	2,1

TABLE 2. Corrections and Experimental Errors of Measurements of $^{237}Np/^{239}Pu$ and $^{241}Am/^{239}Pu$ Fission Cross Section Ratios (Glass Method, $E_n = 3$ MeV), %

Sources of corrections and errors	$^{237}Np/^{239}Pu$		$^{241}Am/^{239}Pu$	
	correction	error	correction	error
Ratio of Nos. of fissionable nuclei	—	0,9	—	1,3
Scanning of glass detectors	—	0,5	—	0,5
Statistical error	—	0,9	—	1,4
Angular anisotropy of fission	0,5	0,3	0,8	0,3
Fission of minority isotopes	0,2	0,1	0,2	0,1
Difference of neutron fluxes through layer	—	0,2	—	0,2
Inelastic scattering of neutrons	—	0,4	—	0,4
Neutron background in laboratory	$\leqslant 0,2$	0,2	$\leqslant 0,2$	0,2
Bkgd. of neutrons scattered from target structure	0,6	0,3	1,4	0,3
Bkgd. of neutrons from accompanying (p, n) reactions	0,8	0,2	1,2	0,3
Total error	—	1,5	—	2,1

trons by the backings. No correction was introduced for the inelastic scattering of neutrons, but an upper estimate of its possible effect (0.3-0.4%) was included in the value of the experimental error.

The absolute values of the $^{237}Np/^{239}Pu$ and $^{241}Am/^{239}Pu$ fission cross section ratios measured by the glass method are listed in Table 1. The value listed for the total experimental error is the rms sum of the uncertainties. Table 2 shows the structure of the characteristic corrections and errors for $E_n = 3$ MeV. The results of the ionization chamber measurements are shown in Table 3 for the whole range of energies studied. The total error listed in Table 3 is the rms sum of the uncertainty of the energy dependence data obtained by the ionization method (statistical error and the errors related to the experimental and calculational corrections), the average error of the absolute values of the ratios of $\sigma_f^{237}Np/\sigma_f^{239}Pu$ (1.5%), $\sigma_f^{241}Am/\sigma_f^{239}Pu$ (2%), and the uncertainty in the normalization of the energy dependence data to the absolute values (0.25%).

For $E_n \geq 6$ MeV the increase in the total error results from the increase in the background of accompanying (d, n) reactions, and for $E_n \leq 1$ MeV from the decrease in statistical accuracy and the increase in the error related to the correction for the background of neutrons scattered by the target structure.

To compare our data with the results of other experiments, the $\sigma_f^{237}Np/\sigma_f^{239}Pu$ and $\sigma_f^{241}Am/\sigma_f^{239}Pu$ ratios were converted to $\sigma_f^{237}Np/\sigma_f^{235}U$ and $\sigma_f^{241}Am/\sigma_f^{235}U$ ratios by multiplying by the $^{239}Pu/^{235}U$ fission cross section ratio [3]. This procedure increases the total error of the results by 0.3-0.5%.

There is good agreement with the data of [6, 7] for the $^{237}Np/^{235}U$ fission cross section ratio. For E_n = 1.5-6 MeV there is a systematic deviation from the preliminary data of [8], but below 1.5 MeV the two results are in general agreement when possible small differences in the calibration of the energy scale are taken into account. For $E_n > 6$ MeV the energy dependences of the results are different.

TABLE 3. $^{237}Np/^{239}Pu$ and $^{241}Am/^{239}Pu$ Fission Cross Section Ratios

E_n, MeV	ΔE_n, keV	σ_f^7/σ_f^9	$\Delta(\sigma_f^7/\sigma_f^9)$, %	σ_f^{41}/σ_f^9	$\Delta(\sigma_f^{41}/\sigma_f^9)$, %	E_n, MeV	ΔE_n, keV	σ_f^7/σ_f^9	$\Delta(\sigma_f^7/\sigma_f^9)$, %	σ_f^{41}/σ_f^9	$\Delta(\sigma_f^{41}/\sigma_f^9)$, %
0,130	21	0,015	4,8	0,012	4,3	1,90	64	0,830	1,7	0,936	2,3
0,180	20	0,022	4,3	0,016	4,4	2,00	66	0,836	1,8	0,937	2,2
0,230	19	0,025	4,1	0,019	4,2	2,10	68	0,841	1,7	0,948	2,3
0,280	18	0,034	4,0	0,024	4,5	2,20	69	0,841	1,8	0,946	2,2
0,350	38	0,068	3,5	0,030	3,6	2,30	70	0,844	1,8	0,956	2,2
0,400	37	0,107	2,9	0,037	3,2	2,40	71	0,854	1,8	0,960	2,2
0,450	36	0,174	2,7	0,050	3,3	2,50	73	0,862	1,7	0,970	2,2
0,500	34	0,265	2,6	0,064	3,1	2,60	75	0,861	1,7	0,971	2,3
0,550	33	0,356	2,4	0,091	3,3	2,70	77	0,863	1,7	0,977	2,2
0,600	32	0,441	2,3	0,112	3,3	2,80	78	0,868	1,7	0,984	2,2
0,650	32	0,539	2,6	0,171	3,2	2,90	80	0,868	1,7	0,984	2,2
0,700	32	0,613	2,3	0,232	3,3	3,00	82	0,866	1,7	0,994	2,2
0,750	32	0,650	2,3	0,314	3,4	3,60	190	0,858	1,8	1,027	2,4
0,800	31	0,686	2,3	0,388	3,2	3,80	180	0,864	1,8	1,027	2,4
0,850	31	0,731	2,1	0,494	3,1	4,00	145	0,859	1,8	1,038	2,4
0,900	31	0,763	2,1	0,565	3,2	4,20	140	0,865	1,8	1,049	2,4
0,950	31	0,781	2,0	0,658	3,1	4,40	130	0,861	1,7	1,055	2,4
1,00	31	0,810	1,9	0,734	2,7	4,60	128	0,861	1,7	1,061	2,3
1,05	34	0,814	1,9	0,786	2,8	4,80	124	0,860	1,7	1,066	2,4
1,10	37	0,812	1,9	0,807	2,7	5,00	125	0,854	1,7	1,062	2,3
1,15	40	0,812	1,9	0,857	2,8	5,20	128	0,859	1,7	1,066	2,3
1,20	42	0,811	1,9	2,876	2,6	5,40	130	0,852	1,8	1,072	2,3
1,25	44	0,807	1,9	0,902	2,6	5,60	133	0,857	1,9	1,077	2,5
1,30	45	0,804	1,8	0,907	2,6	5,80	136	0,874	1,9	1,072	2,5
1,35	46	0,805	1,8	0,911	2,6	6,00	140	0,905	2,0	0,059	2,6
1,40	47	0,809	1,7	0,921	2,6	6,20	144	0,939	2,2	1,051	2,8
1,45	48	0,811	1,7	0,924	2,5	6,40	150	0,974	2,2	1,070	2,7
1,50	49	0,814	1,7	0,928	2,3	6,60	157	0,986	2,5	1,081	2,7
1,60	58	0,820	1,7	0,924	2,4	6,80	165	0,993	2,3	1,056	2,7
1,70	59	0,828	1,7	0,928	2,3	7,00	172	0,983	2,5	1,064	2,9
1,80	61	0,835	1,7	0,931	2,4						

The data on the $\sigma_f^{241}Am/\sigma_f^{235}U$ ratio [9], reduced to the half-life of ^{241}Am (432 ± 4 years), vary more rapidly with energy, particularly for $E_n > 2$ MeV. Preliminary results in [10] in the 1-6 MeV range are systematically higher than our values by 3-7%. Below 1 MeV the agreement of the results is very good, but for $E_n > 6$ MeV there is a difference in the shape of the energy dependence, as is the case for $\sigma_f^{237}Np/\sigma_f^{235}U$. This leads to the conclusion that the difference results from the shape of the $^{239}Pu/^{235}U$ cross section ratio for $E_n > 6$ MeV.

The authors thank S. E. Lavrov, F. B. Samylin, and M. K. Golubevaya for participating in the work.

LITERATURE CITED

1. B. I. Fursov, V. M. Kupriyanov, and G. N. Smirenkin, in: Proceedings of a Conference on Neutron Physics [in Russian], Vol. 3, TsNIIAtominform, Moscow (1977), p. 144.
2. B. I. Fursov et al., At. Energ., 43, 181 (1977).
3. B. I. Fursov et al., At. Energ., 43, 261 (1977).
4. S. A. Baranov, A. G. Zelenkov, and V. M. Kul'kov, At. Energ., 41, 342 (1976).
5. F. Brauer et al., J. Inorg. Nucl. Chem., 12, 234 (1960).
6. W. Stein, R. Smith, and H. Smith, in: Proceedings of the Conference on Neutron Cross Sections and Technology, Vol. 1, Washington (1968), p. 627.
7. P. White, J. Hodgkinson, and G. Wall, in: Proceedings of the Symposium on Physics and Chemistry of Fission, Vol. 1, Salzburg, May 22-26, (1965), p. 219; P. White and G. Warner, J. Nucl. Energy, 21, 671 (1967).
8. J. Behrens, J. Magana, and J. Browne, Report UCID-17370 (1977).
9. É. F. Fomushkin and E. K. Gutnikova, Yad. Fiz., 10, 971 (1969).
10. T. Behrens and J. Browne, Report UCID-17324 (1976).

EXPERIMENTAL RESEARCH ON THE PRODUCTION AND STORAGE OF ULTRACOLD NEUTRONS

V. I. Morozov

UDC 539.125.5

Ultracold neutrons (UCN) have energies of 10^{-7} eV or less [1]. Since 1968, when the first report [2] on the production of UCN was published, the number of experimental and theoretical studies of their properties has grown continuously. The state and prospects of research with UCN are analyzed in detail in [3-6]. During the last few years, a great many experimental papers on UCN have been published. A majority of them deal with techniques for producing intense sources of UCN and storing them in traps of various kinds. In the present paper we give a brief summary of recent experimental research in the USSR on the production and storage of UCN.

The commonest method of obtaining UCN is to extract them directly from a moderator by guide tubes with reflecting walls. In the horizontal method of extraction the experimental room is connected to a reactor core by an evacuated bent horizontal guide tube with walls having a high limiting energy $E_{lim.n} = h^2 N b_{coh}/2\pi m$ in the range of UCN, where N is the number of nuclei per unit volume, b_{coh} is the coherent scattering length, m is the mass of a neutron, and h is Planck's constant. An auxiliary moderator (converter) is located in the guide tube close to the core. When the converter is irradiated with thermal neutrons. part of them lose energy as a result of inelastic scattering and enter the range of UCN. The UCN are extracted from the converter as a result of their total reflection from the vacuum–medium interface for any angles of incidence if $E < E_{lim}$ of the medium. The UCN emerging from the converter reach the guide-tube exit after a number of reflections from the walls of the tube. If the guide tube is long and has sharp bends the spectrum of the extracted neutrons has an upper bound $E = E_{lim.n}$. The flux of UCN at the guide-tube exit is determined by the flux of UCN from the converter and the transmission of the guide tube. The neutron flux from a unit area of the converter in the energy range from E to E +dE is

$$d\Phi = \frac{\Phi_T G(T_c, T_n)}{4} E\, dE, \tag{1}$$

where Φ_r is the thermal neutron flux density, $G(T_c, T_n) = \bar{\sigma}_{cool}(\sigma_{cap} + \sigma_{heat})^{-1} T_n^{-2} E^{-1}$, $\bar{\sigma}_{cool}$ is the cross section for the production of neutrons of energy E, averaged over the thermal neutron spectrum, σ_{cap} is the cross section for the capture of neutrons of energy E, σ_{heat} is the heating cross section equal to σ_{inel} – the cross section for the inelastic scattering of neutrons of energy E, and T_n and T_c are, respectively, the temperatures of the neutron spectrum and the converter [3]. For $T_c = T_n$ and $\sigma_{cap} \ll \sigma_{heat}$ the neutron flux from the converter corresponds to the flux in the equilibrium Maxwellian spectrum:

$$d\Phi = \Phi_T E\, dE/4T_n^2. \tag{2}$$

Equations (1) and (2) are valid when the limiting energy of the converter material is zero. For $E_{lim.c} > 0$ the flux will be smaller because of the reflection of UCN from the converter-vacuum interface, and its spectrum has the lower bound $E = E_{lim.c}$, since neutrons in a vacuum acquire an additional energy $E_{lim.c}$. In view of this the converter material should have a small value of $E_{lim.c}$ in comparison with $E_{lim.n}$ in order to obtain a sufficiently broad spectrum of UCN.

Technically it is simplest to extract UCN from a converter when its temperature is close to that of the neutron spectrum (not cooled to low temperatures). Techniques for extracting UCN from uncooled converters are described in [7-15] where tests of practically all the converter materials suitable for horizontal guide tubes (water, aluminum, magnesium, zirconium hydride) are reported. These experiments showed that a zirconium hydride converter is optimum from the point of view of yield of UCN, radiation stability, and the possibility of using it uncovered in a vacuum. Stainless steel with its large limiting energy ($\sim 1.9 \cdot 10^{-7}$ eV) and high corrosion resistance in strong γ fields turned out to be the most suitable material for guide tubes.

Figure 1 shows a schematic diagram of one of the best horizontal guide tubes, constructed at the SM-2 reactor [14]. The guide tube is 70-90 mm in diameter, 5.5 m long, and is made of electropolished stainless

Translated from Atomnaya Énergiya, Vol. 45, No. 6, pp. 442-449, December, 1978. Original article submitted May 22, 1978.

0038-531X/78/4506-1179$07.50

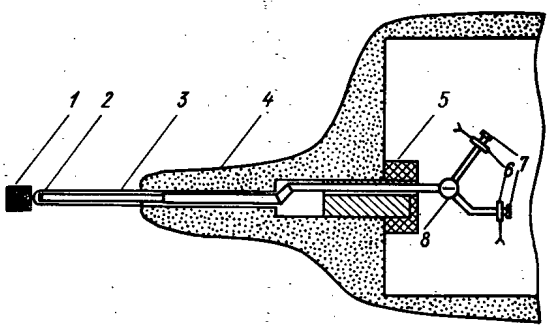

Fig. 1

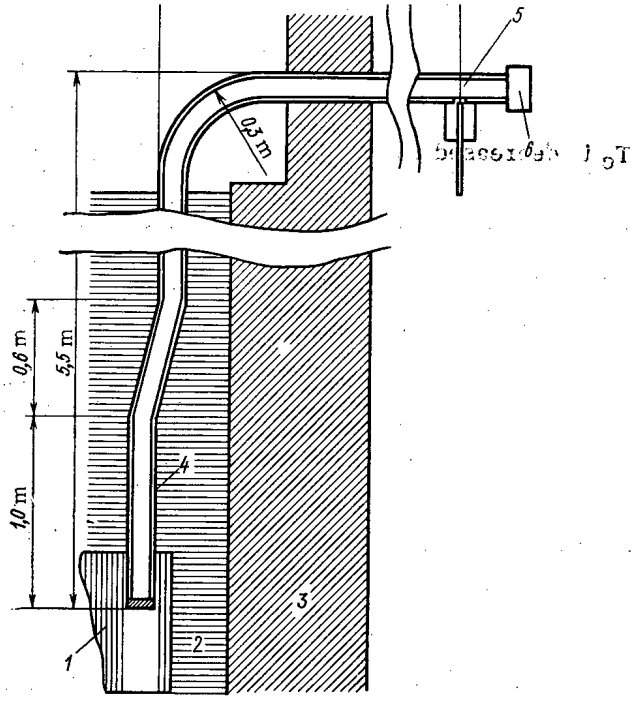

Fig. 2

Fig. 1. Schematic diagram of arrangement for obtaining UCN from the SM-2 reactor: 1) core; 2) converter, 3) entrance region of guide tube; 4) reactor shield; 5) additional shielding; 6) vacuum valves; 7) exit pipes; 8) UCN flux commutator.

Fig. 2. Schematic diagram of vertical guide tube for extracting UCN from the VVR-M reactor: 1) core; 2) beryllium converter; 3) reactor shield; 4) mirror guide; 5) screen for determining background; 6) detector.

steel. The converter is a thin plate of zirconium hydride with $T_c = 350°K$, irradiated with a thermal neutron flux density of $(2-4) \cdot 10^{14}$ neutrons/cm^2 · sec. The total flux of UCN with velocities from 3.2 to 5.7 m/sec at the guide-tube exit where the cross-sectional area is 60 cm^2 is $2 \cdot 10^3$ neutrons/sec. The flux of extracted neutrons with velocities above 5.7 m/sec does not exceed 50 neutrons/sec.

In using a vertical variation of the extractor [5, 9, 16], a wider range of converter materials is possible. Since neutrons from the converter can be slowed down in the gravitational field to energies in the UCN range, it is possible to use converter materials with a high limiting energy (in rising 1 cm a neutron loses $\sim 10^{-9}$ eV of kinetic energy). One such material is beryllium ($E_{lim} = 2.4 \cdot 10^{-7}$ eV, $\sigma_{cap} \ll \sigma_{inel}$) which has a higher radiation resistance than zirconium. Beryllium was used as a converter in the vertical guide tube of the VVR-M reactor [9] (Fig. 2). The guide tube consists of a vertical portion 5.5 m long, a smooth bend, and a horizontal portion 3 m long. The entrance section of the guide tube is 60 × 70 mm in cross section and is made of stainless steel; the horizontal part of the tube is 60 × 60 mm in cross section, and the bend is made of glass mirrors (^{58}Ni dusted on glass). For a thermal neutron flux density of $(3-5) \cdot 10^{13}$ neutrons/cm^2 · sec in the converter region there were 1500 UCN/sec at the exit of the horizontal part of the guide tube with velocities between 3.2 and 6.8 m/sec. There were 8500 neutrons/sec with velocities between 6.8 and 20 m/sec.

The guide tubes described in [9, 14] illustrate the possibilities of the method of extracting UCN by using uncooled converters of the most suitable materials (beryllium, zirconium hydride). It is shown in [9] that by raising the quality of the guide-tube surface and improving its transmission, the flux density of UCN extracted with velocities between 3.2 and 6.8 m/sec can in practice be brought up to 100 neutrons/cm^2 · sec for $\Phi_T = 10^{14}$ neutrons/cm^2 · sec. However, the suitability of a guide tube for experiments with UCN is determined not only by the magnitude of the extracted neutron flux but also by its spectral composition. Guide tubes which extract a flux which is sharply limited at $E = E_{lim.n}$ are more suitable for experiments on the storage of UCN, spectral measurements, and the formation of monoenergetic lines. Slightly curved mirror guides having a high transmission for UCN but furnishing a large number of neutrons with $E > E_{lim.n}$ are suitable only for experiments in which the presence of a background of very cold neutrons is unimportant. An increase in the ex-

tracted flux of UCN resulting from an improvement of the transmission of guide tubes will be accompanied by an increase in the ratio of background to effect, and this makes sense only in certain cases.

Low-temperature converters offer much more promise for increasing the flux of UCN [17, 18]. As T_c is decreased relative to T_n, both σ_{heat} and σ_{cool} decrease, but σ_{cool} falls more slowly and $G(T_c, T_n)$ increases.

According to calculations in [17, 18] the increase in the flux of UCN should be particularly large if σ_{cap} remains appreciably smaller than σ_{heat} during cooling, and the converter material has a high Debye temperature. These requirements are satisfied by beryllium for which $G(T_c, T_n)$ should increase by a factor of 14 for cooling from 300 to 50°K [18].

A low-temperature beryllium converter was used for the first time in an arrangement for extracting UCN from the VVR-M reactor [19]. When the converter was cooled from 300 to 30°K by gaseous helium the flux of UCN was increased by a factor of 8. The flux of UCN was $(1.5\text{-}2)\cdot 10^4$ per sec with velocity components in the following ranges: v_z (along the axis of the horizontal portion) from 3.2 to 6.8 m/sec, v_x and v_y (perpendicular to the axis) from -6.2 to $+6.2$ m/sec. The count of background neutrons with $v_z > 6.8$ m/sec was increased by a factor of 6-7. This arrangement with a low-temperature beryllium converter is the most intense source of UCN in existence at the present time.

An appropriate material for a low-temperature converter in a horizontal guide tube was sought in [17, 20, 21]. According to data in [17] the cooling of zirconium hydride was ineffective. Cooled gases in an aluminum ampul and hydrogenous materials (water and alcohol) frozen onto a cooled backing were investigated as converters in the horizontal guide tube of the VVR-K reactor [20, 21]. Water and hydrogen were the best of the converters tested, having identical yields at 300°K. After cooling hydrogen in the ampul to 80°K and freezing water onto bare backing at 80°K the yield of UCN from hydrogen increased by a factor of 3.2, and that from frozen water by a factor of 17 in comparison with water in an ampul. Taking account of the reflection of UCN from the window of the ampul the observed increase in the yield from water was almost twice as large as the value 5.8 calculated in [17].

These results show that the optimum material for a low-temperature converter in a horizontal guide tube is water frozen onto a backing. A hydrogen converter is less efficient because of the reflection of UCN from the aluminum window which is required to separate the gas from the evacuated guide tube. A parahydrogen converter appears to be rather promising. According to preliminary data [21] its yield at 80°K is 3 times as high as that of ordinary hydrogen.

The results in [19-21] show that by using low-temperature converters of beryllium and water frozen onto a backing at stationary reactors with $\Phi_T = 10^{14}$ neutrons/cm$^2\cdot$sec the density of the extracted fluxes of UCN with velocities from 3.2 to 6.8 cm/sec can be increased to about 10^3 neutrons/cm$^2\cdot$sec. Further technically realizable ways of improving the method of extracting UCN by using guide tubes are not evident. For this reason there is great interest in the development of methods of obtaining UCN by using pulsed reactors.

A recently developed method for obtaining UCN by storing them in portable traps [22-24] is promising. Experiments have been performed [22] on the storage of UCN in quartz and beryllium bottles which were inserted into the core of a stationary reactor and then together with their contents of UCN withdrawn from the core to the surface of the shield. This method is particularly promising with a pulsed reactor. If the neutron bottle is open to the entrance of UCN at the beginning of the reactor pulse and closed at the end, the density of the stored UCN will be determined by the peak neutron density in the moderator, and this is appreciably greater than the average.

This method was first realized in practice at the IIN reactor [24]. The UCN were stored in a copper bottle 40 cm in diameter and 40 cm high (Fig. 3). The lid of the neutron bottle is a fast-acting shutter with an operating time of 20 msec. Over the shutter there is a polyethylene moderator and a cooled polyethylene converter. After a reactor pulse of 2 msec, during which 10^{17} neutrons are emitted, the neutron bottle is conveyed to the measuring room where measurements are begun after 70-80 sec. At the beginning of the measurements 10^3 neutrons remained in the bottle (density of 20 neutrons/liter), while immediately after the reactor pulse the bottle contained $5\cdot 10^3$ neutrons. This density is of the same order of magnitude as that achieved in filling neutron bottles from the guide tube of the SM-2 reactor [14] using an uncooled converter (15-25 neutrons/liter). However, with further improvement of the trap there is the possibility of increasing the number of stored UCN by another factor of 30, and by using the GIDRA reactor the density may be increased by more than 3 orders of magnitude [25].

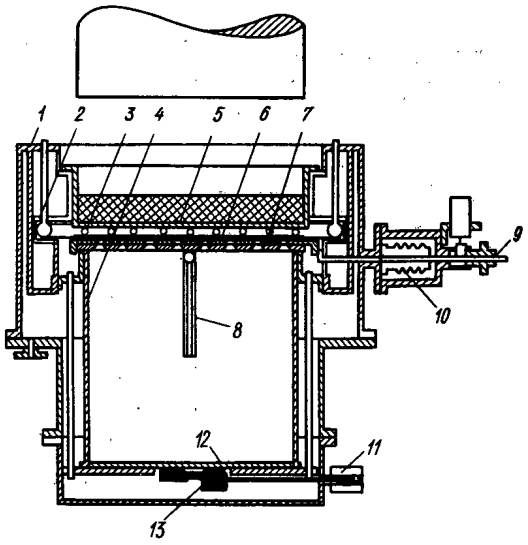

Fig. 3

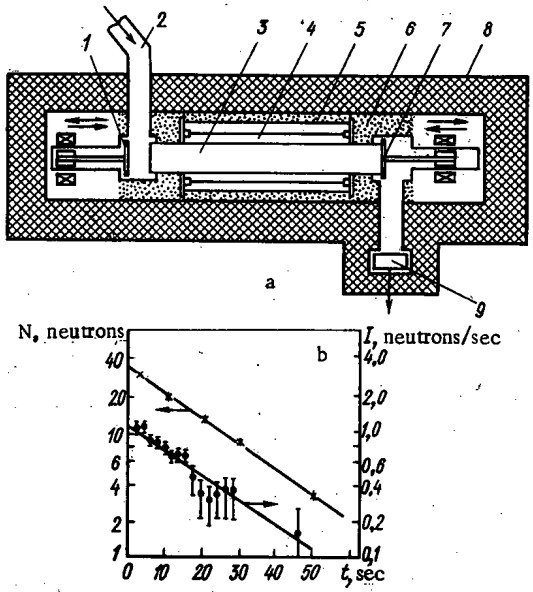

Fig. 4

Fig. 3. Arrangement for storing UCN at the ПН reactor: 1) reactor vessel; 2) converter cooling system; 3) converter; 4) neutron bottle; 5) moderator; 6, 7) fast shutter; 8) slow shutter; 9) shaft; 10) sylphon assembly; 11) solenoid; 12) device for moving filters; 13) detectors.

Fig. 4. Schematic diagram and results of an experiment on the anomalous heating of UCN: a: 1) entrance shutter; 2) entrance pipe; 3) UCN bottle; 4) external proportional counter; 5) cadmium; 6) boron carbide; 7) exit shutter; 8) borated polyethylene; 9) UCN detector; b: time dependence of UCN stored in bottle and neutron counts of external detector.

While there has been considerable success in producing a dense gas of UCN, the problem of storing it for a long time is still unsolved. Study of the storage process, stimulated by the possibility of using UCN in experiments to determine the basic characteristics of the neutron (dipole moment, charge, lifetime), has acquired independent interest. The main reason for the increased attention to the problem of storing UCN is the anomalously short storage times found experimentally.

Theoretically [3, 26] the escape of UCN from a bottle can occur as the result of capture and inelastic scattering in collisions with the bottle walls. The effective absorption coefficient of UCN per collision, averaged over the angles of incidence, is

$$\bar{\mu} = \frac{k(\sigma_{cap}+\sigma_{ind})}{4\pi b_{coh}}(\arcsin y - y\sqrt{1-y^2}), \qquad (3)$$

where $y^2 = E/E_{lim}$ and k is the wave number.

However, in almost all the experiments performed on the storage of UCN [7-9, 13, 14, 24, 27-29] the storage times actually attained were considerably shorter than those calculated by using data on the cross sections σ_{cap} and σ_{inel} extrapolated into the UCN region. The minimum experimental value of the cross section for the "removal" of UCN from neutron bottles is $\sim 2 \cdot 10^3$b for v = 10 m/sec, including materials with very small σ_{cap} and σ_{inel} cross sections – glass, beryllium, graphite, etc. In view of this, the attainable storage time of UCN does not exceed 300 sec even for neutrons with $E \ll E_{lim}$ stored in a bottle of optimum geometry [29]. So short a storage time does not permit the use of UCN to solve one of the fundamental problems – the precision measurement of the neutron lifetime from the decrease of density of a neutron gas stored in a bottle [3].

The observed anomalous leakage is difficult to account for by the presence of any strongly absorbing surface impurity, since the experiments were performed with bottles of various materials processed in different ways. The assumption of a hydrogenous film or an admixture of ~10% hydrogen 100 Å thick on the bottle walls seems more probable. In this case a strong dependence of the storage time on the temperature of the bottle walls should be observed, but experiments on the storage of UCN in bottles whose wall temperatures were varied from 120 to 700°K did not show such a dependence.

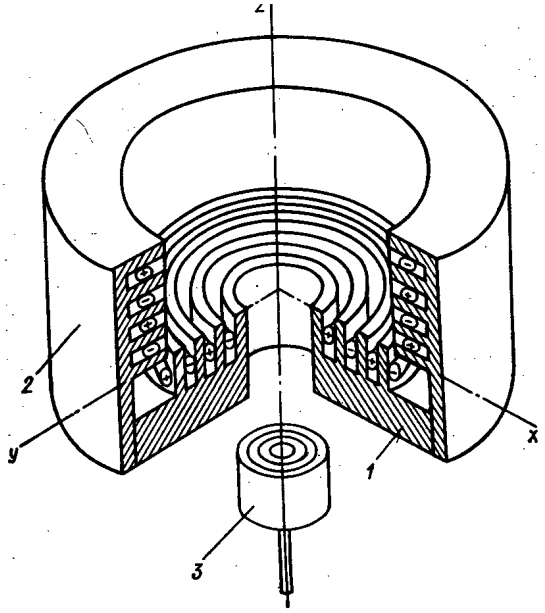

Fig. 5. Schematic diagram of trap: 1, 2) horizontal and vertical mirrors; 3) magnetic plug.

The results obtained lead to the conclusion that heating and capture are improbable causes of the anomalous leakage of UCN from bottles. However, a direct experiment reported in [30] showed that the anomalously short storage time, at least for copper bottles, is due to the heating up of the UCN to thermal energy. A schematic diagram of the experimental arrangement is shown in Fig. 4a. A copper bottle for storing UCN was located inside a six-chamber proportional helium detector whose efficiency for recording thermal neutrons was ~100%. One of the bottle shutters admitted UCN, and the second released the remaining UCN to the gas proportional detector. The purpose of the experiment was to observe the heating up and leakage of the UCN by means of the external detector.

Figure 4b shows the storage curve of UCN in a bottle with a storage time of 23 sec. This storage time is close to the maximum attainable for such bottles. The figure also shows the time dependence of the neutron counting rate of the external detector. The two curves have the same slope, and the number of neutrons recorded by the external detector, according to the calculations in [30], is from 90 to 110% of the total number of UCN stored in the bottle. This shows that the neutrons recorded by the external detector are former UCN.

The physical nature of the observed heating of the UCN is still not clear. The most realistic cause of the heating appears to be the presence of hydrogen on the bottle walls, although this contradicts the temperature independence of the storage time. This contradiction would be lessened somewhat if the assumption [31, 32] that hydrogen is strongly bound in the direction of the normal to a container surface but free to move along the surface is confirmed. In this case when a neutron is inelastically scattered by a proton it could gain an energy of the order of thermal. The cross section for this process $\sigma \sim \sqrt{T}$, where T is the wall temperature, and therefore the experiments might show a weak dependence of the storage time on temperature. The testing of the hydrogen hypothesis is of great interest. If it is confirmed, the problem of a long storage time can obviously be solved by using clean containers as proposed in [30]. Otherwise the problem of extended containment of UCN in bottles remains open until the physical nature of the anomalous heating is explained.

In principle, the reduction of the storage time of UCN because of anomalous heating can be avoided by using magnetic traps for storage [33]. A neutron introduced into a closed magnetic cavity in which the field increases from the center to the periphery should be retained in it so long as its spin is directed along the field $E < \mu H_{max}$, where $\mu = -6.03 \cdot 10^{-12}$ eV/Oe is its magnetic moment, and H_{max} is the magnetic field intensity at the edge of the cavity. The condition for the preservation of the orientation of the spin relative to the field is given by $\omega \ll 2\mu H/n$, where ω is the angular velocity of the field vector in the coordinate system moving with the neutron. From the point of view of depolarization the most dangerous regions are those where the field changes its direction rapidly or is close to zero. Estimates in [33] show that if there are no regions in the trap with a field intensity close to zero, the probability of depolarization may be appreciably smaller than the probability of neutron decay ($\sim 10^{-3}$/sec).

Experiments on the use of magnetic fields to trap UCN began relatively recently. Total reflection of UCN from an energy barrier produced by a magnetic field was reported in [34]. The probability of depolarization of UCN stored in a cylindrical copper bottle closed at one end by a magnetic energy barrier was reduced to ~0.01/sec [35]. Results in [35, 36] showed the practicability of constructing a magnetic trap with a storage time for UCN of ~10-100 sec.

A specific configuration of a magnetic system for producing a magnetic field which, together with the gravitational field, might be used to store UCN, was proposed and described in [37]. The system was made in the form of a cup of magnetic mirrors formed by annular conductors with periodically varying current directions. Estimates in [37] showed that the storage time of UCN in this trap should be ~100 sec, and in principle might be increased to 10^4 sec by eliminating regions of zero field intensity.

A similar structure was developed and built at the SM-2 reactor where the first experiments on the storage of UCN were performed [38]. The magnetic system of the trap consists of a plane horizontal mirror and a cylindrical vertical mirror 64 cm in diameter with a maximum field intensity of 2.5 kOe (Fig. 5). The central part of the horizontal mirror plays the role of a magnetic plug. Ultracold neutrons enter the trap through the opening in the plug and leave through it for recording. The magnetic system in conjunction with the gravitational field ensures the trapping of UCN with energies up to $9 \cdot 10^{-9}$ eV. In preliminary experiments 1.05 ± 0.15 neutrons were stored in the trap with an average storage time of 35 ± 10 sec. The result obtained showed the possibility of storing UCN for at least several tens of seconds by using a magnetic field. The problem of attaining the theoretical storage time in such a trap will finally be solved after eliminating the regions of zero field and stabilizing the field of the magnetic system. It should also be noted that the storage time of UCN in the trap should depend strongly on the neutron energies and trajectories in the working volume. The accuracy achieved in the preliminary experiments is clearly inadequate to account in detail for the shape of the curve for the storage of UCN. An improvement in accuracy requires a substantial increase in the density of neutrons stored in the trap.

In conclusion, the author thanks I. M. Frank, V. I. Lushchikov, A. V. Strelkov, V. K. Ignatovich, Yu. N. Pokotilovskii, A. P. Serebrov, V. I. Mikerov, Yu. N. Panin, A. I. Frank, P. E. Spivak, B. G. Erozolimskii, Yu. G. Abov, P. A. Krupchitskii, V. V. Vasil'ev, V. A. Konks, Yu. S. Zamyatnin, Yu. A. Kushnir, Yu. Yu. Kosvintsev, G. I. Terekhov. and V. N. Nefedov for numerous discussions of the papers cited in the present article.

LITERATURE CITED

1. Ya. B. Zel'dovich, Zh. Eksp. Teor. Fiz., 36, 1952 (1959).
2. V. I. Lushchikov et al., Pis'ma, Zh. Eksp. Teor. Fiz., 9, 23 (1969).
3. F. L. Shapiro, JINR Report R3-7135, Dubna (1973).
4. V. I. Lushchikov, in: Second International School of Neutron Physics (Collected Lectures) [in Russian], JINR, Dubna (1974), p. 7.
5. I. M. Frank, ibid., p. 19.
6. A. Shtaierl, ibid., p. 42.
7. L. V. Groshev et al., Preprint JINR R3-5392, Dubna (1970).
8. L. V. Groshev et al., Preprint JINR R3-7282, Dubna (1973).
9. A. I. Egorov et al., Yad. Fiz., 19, 300 (1974).
10. E. Z. Akhmetov et al., Preprint JINR R3-7457, Dubna (1973).
11. E. Z. Akhmetov et al., At. Energ., 37, 35 (1974).
12. Yu. S. Zamyatnin et al., JINR Report R3-7946, Dubna (1974).
13. Yu. Yu. Kosvintsev et al., Nucl. Instrum. Methods, 143, 133 (1977).
14. Yu. Yu. Kosvintsev, Yu. A. Kushnir, and V. I. Morozov, in: Proceedings of a Conference on Neutron Physics, Part 1 [in Russian], TsNIIatominform, Moscow (1977), p. 152.
15. E. Z. Akhmetov et al., ibid., p. 178.
16. A. V. Antonov et al., ibid., p. 187.
17. V. V. Golikov, V. I. Lushchikov, and F. L. Shapiro, JINR Preprint R3-6556, Dubna (1972).
18. G. D. Porsev and A. P. Serebrov, Preprint LIYaF Akad. Nauk SSSR, No. 38, Leningrad (1973).
19. I. S. Altarev et al., Preprint LIYaF Akad. Nauk SSSR, No. 246, Leningrad (1976).
20. E. Z. Akhmetov et al., JINR Report R3-8470, Dubna (1974).
21. E. Z. Akhmetov et al., [see Ref. 14], p. 182.
22. V. A. Anikolenko et al., FIAN Preprint No. 92, Moscow (1973).
23. A. V. Antonov et al., Pis'ma Zh. Eksp. Teor. Fiz., 10, 380 (1969).

24. A. V. Antonov et al., Pis'ma Zh. Eksp. Teor. Fiz., 24, 387 (1976).
25. V. I. Mikerov, Author's Abstract of Candidate's Dissertation, Moscow (1977).
26. V. I. Ignatovich, JINR Preprint R4-6553, Dubna (1972).
27. L. V. Groshev et al., in: Proceedings of a Conference on Neutron Physics, Part 2 [in Russian], TsNIIatominform, Moscow (1976), p. 166.
28. A. Steyerl and W. Trustedt, Z. Phys., 267, 379 (1974).
29. Yu. Yu. Kosvintsev, Yu. A. Kushnir, and V. I. Morozov [see Ref. 14], p. 173.
30. A. V. Strelkov and M. Khettsel't, JINR Preprint R3-10815, Dubna (1977).
31. V. K. Ignatovich and L. M. Satarov, IAE Preprint No. 2820, Moscow (1977).
32. L. I. Blokhintsev and I. M. Plakida, JINR Preprint R4-10381, Dubna (1977).
33. V. V. Vladimirskii, Zh. Eksp. Teor. Fiz., 39, 1065 (1960).
34. Yu. Yu. Kosvintsev, Yu. A. Kushnir, and V. I. Morozov, Pis'ma Zh. Tekh. Fiz., 23, No. 2, 293 (1976).
35. Yu. Yu. Kosvintsev, Yu. A. Kushnir, and V. I. Morozov, Pis'ma Zh. Eksp. Teor. Fiz., 23, 135 (1976).
36. Yu. Yu. Kosvintsev et al., Preprint NIIAR P-15 (281), Dimitrovgrad (1976).
37. Yu. G. Abov et al., Preprint ITÉF-44, Moscow (1976).
38. P. G. Aver'yanov et al., [see Ref. 14], p. 167.

CYCLOTRON X-RAY SPECTRAL ANALYSIS OF THE ELEMENTS FROM TITANIUM TO CESIUM

V. A. Muminov, R. A. Khaidarov, and Kh. Isaev

UDC 543.422.8 +539.186.2

Excitation of characteristic x rays by means of charged-particle accelerators has attracted increased attention in recent years as a method of elemental analysis; distinctive features are the high sensitivity, the scope for determining practically all elements, and the instant response, because the radiation is recorded directly during the bombardment [1].

We have examined the analysis of substances by the excitation of K x rays by means of protons of energy between 2-6 MeV produced by a cyclotron.

Principles. The number of x-ray quanta recorded by a detector is as follows when the contribution from secondary fluorescence can be neglected:

$$Y = 6.3 \cdot 10^{12} \frac{N}{A} Q \eta_{T_j} p \int_0^{R \cos \theta_1} \sigma_{T_j}(x) \times$$

$$\frac{\exp[-\mu x/\cos\theta_2]\,dx}{\cos\theta_1} = 10^6 Q \eta_{T_j} p \times \int_{E_H}^{E_k} B_{x\,tn}(E) \frac{\exp[-\mu t(E)]}{S(E)} dE;$$

$$t(E) = \int_{E_H}^{E} \frac{\cos\theta_1\, dE}{S(E)\cos\theta_2}, \qquad (1)$$

where N is Avogadro's number; A, atomic mass of the element; E, charged-particle energy in MeV; R, range of the latter in the target in g/cm^2, Q, total charge delivered in μCu; σ_{T_j}, excitation cross section of the T_j series in cm^2; η_{T_j}, recording efficiency for the characteristic x rays, which is determined by the characteristics of the detector and the geometry used; μ, mass-absorption coefficient for the x rays in cm^2/g; θ_1 and θ_2, angles between the normal to the irradiated surface made by the beam and the direction to the detector, respectively; p, element concentration in the target (for homogeneous distribution); S(E), stopping power for the charged particles in MeV · cm^2/g; and B_{xtn}, yield of characteristic x rays from a thin target (this is the number of quanta from the T_j series emitted on irradiating material of mass 1 μg/cm^2 with a total charge of 1 μCu). The quantity $B_{xtn}(E)$ gives a better indication of the scope for using the method than does $\sigma_x(E)$.

Translated from Atomnaya Énergiya, Vol. 45, No. 6, pp. 449-452, December, 1978. Original article submitted December 19, 1977.

0038-531X/78/4506-1185 $07.50

In any absolute method of analysis, the accuracy is dependent to a large extent on the errors in determining numerous parameters (η, B_{xtn}, μ, θ_1, θ_2), so a relative method is preferable. The most accurate results and the simplest relationships are obtained if the thickness and composition are identical for the major components of the standards and specimens (major components are elements whose concentrations are such that the self-absorption and secondary fluorescent emission in the specimen and standard are identical within the acceptable errors):

$$m_0 = \frac{Y_0}{Y_S}\frac{Q_S}{Q_0}m_S; \quad p_0 = \frac{Y_0}{Y_S}\frac{Q_S}{Q_0}p_S, \tag{2}$$

where m is the content of the element.

One of the advantages of the method is that numerous elements can be determined together. Calculations from (2) become laborious if there are many components, since standards must be available for all the elements. It is much simpler to plot curves of the following type for a few standard elements for the appropriate x-ray energy range:

$$f_1(Z, E) = \frac{Y_S(Z, E)}{m_S Q_S}; \quad f_2(Z, E) = \frac{Y_S(Z, E)}{p_S Q_S}, \tag{3}$$

from which the contents of the elements can readily be determined:

$$m_0 = \frac{Y_0}{f_1(Z, E)}\frac{1}{Q_0}; \quad p_0 = \frac{Y_0}{f_2(Z, E)}\frac{1}{Q_0}. \tag{4}$$

Excitation Cross Sections and X-Ray Yields. The scope for using the method under particular conditions was evaluated and optimum conditions were defined by reference to the excitation cross section or x-ray yields. Existing theories give a good description of the cross sections, but the values calculated for $\sigma_x(E)$ agree with measured values only for restricted energy and element ranges [2]. Therefore, experimental data have to be used in practice.

The excitation cross sections $\sigma_x(E)$ and the x-ray yields $B_{xtn}(E)$ were measured by using absolute and relative methods in parallel, which serves to eliminate possible systematic errors. In the absolute method, the formula used for $\sigma_x(E)$ was

$$\sigma_x = \frac{A\cos\theta_1}{6.3\cdot 10^{19} mNQ}\sum_j \frac{S_{T_j}}{\eta_{T_j}}, \tag{5}$$

where S_{T_j} is the area of the photopeak.

In the relative method, $\sigma_x(E)$ is deduced from the following formula when the target contains the working and standard elements:

$$\frac{\sigma_{xu}}{\sigma_{xS}} = \frac{A_u}{A_S}\frac{m_S}{m_u}\left(\sum_j \frac{S_{T_j u}}{\eta_{T_j u}}\right)\left(\sum_j \frac{S_{T_j S}}{\eta_{T_j S}}\right)^{-1}. \tag{6}$$

As the ratio m_S/m_u is determined with higher precision than the mass of the target, the error in measuring $\sigma_x(E)$ is dependent in the main on the error in the cross section for the standard element.

We measured $\sigma_x(E)$ for the K series as excited by protons of energy between 2 and 6 MeV for the elements from titanium (Z = 22) to cesium (Z = 55), apart from krypton, technetium, and xenon. The targets were prepared from solutions of salts, which were evaporated onto thin polystyrene films (thickness 1 mg/cm^2) to produce layers of 40-500 μg/cm^2. The standards were copper and iron.

The 150-cm cyclotron at the Institute of Nuclear Physics, Academy of Sciences of the Uzbek SSR, was used; the initial beam energy was 8 MeV, and the beam was passed through a shaper, which provided remote control of the proton energy by means of aluminum foils, after which the beam passed through a system of collimators of diameter up to 5 mm, the target set at 45° to the beam, and an aluminum Faraday cylinder of length 100 mm. The target holder was placed in the Faraday cylinder at a depth of 50 mm to ensure complete charge collection. The total incident charge was determined with a current integrator, whose error of measurement was 2%. The characteristic x rays were recorded with an Si(Li) detector having a resolution of 320 eV for the 6.4 keV line of ^{57}Co.

Table 1 gives the measured excitation cross sections; the error of measurement for $\sigma_x(E)$ was not more than 12%. We also give the published values of $\sigma_x(E)$ for comparison.

Table 2 gives values of $B_{xtn}(E)$ for the K series for thin targets; we also measured the K_α/K_β intensity ratio with an error not more than 12%. It was found that these quantities did not vary with the proton energy within the error of measurement and were in agreement with the theoretical values [4]. The results are therefore not given.

TABLE 1. Excitation Cross Sections for the K Characteristic X-Rays in Barns

Z	Energy, MeV					Z	Energy, MeV				
	2	3	4	5	6		2	3	4	5	6
22	240 221 [9] 218 [10] 259 [6] 252 [11]	440 369 [9] 383 [10] 441 [11]	560 490 [9] 562 [11]	610 553 [9] 583 [10]	625 [9]	33	21 [11] 17 15,9 [3]	44	76	110	140
23	190 197 [6]	340	480	570		34	14 11,5 [5]	36	63	89	110
24	150 167 [6]	280	380	470		35	10 10,4 [5]	29	51	75	96
25	120 133 [6]	230 226 [12]	330	410	460 446 [2]	37	7,7 5,43 [5]	20 20 [11]	35 37 [11]	52 48 [11]	70
26	100 76,5 [13] 88 [10] 77 [8]	180 100 [2] 177 [10] 177 [11]	270 268 [2] 228 [11]	340 311 [2] 305 [11]	420 404 [2]	38	7 [11] 5,0 5,28 [5]	15	29	43	58
27	82 59 [3] 70 [10] 60 [8] 86 [6] 81 [11]	160 146 [10] 150 [11]	220 207 [11]	280 272 [10] 269 [11] 269 [9]	330	39	3,8 3,94 [5]	12 12,5 [2]	23 25,3 [2]	35 35,7 [2]	48
28	63 57 [10] 68 [6] 58 [11]	130 123 [2] 120 [10] 135 [11]	190 182 [2] 178 [11]	250 249 [2] 254 [11] 294 [9]	300 267 [2]	40	2,9 3 [11]	9,5 9 [11]	19 17 [11]	29 26 [11]	40
29	44 39 [3] 43 [10]	100 98 [2] 95 [10]	170 156 [2]	220 208 [2] 186 [10]	260 252 [2]	42	1,7 2,05 [5]	5,7 5,37 [2]	12 10 [2]	20 17,1 [2]	28 22,6 [2]
30	36 31,9 [3]	83 78 [2]	140 134 [2]	180 171 [2]	220 212 [2]	44	1,0	3,7	8,3	13	20
31	30 28,3 [3] 28 [8]	71	120	150	190	45	0,84	2,9	6,7	11	16
32	25 18,5 [3] 19 [8]	60 52 [11]	99 92 [11]	130 124 [11]	170	46	0,70 0,755 [5]	2,3	5,4	8,9	13
						47	0,57 0,67 [7] 0,7 [10]	1,8 1,9 [2] 2,4 [10]	4,3 4,17 [2]	7,0 6,8 [2] 7,7 [10]	11 8,87 [2]
						48	0,45 0,54 [7]	1,5 1,64 [2]	3,4 3,86 [2]	5,9 5,5 [2]	9,6 8,7 [2]
						49	0,36	1,3	2,8	5,2	7,6
						50	0,28 0,32 [7]	1,1	2,5	4,4	6,4
						51	0,23 0,34 [7]	0,90	2,1	3,9	5,6
						52	0,19 0,18 [7]	0,75	1,8	3,3	4,7
						53	0,15	0,63	1,5	2,8	4,1
						55	0,089	0,40	1,1	2,0	2,8

TABLE 2. Yields of K-Series Characteristic X Rays from Thin Targets in 10^5 Quanta/$\mu g \cdot cm^{-2} \cdot \mu Cu$

Z	Proton energy, MeV					Z	Proton energy, MeV				
	2	3	4	5	6		2	3	4	5	6
22	180	330	420	480	540	38	2,2	6,6	12	19	25
23	140	250	350	420	460	39	1,6	5,3	9,8	15	20
24	93	180	240	300	340	40	1,2	4,0	7,9	12	17
25	84	150	220	280	310	41	0,90	2,9	7,7	9,8	14
26	73	120	170	220	270	42	0,66	2,2	4,8	7,7	11
27	52	95	140	180	210	44	0,40	1,4	3,1	5,0	7,4
28	42	87	130	160	200	45	0,30	1,0	2,5	4,0	5,7
29	26	62	98	130	160	46	0,25	0,80	1,9	3,2	4,6
30	21	48	81	100	130	47	0,20	0,64	1,5	2,5	3,8
31	16	39	64	84	100	48	0,15	0,51	1,2	2,0	3,1
32	13	31	51	69	87	49	0,12	0,43	0,93	1,7	2,5
33	8,6	22	39	54	69	50	0,090	0,36	0,80	1,4	2,0
34	6,7	17	30	43	55	51	0,070	0,28	0,66	1,2	1,7
35	4,9	13	25	34	45	52	0,056	0,22	0,52	0,99	1,4
37	3,3	8,3	15	24	30						

Pros and Cons of the Cyclotron in the Analysis of Air. We consider the analysis of air contaminants (from filters) to illustrate the pros and cons; the elements were Mn, Fe, Cu, Zn, Ga, Ge, As, Se, Mo, Sb, Te.

Firstly, the yields of the characteristic x rays (Table 2) indicate that the limit of detection for E_p around 6 MeV is better by 1-2 orders of magnitude than that for E_p of ~2-3 MeV, which is the range normally employed in elemental analysis.

Secondly, the energy of the charged particles can be varied over a wide range (from 2 up to about 6 MeV), so the method is more flexible and can handle more elements. In fact, the atomic number and the incident energy have marked effects on the excitation cross sections, so there is no single optimal energy if one has to determine elements differing substantially in atomic number, in contrast to the assertion of [1]. The experiments showed that the elements listed can be determined at levels of 10^{-7}-10^{-10} g/cm^2 by irradiation first at 2 MeV and then at 5 MeV. The Mo, Sb, and Te are determined in the second case. The limit of detection was unsatisfactory at the low bombardment energy. The lower elements cannot be determined

TABLE 3. Some Results from the Analysis of Air Samples, 10^{-7} g/cm^2

Mn	Fe	Cu	Zn	Ga	Ge	As	Se	Te
7,1 (6,6)	3,7	4,9	—	1,1	0,88	0,45	—	—
3,4 (3,0)	22	4,2	8,6(9,3)	—	—	0,82	—	—
47 (50)	50	17 (19)	—	—	—	0,091	3,0	7,1

adequately for a proton energy of 5 MeV, because there is a marked rise in the background in the low-energy region, while the count rates provided by the light elements become excessive, so the corresponding radiations are suppressed by means of an aluminum absorber of thickness 200 μ. In both cases the bombardment current was 10-30 nA and the measurement time was 5-10 min. The standards were prepared by evaporating solutions of salts sprayed onto filters.

The method was tested on 42 specimens made in the same way as the standards; also, 12 air samples were examined for certain elements by neutron activation. These checks showed that the error in determining element contents at the 10^{-7}-10^{-10} g/cm^2 level is not more than 15% at the 0.9 confidence level. The limit of detection was defined by taking the minimum number of pulses in a peak as $3\sqrt{N_b}$, where N_b is the background as found in measurement on the above specimens. The limit of detection was 10^{-9}-10^{-11} g/cm^2, the atomic number being the decisive factor. Table 3 gives typical results (the results from neutron-activation analysis are given in parentheses).

A disadvantage of a cyclotron is that the particles are produced in pulses; it is very difficult to correct for the dead time of the equipment under these conditions, but it is possible to select an irradiation current such that the dead-time correction is negligible. For this purpose it is sufficient to alter the markspace ratio of the beam at a given mean current. If the count rate due to the characteristic x rays remains constant, the current has been chosen correctly.

Cyclotrons providing proton energies up to about 6 MeV thus provide substantial improvement in the sensitivity and can handle more elements. The energy can be adjusted, which allows one to determine elements with Z between 22 and about 50 with a limit of detection of 10^{-9}-10^{-11} g/cm^2, the exact value being dependent on the atomic number.

LITERATURE CITED

1. A. Johansson and I. Johansson, Nucl. Instrum. Methods, 137, 473 (1976).
2. R. Liebert, Phys. Rev., A., 8, 2336 (1973).
3. R. Lear and T. Gray, ibid, p. 2469.
4. J. Scofield, Phys. Rev., A, 9, No. 3, 1041 (1974).
5. T. Griswell and T. Gray, Phys. Rev., A, 10, 1145 (1974).
6. F. Bodart, G. Deconninck, and S. Wiek, X-Ray Spectrom., 4, 90 (1975).
7. N. Khelil and T. Gray, Phys. Rev., A., 11, No. 3, 893 (1975).
8. G. Deconninck, G. Demortier, and F. Bodart, At. Energy Rev., 13, No. 2, 367 (1975).
9. G. Bissinger et al., Phys. Rev., A, 1, No. 3, 841 (1970).
10. A. Akselsson and T. Johansson, Z. Phys., 266, 245 (1974).
11. J. McCoy and J. Duggan, in: Proceedings of the Symposium on Nuclear Techniques in the Basic Metal Industries, IAEA Vienna, (1973), p. 591.

LETTERS

MEASUREMENT OF NEUTRON TOTAL CROSS SECTIONS AND RESONANCE PARAMETERS OF ^{147}Pm

V. A. Anufriev, T. S. Belanova,
Yu. S. Zamyatnin, A. G. Kolesov,
S. N. Nikol'skii, V. A. Poruchikov,
S. M. Kalebin, V. S. Artamonov,
and R. N. Ivanov

UDC 621.039.556

We present the results of measurements of neutron total cross sections of ^{147}Pm ($T_{1/2}$ = 2.652 yr) by the time-of-flight method. The experiment was performed at the SM-2 reactor [1] using a selector with synchronous rotors suspended in a magnetic field [2]. The neutron detectors were ^{3}He filled counters. The best resolution of the spectrometer was 70 nsec/m. The statistical accuracy of the measurements was maintained between 0.5 and 1.5%, and the neutron background did not exceed 4%.

The targets were plates of promethium metal with the following admixtures, %: ^{147}Sm 2; ^{145}Nd 0.4; Si 8; Mn < 0.1; Mg and Fe < 0.08; Cr, Fe, Al < 0.4; Cd and Ni < 0.6; Ce < 0.2; Eu < 0.01. The transmission of the samples was measured for thicknesses of 0.12, 0.75, and 4.0 mm, corresponding to ^{147}Pm contents of $0.27 \cdot 10^{21}$, $1.78 \cdot 10^{21}$, and $9.97 \cdot 10^{21}$ atoms/cm^2. The neutron energies varied from 0.02 to 250 eV. Up to 50 eV the neutron resonance parameters were calculated by shape fitting, and above 50 eV by area analysis. The value of the neutron width $2g\Gamma_n$, the total width Γ, and the position of the E_0 level are listed in Table 1.

Figure 1 shows the energy dependence of the ^{147}Pm neutron total cross section from 0.02 to 250 eV. Of the 28 resonances found in ^{147}Pm below 180 eV the levels at 21, 53, and 23.09 eV were observed for the first time. The measured value of the total thermal neutron cross section was $\sigma_t = 190 \pm 15$ b. A negative resonance with an energy of 1.58 eV was introduced to make σ_t in the thermal region calculated from the positive resonances agree with the experimental value.

The resonance parameters are in general agreement with those in [3-6] except for the level at 5.37 eV for which the neutron and total widths differ appreciably from the values in [3] ($2g\Gamma_n = 37 \pm 2$ MeV and $\Gamma = 104 \pm 6$ MeV). The value $I = 1840 \pm 280$ b for the total resonance integral calculated from the neutron resonance parameters is 10-15% smaller than the values in [3-6] as a result of the difference in the resonance parameters of the 5.37 eV level noted above.

The graph in Fig. 2 of the distribution of the number of levels as a function of the neutron energy shows that the omission of levels begins at 55 eV. Using the tabulated data for levels below 55 eV, the average distance between levels is $\bar{D} = 3.58 \pm 0.50$ eV, the average reduced neutron width is $2g\bar{\Gamma}_n^0 = 1.68 \pm 0.62$ MeV, and the value of the neutron strength function is $S_0 = (2.9 \pm 1.1) \cdot 10^{-4}$.

TABLE 1. Neutron Resonance Parameters of ^{147}Pm

E_0, eV	Γ, MeV	$2g\Gamma_n$, MeV	E_0, eV	$2g\Gamma_n$, MeV
−1,53		2,1	52,21±0,18	2,79±0,45
5,370±0,012	144±5	20,57±0,50	55,55±0,18	1,93±0,41
6,580±0,015	54±4	1,39±0,04	65,20±0,19	55,4±6,3
6,930±0,015	72±7	3,81±0,24	82,1±0,2	30,8±5,9
15,17±0,07	87±4	1,27±0,02	85,1±0,2	34,6±6,3
19,54±0,07	79±4	4,04±0,05	94,7±0,3	21,2±3,7
21,53±0,08		0,026±0,013	98,9±0,4	38,2±7,5
23,09±0,09		0,06±0,02	114,3±0,5	56,6±6,8
29,20±0,12	123±14	2,12±0,06	130,3±0,6	138±21
35,31±0,15	149±50	0,42±0,08	139,8±0,6	9,1±6,7
38,02±0,15	137±10	20,72±0,56	143,1±0,7	15±5
39,84±0,15	138±12	17,17±0,46	146,5±0,7	92±24
45,46±0,16	139±12	21,38±0,52	153,2±0,7	87±26
47,98±0,16	95±13	18,67±0,41	172,2±0,8	336±55
			177,7±0,9	25±15

Translated from Atomnaya Énergiya, Vol. 45, No. 6, pp. 453-455, December, 1978. Original article submitted October 4, 1976; revision submitted May 12, 1978.

0038-531X/78/4506-1189 $07.50

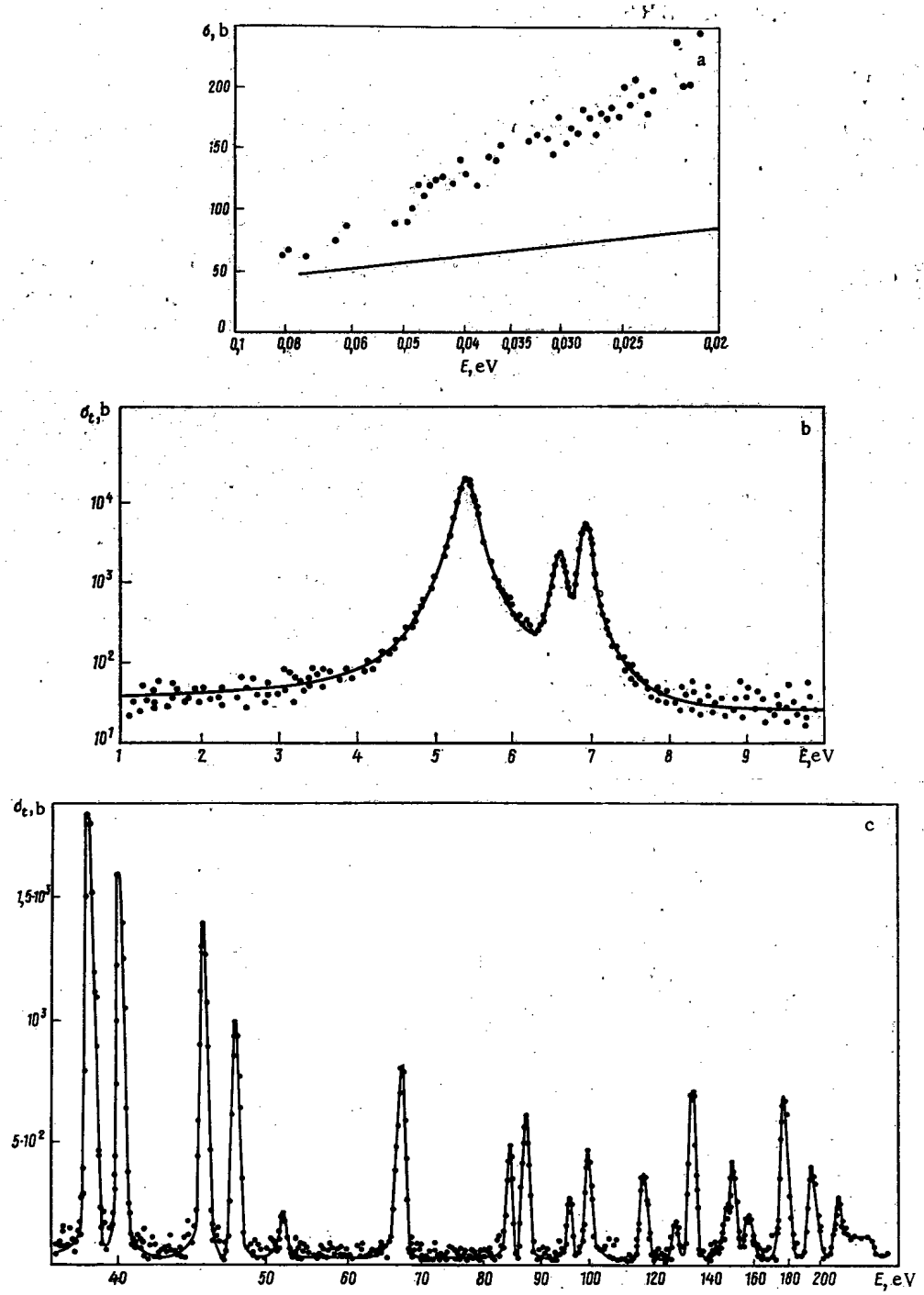

Fig. 1. Neutron total cross section at a) 0.02-0.08 eV; b) 1-10 eV; c) 36-250 eV: •) experiment; —) calculated from resonance parameters of Table 1.

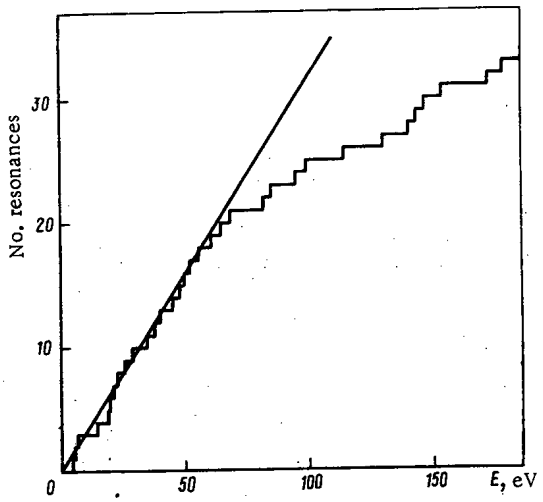

Fig. 2. Number of ^{147}Pm resonances as a function of neutron energy.

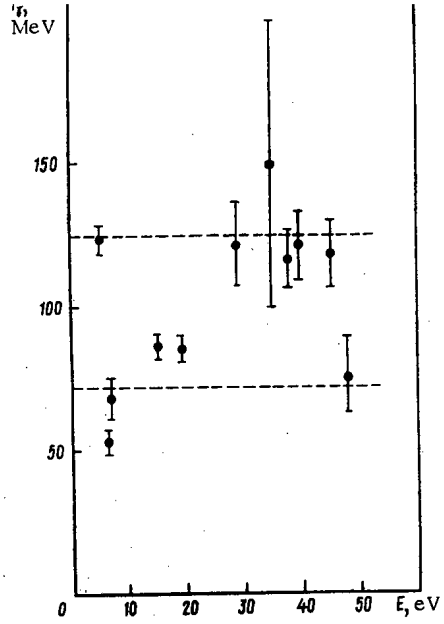

Fig. 3. Distribution of values of radiation width of ^{147}Pm levels.

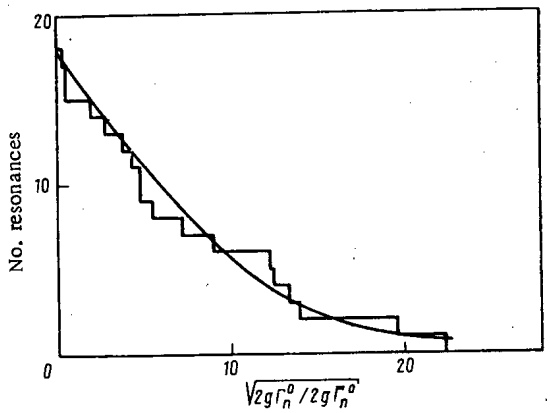

Fig. 4. Integrated distribution of values of the reduced neutron width of ^{147}Pm: ——) Porter–Thomas distribution for one degree of freedom; the histogram is the experimental distribution.

The radiation width $\Gamma_\gamma = \Gamma - 2g\Gamma_n$ can be calculated for 11 resonances. It is clear from the graph in Fig. 3 that the values of Γ_γ are grouped around two average values: 72 ± 6 MeV (5 resonances) and 125 ± 9 MeV (6 resonances). The average value ($\bar{\Gamma}_\gamma$ = 100 MeV) was used in calculating the neutron resonance parameters by area analysis.

Statistical processing of the resonance data below 55 eV shows that the values of the reduced neutron widths follow the Porter–Thomas distribution with one degree of freedom (Fig. 4).

LITERATURE CITED

1. G. A. Bat', A. S. Kochenov, and L. P. Kabanov, Research Reactors [in Russian], Atomizdat, Moscow (1972).
2. T. S. Belanova et al., NIIAR Preprint P-6 (272), Dimitrovgrad (1976).
3. G. Kirouac et al., Nucl. Sci. Eng., 52, 310 (1973).
4. BNL-325, Third Edition, New York (1973).
5. J. Codding et al., Nucl. Sci. Eng., 43, 58 (1971).
6. J. Harvey et al., in: Proceedings of the Second International Conference on Peaceful Uses of Atomic Energy, Geneva, 16, 150 (1958).

USE OF SMALL DEUTERON ACCELERATOR FOR NEUTRON-ACTIVATION DETERMINATION OF FLUORIDE

Yu. I. Bondarenko and V. S. Rudenko

UDC 543.53

The neutron-activation method of fluorine determination, based on the use of the $^{19}F(n, \alpha)^{16}N$ nuclear reaction with subsequent detection of the γ radiation of the nuclide ^{16}N formed ($T_{1/2} = 6.3$ sec, $E_\gamma \approx 6-7$ MeV), has found widespread application in the analysis of various materials. This has been furthered by the speed, selectivity, and simplicity of the method, especially when isotopic neutron sources are used as activation sources [1-3]. In view of their limited neutron yield, however, isotopic sources are used to determine fluorine when its content $\geq 10^{-2}$ wt. % [1, 2]. More intense neutron sources are required to determine a fluorine concentration of 10^{-3} wt. % or less.

High neutron fluxes with an energy of less than 10 MeV, which is suitable for determining fluorine from the $^{19}F(n, \alpha)^{16}N$ reaction (reaction threshold 1.57 MeV) without interference from oxygen from the $^{16}O(n, p)^{16}N$ reaction (reaction threshold 10.2 MeV), can be obtained in charged-particle accelerators, e.g., from the $^{9}Be(\alpha, n)^{10}B$ reaction. The neutron yield is $\sim 2 \cdot 10^9$ neutrons/sec when a thick beryllium target is irradiated with neutrons with an energy of 3 MeV and a current of 1 μA. Moreover, the neutron angular distribution has a sharp maximum for angles near 0° with respect to the direction of the accelerated deuterons. This makes it possible to obtain higher neutron fluxes in the specimen than with isotopic sources with the same integrated neutron yield but with an isotropic distribution.

The comparatively low energy of the neutrons (~6 MeV) at which the cross section for the (n, α) reaction in fluorine is a minimum permits highly sensitive fluorine determination to be carried out with low-energy deuteron accelerators. Thus, Jinno and Ishii [4] employed a 2-MeV Van de Graaf electrostatic accelerator for fluorine determination. This method did not, however, find widespread application because of the lack of suitable, easily operated deuteron accelerators which could be used under industrial conditions.

In the present paper we consider the possibility of a small 3-MeV deuteron accelerator (MLUD-3), with a pulse current of 250 μA, which has been developed in our country [5] being used as a source of neutrons for activation analysis and, in particular, for fluorine determination. The experiment was performed on a prototype of such a linear accelerator which occupies an area of about 20 m^2 (apart from the control panel) and has the following operating parameters: energy of accelerated deuterons 3 MeV, mean current 0.3 μA, and beam diameter on beryllium target ~25 mm.

The beryllium target with a diameter of 30 mm and a thickness of 2 mm was installed in the path of the deuteron beam in the ion guide of the accelerator (see Fig. 1) and at the same time served as the bottom of a Faraday cylinder used to measure the deuteron current. The sample-irradiation chamber was placed on the outside of the ion guide (minimum distance between Be target and sample ~5 mm). Samples of materials containing fluorine were packed in polyethylene ampuls with a diameter of 18 mm and a height of 40 mm and after irradiation were delivered to the detection station. The induced activity was detected by the ^{16}N γ radiation in the energy range 4.0-7.2 MeV by using a scintillation detection unit with a NaI(Tl) crystal of 150 × 150 mm with a well, connected to an LP-4840 pulse-height analyzer or with a single-channel analyzer.

The fluorine in the samples was determined by comparison with a standard sample or by separate cyclic irradiation of the samples and measurement with irradiation for 25 sec, cooling for 2 sec, and detection for 15 sec, for six cycles. The neutron flux was monitored by the deuteron current on the target during irradiation of the sample.

The procedure for determining fluorine by using the MLUD-3 as a neutron generator was tested in the analysis of zirconium samples. The fluorine by using the MLUD-3 as a neutron-activation technique for five zirconium samples was 0.011, 0.019, 0.033, 0.11, and 0.79 wt. % as compared to 0.010;

Translated from Atomnaya Énergiya, Vol. 45, No. 6, pp. 456-457, December, 1978. Original article submitted February 16, 1978.

0038-531X/78/4506-1192$07.50

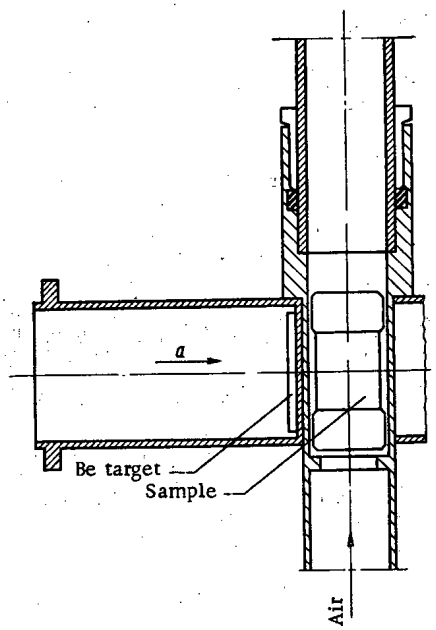

Fig. 1. Irradiation position.

0.018; 0.034; 0.11, and 0.80 wt. %, respectively, by the chemical method. The standard deviation of the results of fluorine determination by activation analysis is 5% for a fluorine content of 0.02 wt. % and for a series of 11 parallel measurements. This characterizes good accuracy and reproducibility of analysis in a linear accelerator with the chosen method of neutron flux monitoring.

The lower limit of detection of fluorine is 0.1 mg (which corresponds to 10^{-3} wt. % for a 10-g sample) with a deuteron current of 0.3 μA and an analysis time of 4 min (6 cycles). For comparison, it may be pointed out that when a ^{238}Pu–Be neutron source with a total yield of 10^8 neutrons/sec is used for activation, the lower limit of fluorine detection by the given technique is 1 mg, all other conditions being equal [2]. An increase in the deuteron current by two orders of magnitude, which in principle can be attained in a MLUD-3 accelerator [6] or in accelerators with similar characteristics permits a practically proportional increase in the neutron flux and enhancement of the sensitivity of neutron-activation determination, of fluorine in the given case. Along with their small size, simplicity of control, and stability of neutron yield, such accelerators create favorable prerequisites for the introduction of neutron-activation techniques employing small acclerators in technological inspection.

LITERATURE CITED

1. T. Lauff, E. Champlin, and E. Przybylowicz, Anal. Chem., 45, No. 1, 52 (1973).
2. V. I. Melent'ev, V. V. Ovechkin, and V. S. Rudenko, At. Energ., 34, No. 1, 35 (1973).
3. I. N. Ivanov, N. Yu. Markun, and A. S. Shtan', in: Proceedings of the All-Union Research Institute for Radiation Technology [in Russian], Atomizdat, Moscow, No. 6 (1971), p. 131.
4. K. Jinno and D. Ishii, Radioisotopes, 19, No. 9, 406 (1970).
5. L. N. Baranov et al., in: Problems of Atomic Science and Engineering, "High-Energy and Nuclear Physics" Series [in Russian] Izd. Fiz. Tekhn. Inst. Akad. Ukr. SSR, Kharkov, No. 1 (13) (1975), p. 15.
6. L. N. Baranov et al., in: Digests of Papers of Fourth All-Union Seminar on Linear Accelerators [in Russian], Izd. Fiz.-Tekh. Inst. Akad. Ukr. SSR, Kharkov (1976), p. 10.

RADIAL REACTOR STABILITY AND AUTOMATIC REGULATOR

B. Z. Torlin

UDC 621.039.562

It was shown in [1] that the effect of an automatic regulator (AR) on the axial xenon stability of a neutron field could be substantial. A detailed analysis of the radial stability of a reactor can also be carried out by practically the same method. As will be shown below, the automatic regulator in this case has a radical effect on the spatial stability.

To begin with, let us consider the very common case in which the automatic regulation rod is located in the center of a cylindrical reactor of radius R. It is convenient to express all dimensions in fractions of R. Therefore, R = 1. As was done in [1], we shall evaluate the degree of stability of the neutron field in a reactor with the material parameter B_0 as the value of the minimum eigenvalue μ of the boundary-value problem

$$\Delta\varphi + B_0^2\varphi + \mu\varphi = 0 \tag{1}$$

with uniform boundary conditions at the outer reactor surface and at the absorbing-rod surface. The necessary controlling action of the rod is attained by choosing such boundary conditions at its surface that would satisfy the algorithm for the operation of a high-speed astatic regulator:

$$\int_V K\varphi\, dV = 0, \tag{2}$$

where K is the weight function for shaping the control signal from the detectors. The form of function K and condition (2) for local and distributed systems for the collection of neutron-field data were discussed in [1]. For example, a single local detector installed at point r_d with polar coordinates $\{r_d, \vartheta_d\}$ turns condition (2) into the condition

$$\varphi(r_d) = 0. \tag{3}$$

For a homogeneous reactor satisfying condition (3), the solutions of Eq. (1) are of the form

$$\text{a)}\ \varphi_0 = J_0(Br) - N_0(Br)\, T_0(B), \tag{4}$$

where J_n and N_n, respectively, are Bessel and Neumann functions of order n, and $T_n(B)$ is determined by the boundary conditions at the outer surface; for a reactor with an unflattened steady-state distribution of the neutron field in the form $J_0(B_0 r)$ for $B_0 = 2.405$, we have

$$T_n(B) = J_n(B)/N_n(B); \tag{5}$$

for a reactor with a completely flattened steady-state neutron field for $B_0 = 0$, we have

$$T_n(B) = J_n'(B)/N_n'(B). \tag{6}$$

The eigenvalue B is found from

$$J_0(Br_d)/N_0(Br_d) = T_0(B). \tag{7}$$

$$\text{b)}\ \varphi_n^{(1)} = J_n(Br)\sin n(\vartheta - \vartheta_d), \quad n \geqslant 1, \tag{8}$$

where B is the root of the Bessel function. We have

$$J_n(B) = 0, \tag{9a}$$

if $B_0 = 2.405$, or

$$J_n'(B) = 0, \tag{9b}$$

if $B_0 = 0$

$$\text{c)}\ \varphi_n^{(2)} = J_n(Br)\cos n(\vartheta - \vartheta_d) - A_n\varphi_0(r), \quad n \geqslant 1. \tag{10}$$

Translated from Atomnaya Énergiya, Vol. 45, No. 6, pp. 457-459, December, 1978. Original article submitted March 6, 1978.

0038-531X/78/4506-1194$07.50

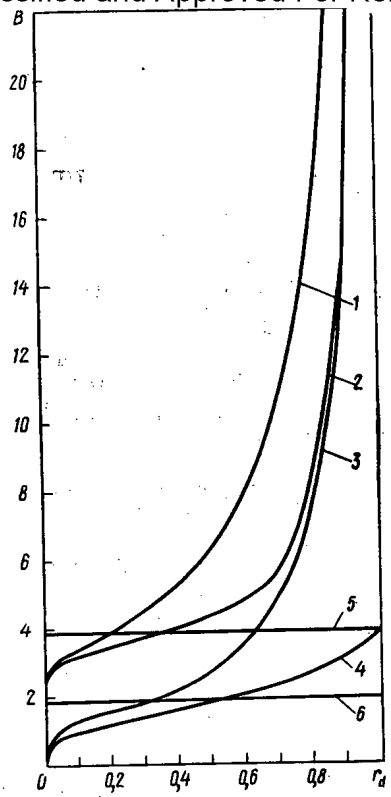

Fig. 1

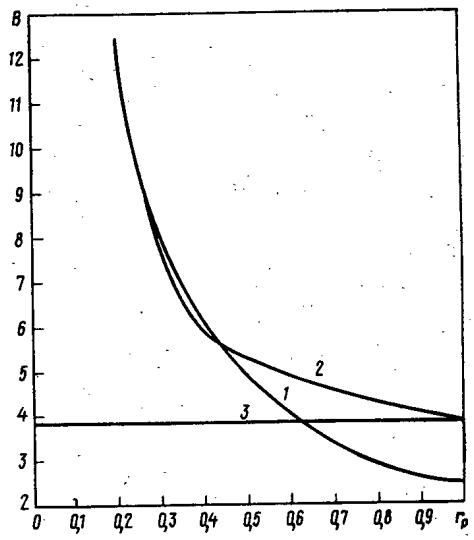

Fig. 2

Fig. 1. Minimum eigenvalues for radial mode (1-4) and axial modes (5-6) of reactor with central automatic regulator: 1, 2, and 5) unflattened distribution of neutron field [in form $J_0(B_0 r)$, $B_0 = 2.405$]; 3, 4, and 6) completely flattened neutron field ($B_0 = 0$); 1, 3) automatic regulation detectors installed at distance r_d from reactor axis; 2, 4) automatic regulator maintains power in zone of radius r_d.

Fig. 2. Minimum eigenvalues for radial mode of reactor with automatic regulator rods arranged at distance r_p from axis: 1) automatic regulator controlled by external ionization chambers; 2, 3) automatic regulator maintains full reactor power with, respectively, unflattened and completely flattened radial neutron field.

where

$$A_n = J_n (Br_d)/\varphi_0 (r_d), \tag{11}$$

and B is found from Eq. (9).

Henceforth B will be related to μ by

$$B^2 = B_0^2 + \mu. \tag{12}$$

The characteristic solution of Eq. (4) will be called the radial mode and the other solutions, the azimuthal modes. It is a priori clear that the central regulator cannot affect the stability of the azimuthal mode and alter the spectrum of their eigenvalues [2].

The solutions given above were obtained for an automatic regulator controlled by an individual sensor. The signal from a group of sensors is practically always used in automatic regulation systems. Suppose, e.g., that this is the signal from a group of identical detectors placed symmetrically with respect to the azimuthal angle ϑ at a distance r_d from the reactor axis. It is easily shown that in comparison with the solutions given above, there will be a change only in the form of the eigenfunction $\varphi_n^{(2)}$. The spectrum of the eigenvalues and, therefore, the stability of the system remain the same as before. The eigenvalue spectrum of the radial mode is changed when the automatic regulator maintains the power in an entire zone of radius r_d about the

center of the reactor, i.e., $\int_0^{2\pi} d\vartheta \int_0^{r_d} \varphi\, r dr = 0$ (obviously, when $r_d = 1$ the regulator will maintain full reactor power). Although in this case the radial mode will be of the form (4) and their eigenvalues will be found from

$$[N_1(Br_d) + 2/\pi Br_d]\, T_0(B) = J_1(Br_d). \tag{13}$$

The eigenvalues B for the radial mode were found as a function of r_d by solving Eqs. (4) [3] and (13); their minimum values are shown in Fig. 1 (1-4); curves 5 and 6 correspond to the minimum eigenvalues for azimuthal modes: B = 3.83 from Eq. (9a) and B = 1.84 from Eq. (9b).

Comparison of curves 1 and 2 with 5 and curves 3 and 4 with 6 shows that if the detectors are at an insufficient distance from the automatic regulation rod, the spatial stability of the reactor will be determined by the radial mode and not the axial modes, as follows from [2, 4]. If the sensors are placed too close to the rod, there is a considerable deterioration of the radial stability of the reactor and in fact it becomes impossible to maintain its power. Conversely, arrangement of the sensors so that the control signal is produced by the variation of neutron field at the boundary of the reactor (Fig. 1, curves 1 and 3 as $r_d \to 1$) altogether eliminates the possibility of radial instability ($B \to \infty$ for the radial mode). This conclusion is an important argument in favor of the traditional arrangement of ionization chambers for the automatic regulation at the periphery of the reactor. Curves 2 and 4 show that the same tendencies also hold for an automatic regulator set to maintain power. It has turned out, it is true, that for a reactor with a flattened radial neutron field a central automatic regulator maintaining the power does not entirely eliminate the possibility of radial instability (B = 3.83 as $r_d \to 1$). Let us next consider an automatic regulator whose actuator consists not of an individual rod but of a group of identical absorption rods which are moved simultaneously and which are arranged symmetrically about the azimuth ϑ at a distance r_p from the reactor axis. By the "addition theorem" [3] for Bessel functions we transform the weighting functions of these rods to a system of polar coordinates with center on the reactor axis, this transformation being the usual transformation of heterogeneous theory [5].

The radial mode φ_p will be of the form

$$\varphi_p = \left\{ \begin{matrix} J_0(Br)\,\varphi_0(r_p) \text{ for } 0 \leqslant r \leqslant r_p \\ J_0(Br_p)\,\varphi_0(r) \text{ for } r_p \leqslant r \leqslant 1 \end{matrix} \right\} + 2D(r, \vartheta). \tag{14}$$

The form of the functions D (r, ϑ) depends on the number of rods in the group. For example, for four rods with coordinates (r_p, 0), (r_p, $\pi/2$), r_p, π), and (r_p, $-\pi/2$) it is of the form

$$D(r, \vartheta) = \begin{cases} \sum_{n=1}^{\infty} J_{4n}(Br)[J_{4n}(Br_p) - N_{4n}(Br_p)T_{4n}(B)] \\ \qquad \text{for } 0 \leqslant r \leqslant r_p; \\ \sum_{n=1}^{\infty} J_{4n}(Br_p)[J_{4n}(Br) - N_{4n}(Br)T_{4n}(B)] \\ \qquad \text{for } r_p \leqslant r \leqslant 1. \end{cases} \tag{15}$$

The minimum eigenvalues of the radial mode in the case when the signal controlling the automatic regulator is formed by a group of peripheral ionization chambers is described by (curve 1, Fig. 2):

$$B = 2.405/r_p. \tag{16}$$

Curves 2 and 3 show the r_p dependence of the minimum eigenvalues of the radial mode (14), determined from

$$J_0(B) = J_0(Br_p) \tag{17}$$

or

$$J_1(B) = 0 \tag{18}$$

for the case when the automatic regulator maintains full reactor power with unflattened or flattened radial neutron field. Curves 1 and 2 illustrate the tendency for the radial stability of the system to improve as r_p decreases. This is particularly pronounced with external ionization chambers (curve 1) for a reactor with an unflattened radial field. When the distance of the automatic regulation rod to the ionization chambers is less than 0.38 of the reactor radius from the ionization chambers, the radial mode stability becomes worse than the minimum azimuthal stability.

In conclusion, we note that for an automatic regulator with absorbing rods arranged uniformly in the reactor core the eigenvalue spectrum of the system has the character of a Randall spectrum [2], regardless of the form of the controlled parameter, as shown in [1].

The author is indebted to A. D. Galanin and Ya. D. Shevelev for their interest in the paper and their useful discussion and valuable comments.

LITERATURE CITED

1. A. M. Afanas'ev and B. Z. Torlin, At. Energ., 43, No. 4, 243 (1977).
2. D. Randall and D. John, Nucleonics, 16, 82 (1958).
3. E. Janke, F. Emde, and F. Losch, Special Functions [Russian translation], Nauka, Moscow (1964).
4. A. Hitchcock, Nuclear Reactor Stability [Russian translation], Gosatomizdat, Moscow (1963).
5. A. D. Galanin, The Theory of the Heterogeneous Reactor [in Russian], Atomizdat, Moscow (1971).

EXPERIMENTAL DETERMINATION OF NEUTRON LEAKAGE FROM A MANGANESE BATH

A. V. Sorokina, É. A. Shlyamin,
K. A. Petrzhak, G. E. Lozhkomoev,
A. G. Prusakov, and Ya. M. Kramarovskii

UDC 621.039.512.4:
539.125.5.03

The manganese bath method ensures the highest accuracy of absolute measurements of the total flux of neutrons from various sources. This method is rather simple technically, but requires the introduction of several corrections, including one for the neutron leakage from the bath.

Fast neutrons are slowed down in an aqueous solution of manganese sulfate mainly by elastic scattering from hydrogen nuclei. After the first few collisions a neutron is thermalized and captured in a relatively short distance. The spatial distribution of slow neutrons in a moderator depends on the fast neutrons and on the diffusion process, which plays a more important role near the source because of the large slow-neutron density gradient there. The slow-neutron density at first decreases rapidly with distance from the source and then more slowly. As a result of the $4\pi r^2$ geometry factor, the spatial distribution of slow neutrons in a moderator will have a maximum at a position determined by the moderator properties and the energy spectrum of the source neutrons, and at large distances can be approximated by an exponential function with an exponent α which depends on the average energy of the source neutrons and the moderating properties of the medium [1].

The area under the curve describing the spatial distribution of neutrons in an infinite moderator characterizes the source strength. The fraction l of the neutrons passing beyond a hypothetical spherical surface of radius $r > r_e$ can be found from the ratio of the area under the spatial distribution curve extrapolated exponentially from the spherical surface to ∞, to the total area in an infinite moderator:

$$l(r_s)=\frac{\int_{r_s}^{\infty} n(r_s)\, r_s^2 \exp[-\alpha(r-r_s)]}{S_0}\, dr=\frac{n(r_s)\, r_s^2}{\alpha S_0}.$$

Since nr_s^2 falls off exponentially from the distance r_e, we have

$$l(r_s)=\frac{n(r_e)\, r_e^2 \exp(\alpha r_e)}{\alpha S_0}\exp(-\alpha r_s)=\frac{C}{\alpha S_0}\exp(-\alpha r_s), \quad (1)$$

where $n(r_s)$ is the neutron density at the hypothetical spherical surface; r_s, distance from the source to this surface; r_e, distance from the source to the place where the spatial distribution becomes exponential; and $n(r_e)$, neutron density at the distance r_e.

The product of all the quantities in front of $\exp(-\alpha r_s)$ is constant for a given source and moderator, and therefore the leakage can be written in the form

$$l=A\exp(-\alpha r) \quad \text{for} \quad r>r_e. \quad (2)$$

Translated from Atomnaya Énergiya, Vol. 45, No. 6, pp. 459-461, December, 1978. Original article submitted April 3, 1978.

0038-531X/78/4506-1197$07.50

To determine the actual leakage it is necessary to take account of the change of moderating conditions beyond the medium-air boundary, i.e., the decrease in the probability of the return of a neutron through the boundary into the moderator. A theoretical estimate [2] shows that ~20% of the thermal neutrons at a water-air boundary diffuse past the boundary. In addition, ~20% of the fast neutrons crossing the boundary and slowing down beyond it do not return to the moderator. Thus, the total fraction of neutrons which do not return to the moderator is ~40%, and consequently the leakage increases by 40%. As a result of the large total cross section for neutron capture by a concentrated solution of manganese sulfate, this value was decreased to 30%. The correction for the difference in the moderating properties of water and a manganese sulfate solution in estimating the effect of the boundary was determined experimentally in [3]. Measurements with indium foils gave an albedo $\gamma = 0.52$ for thermal neutrons in a manganese sulfate solution.

Assuming that

$$\gamma = [d - (2/3)\lambda_{tr}]/[d + (2/3)\lambda_{tr}],$$

and that the neutron transport length λ_{tr} is the same in water and in a manganese sulfate solution, and using an albedo of 0.84 for thermal neutrons in water obtained by Feld [4], Davy [3] calculated the ratio of the extrapolation lengths d for a manganese sulfate solution and water to be 0.28. Since the neutron flux falls to zero at a distance beyond the boundary equal to the extrapolation length, the boundary effect of a manganese sulfate solution is reduced to (0.28) (0.40) = 0.11; i.e., the leakage increases by only 11%. Thus, a factor must be introduced into the expression for the leakage to take account of the boundary effect, i.e.,

$$l = A \cdot B \exp(-\alpha r). \tag{3}$$

We have measured three parameters for neutrons from a ^{252}Cf spontaneous fission source and an AmBe (α, n) source in a spherical manganese bath. The bath was a steel sphere 100 cm in diameter with a practically point source of 11.3 μg of ^{252}Cf or an AmBe (α, n) source at the center. The bath was filled with an aqueous solution of highly purified manganese sulfate with a concentration of 25.98 g/100 g of solution. The thermal neutron density n(r) was measured with a movable Mark SNM-13 boron counter at distances of 2-36 cm from the source. The curves obtained for the spatial distribution of thermal neutrons $n(r)r^2$ had the usual form for hydrogenous moderators with maxima at 8.4 and 10.6 cm and exponential fall-off for $r > 17$ cm and $r > 22$ cm for the Cf and AmBe (α, n) sources, respectively. The exponents α and the parameter C in Eq. (1) were determined at distances of 17-27 cm for the Cf source and 22-36 cm for the AmBe (α, n) source by the method of least squares.

The total areas under the curves for the spatial distribution of neutrons as $r \to \infty$, which determine the number of neutrons emitted by the sources per unit time, were found by adding the areas under the experimental curves from $r = 0$ to $r = 17$ for the Cf source and from $r = 0$ to $r = 22$ for the AmBe (α, n) source, found by numerical integration, to the areas under the curves extrapolated exponentially to ∞ from $r = 17$ cm and $r = 22$ cm respectively.

The rms deviation in determining the total area was 0.8 and 1.1% for the Cf and AmBe (α, n) sources, respectively.

The values of the preexponential factor A in Eq. (2) for the leakage, calculated from the experimental results, were 2.78 ± 0.02 and 2.63 ± 0.05 for neutrons from the Cf and AmBe (α, n) sources, respectively.

The coefficient B in Eq. (3), which takes account of the boundary effect, was determined in a separate experiment for the boundary between the manganese sulfate solution and air. To do this a plastic sphere with an inside diameter of 23 cm was filled with the working solution and placed in a large bath. Either the Cf or the AmBe (α, n) source was placed at the center of the small sphere. After the ^{56}Mn activity was saturated the small sphere was removed from the bath and the induced manganese activity was measured under standard conditions with a 60 × 60 NaI(Tl) crystal in combination with an FÉU-82. The manganese sulfate solution was then removed from the bath and the experiment on the activation of the solution in the small sphere was repeated.

The activity of the solution in the small sphere, reduced to the same time after irradiation, and determining the strength of the neutron source and the leakage from it, can be written in the following form: $A_1 = C(1 - l_1)$; $A_2 = C(1 - l_2)$; $l_2 = Bl_1$, where l_1 and l_2 are the neutron leakages from the small sphere in the first and second cases. The leakage l was found from the spatial distribution of slow neutrons in the manganese sulfate solution by assuming that the moderator was infinite and calculating the ratio of the area under the experimental curve from 0 to 11.5 cm to the total area S_0 (Table 1).

TABLE 1. Characteristics of Two Types of Sources

Source	A_2/A_1	l_1	B
^{252}Cf	0,87	0,429	1,17±0,02
AmBe (αn)	0,78	0,637	1,12±0,03

TABLE 2. Parameters of the Neutron Leakage Formulas for Various Neutron Sources

Type of source	Moderator	N_{Mn}/N_H	Parameters characterizing the leakage		
			α	A	B
^{252}Cf	H_2O	0	0,1439±0,0006	2,94±0,02	1,4*
	Aqueous solution $MnSO_4$	0,02094	0,1599±0,0003	2,77±0,02	1,17±0,02
AmBe (αn)	H_2O	0	0,1015±0,0005	2,35±0,04	1,4*
	Aqueous solution $MnSO_4$	0,02094	0,1162±0,0003	2,63±0,05	1,12±0,03
RaBe (αn)†	H_2O	0	0,1041±0,0004	1,96±0,02	1,4*
	Aqueous solution $MnSO_4$	0,0238	0,1073±0,0012	1,86±0,06	—

*Taken from [2].
†All values for this source are from [5].

In addition, the spatial distributions of slow neutrons from the ^{252}Cf and AmBe(α, n) sources were measured in water, and the parameters A and α which determine the neutron leakage from the sphere filled with water were evaluated (Table 2).

Analysis of the data of [5] permitted the calculation of the parameters α and A of the exponential function determining the neutron leakage for a RaBe (α, n) source in a manganese sulfate solution and the tracing of the dependence of these parameters on the ratio of the number of manganese atoms to the number of hydrogen atoms. Within the limits of experimental error this dependence can be represented by the linear relation $\alpha = 0.1041 + 0.14\,(N_{Mn}/N_H)$; $A = 1.96 - 2.93\,(N_{Mn}/N_H)$.

LITERATURE CITED

1. K. A. Petrzhak and M. A. Bak, in: Proceedings of the V. G. Khlopin Radium Institute [in Russian], Vol. 7, No. 1, (1956), p. 61.
2. G. Hanna and O. Runnalls, Canad. J. Phys., 34, 959 (1956).
3. D. Davy, J. Nucl. Energy, 20, 277 (1966).
4. B. Feld, in: Experimental Nuclear Physics, Vol. 2, Wiley, New York (1953), p. 490.
5. K. A. Petrzhak et al., [see Ref. 1], p. 31.

POSSIBILITY OF ACOUSTICALLY DETECTING THE BOILING OF SODIUM IN A FAST REACTOR BY MEANS OF A PULSED SYSTEM

B. V. Kebadze, K. A. Aleksandrov, and V. V. Golovanov

UDC 631.039.534.6

The main source of acoustic noise during the boiling of sodium is the collapse of vapor bubbles in the underheated liquid, which is why the signals are of a pulsed nature. In the spectral analysis of acoustic signals that is used in most experimental studies on boiling, these characteristic features are not taken into account, and the problem of detecting boiling reduces to monitoring the dispersion of the noise in some frequency band. Since, as a rule, no boiling-specific frequencies are observed in the spectrum, such a detection system is sensitive to a change in the background-noise level, e.g., a change caused by variation of the rate of flow through the reactor. The purpose of the present study is to evaluate the possibility of a detection system which makes use of the pulsed nature of the signals.

In order to study the structure of the acoustic signals in experiments with boiling on the Bor-60 reactor (V. A. Afanas'ev et al., At. Energ., 45, No. 5, 338 (1978)), we used a statistical processing of a tape recording of the signals and a recording on a loop oscillograph. Under some conditions the initial period of boiling is accompanied by an intensive, long-lasting (0.1 sec), practically continuous acoustic noise. An analysis of the signals obtained from the acoustic, temperature, and neutron sensors shows that these conditions are characterized by a rapid boiling of the sodium, with subsequent ejection of a large volume of the vapor phase into the region of underheated liquid and the generation of acoustic noise during the process of bubble collapse. After this comes the steady-state boiling condition, during which individual bubbles of relatively small size separate from the vapor volume and collapse, forming a random sequence of acoustic bursts. (Fig. 1a). Their total duration is a small fraction of the total observation time.

In operating conditions with a "softer" onset of boiling (for example, when the power is increased less rapidly) the initial long-lasting burst is absent, and the nature of the signals corresponds from the outset to the steady-state condition. Let us analyze the special features of the signals and the detection system for such a boiling regime. The duration of short-lived bursts (on the order of milliseconds) is considerably longer than that of the pressure pulse accompanying the collapse of a bubble with the dimension characteristic of this assembly (see the above-mentioned article by V. A. Afanas'ev et al.); this is explained by the fact that the sensor records both direct and multiply reflected pulses. Owing to the resonance properties of the sensors, the pulses are converted to a series of intersecting radio pulses; a burst takes on the form of a noiselike signal (Fig. 1b). Since the dimensions of the bubbles and the coordinates of their points of collapse are statistically distributed, the amplitudes and shapes of the bursts are different. In some cases pulses from different bubbles may be superimposed.

In the process of the experiment, using a diode detector, we formed the envelope of the acoustic signal (Fig. 1c) with a constant of integration corresponding approximately to the duration of the burst (~1 msec). From the acoustic bursts there is formed a sequence of pulses; an analysis of a sample from 2000 such pulses indicated that the distribution of the amplitudes is satisfactorily described by Rayleigh statistics, and the tracking frequency by a Poisson distribution.

A pulsed detection system making use of the "fast" envelope generates a breakdown signal when it has accumulated a specified number of pulses exceeding some threshold during a given interval of time. It is necessary to calculate the probability of a false breakdown signal and the probability that a breakdown situation (boiling) will go undetected. If we disregard the possibility that the background noise will exceed the threshold, the probability of "accumulating" pulses and consequently not detecting a breakdown is increased somewhat, and this must be included in the calculation of the statistical reliability margin of the system. We also

Translated from Atomnaya Énergiya, Vol. 45, No. 6, pp. 461-463, December, 1978. Original article submitted April 7, 1978.

 0038-531X/78/4506-1200$07.50

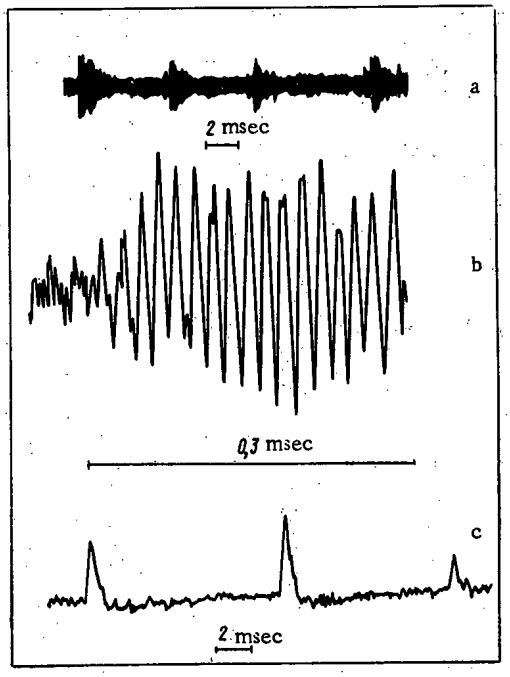

Fig. 1

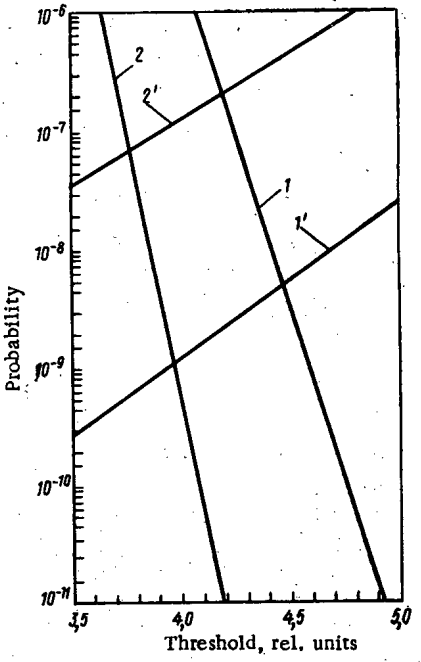

Fig. 2

Fig. 1. Signals from an immersed acoustic sensor in the steady-state boiling conditions: a) sequence of bursts; b) initial phase of burst; c) pulses of "fast" envelope of signal.

Fig. 2. Probability of nondetection (1', 2') and false triggering (1, 2) by a pulsed system, with m = 3 (1, 1') and m = 5 (2, 2') [the threshold value is referred to the standard of the background-noise envelope].

assumed that the distributions of the pulses with respect to amplitude and tracking interval were not correlated with each other. The probability r of exceeding the threshold S is given by the amplitude distribution function:

$$r=\int_S^\infty \frac{a}{\sigma_a^2}\exp\left(-a^2/2\sigma_a^2\right)da; \quad q=1-r,$$

where σ_a is the Rayleigh distribution parameter. Let m be the number of pulses that must be recorded during time T in order to produce the breakdown signal; let λ be the intensity with which the signal pulses appear. The probability that the system will not be triggered is given by the following relation:

$$P_{\text{nd}}=\sum_{k=0}^{m-1}P(k)+\sum_{k=m}^{\infty}P(k)\left[\sum_{i=0}^{m-1}C_k^i q^{k-i}r^i\right],$$

where $P(k)=(\lambda T)^k/k!\,[\exp(-\lambda T)]$ is the Poisson distribution.

Let us determine the probability that the system might be falsely triggered by background noise. The formation of the envelope is a nonlinear operation; it is possible, however, to represent the detected background noise in the form of a sequence of random pulses received by the integrating circuit. Since $\tau_{\text{int}} = 1\ \text{msec} \gg t_g$, where t_g is the average interval between pulses, the fluctuations at the outlet of the envelope former have a nearly normal distribution, a fact which is confirmed by experiment. For a random process with a normal distribution, the average number of times the level S is exceeded per unit time is given by the well-known relation

$$\lambda_{\text{n}}=T_{\text{eff}}^{-1}\exp\left(-S^2/2\sigma_{\text{n}}^2\right),$$

where T_{eff} is the effective period of the fluctuations of the background-signal envelope. Assuming that the times at which the threshold is exceeded have a Poisson distribution, we obtain an estimate for the probability of a false triggering:

$$P_{\text{ft}}=\sum_{k=m}^{\infty}\left[\frac{(\lambda_{\text{n}}T)^k}{k!}\right]\exp\left(-\lambda_{\text{n}}T\right).$$

The results of the calculations for the parameters of the signals used in the experiment ($\sigma_a/\sigma_n = 5.5$; $\lambda = 100$ sec^{-1}, λ_{n0} is the intensity with which the zero level (the threshold) is crossed by the background noise; $\lambda_{n0} = 600$ sec^{-1}) for $T = 0.3$ sec are shown in Fig. 2.

The relation between the probabilities of nondetection of a breakdown and false triggering must be determined from economic considerations. It is clear that a proper choice of threshold can ensure an acceptable probability of error over a short observation period.

ANNIVERSARIES

NIKOLAI NIKOLAEVICH PONOMAREV-STEPNOI

December 3, 1978, was the 50th birthday of Professor Nikolai Nikolaevich Ponomarev-Stepnoi, Dr. Tech. Sci., Deputy Editor-in-Chief of the journal Atomnaya Énergiya and head of the Department of High-Temperature Power Engineering at the I. V. Kurchatov Institute of Atomic Energy.

N. N. Ponomarev-Stepnoi is a representative of the Soviet school of atomic reactor construction founded by I. V. Kurchatov and A. P. Aleksandrov. In the scientific program in the Soviet Union for the construction of high-temperature reactors he has carried out a number of design and theoretical research projects on the physics of high-temperature reactors and has done work on their physical design and on the development of programs for experimental investigations on the principal physical problems of high-temperature power engineering. He is participating in design and construction work on prototypes of reactor facilities for technological purposes and for radiation chemistry, on a helium-cooled fast breeder reactor, etc.

Nikolai Nikolaevich is engaged in research on the direct conversion of energy. He is one of the creators and one of the scientific supervisors of the world's first high-temperature reactor-converter, "Romashka." Many papers by Nikolai Nikolaevich have been devoted to the study of various aspects and salient features of thermionic generator-reactors.

His scientific authority, benevolence, simplicity, and exacting requirements have enabled Nikolai Nikolaevich to put together a team of researchers in the Department of High-Temperature Power Engineering which he heads. Nikolai Nikolaevich infects those around him with his enormous energy and capacity for work. It was not without reason that Igor' Vasil'evich Kurchatov called him "double traction."

Since 1956 Nikolai Nikolaevich has been teaching at the S. Ordzhonikidze Moscow Aviation Institute where he is a professor. He has worked with great creative dedication on the editorial committee of Atomnaya Énergiya and on the editorial council of the Atomizdat publishing house.

The scientific work of N. N. Ponomarev-Stepnoi has been recognized with governmental awards: Two Orders of the Red Banner of Labor and medals.

The management of the I. V. Kurchatov Institute of Atomic Energy and the editorial board of Atomnaya Energiya congratulate Nikolai Nikolaevich on his fiftieth birthday and wish him further successes in his scientific work

---

Translated from Atomnaya Énergiya, Vol. 45, No. 6, p. 465, December, 1978.

0038-531X/78/4506-1203$07.50

FOURTH INTERNATIONAL CONFERENCE ON THE APPLICATION OF ZIRCONIUM IN THE ATOMIC INDUSTRY

B. S. Rodchenkov and A. N. Ivanov

The conference was held in Stratford-on-Avon (Gt. Britain) in June, 1978. Such conferences are held every two years and are the most representative forum of scientists engaged in the development of zirconium alloys as well as in research on their properties and various aspects of their behavior during use as structural reactor materials.

The Fourth Conference, in which more than 210 representatives of 21 countries participated, dealt with a narrow subject matter: the behavior of zirconium cans of fuel elements of nuclear power reactors and enhancement of the reliability of such cans in hypothetical emergency situations. The program envisaged the presentation and discussion of 39 papers from six countries; 18 from the U.S.A. (two jointly with Great Britain and Canada), six each from Great Britain and the Federal German Republic, five from Canada, and two each from Norway and Sweden, as well as a visit to the nuclear laboratories at Berkeley.

The main topics of the papers included:

the resistance of zirconium fuel-element cans to local fracture (behavior under strain, the mechanism of can–fuel interaction, resistance to corrosion-induced cracking under the effect of fission products, and the role of hydrogenation);

factors determining the dimensional stability of the cans (creep resistance, radiation-induced growth);

the characteristic features of the corrosion behavior of cans during the use of fuel elements in a reactor;

the strain behavior, the fracture strength and oxygen embrittlement of cans under unsteady and emergency conditions; simulation of the behavior of cans.

It should be noted that part of the papers reflected the results of investigations carried out in accordance with long-range national programs or programs of joint work by scientific research organizations and companies on the fabrication of fuel elements, e.g., the program of research on the efficiency of fuel elements under hypothetical emergency conditions, realized, in particular, by the U. S. Energy Research Institute in conjunction with five leading companies engaged in the fabrication of fuel elements with zirconium cans, and a program for ensuring the safety of nuclear reactors (Federal German Republic). Most of the papers were of a comprehensive nature and included the development of models of the processes taking place, thus making it possible to determine the general laws governing the effects studied and, within certain limits, to predict the behavior of fuel cans.

At the present time, alloys of the zircalloy type (Zircalloy 2 and 4) are used predominantly in the fabrication of fuel cans for power reactors, and this was reflected in the papers presented. Other well known zirconium alloys, such as those with 1% and 2.5% niobium, were considered only for the purpose of comparison.

In a review paper, J. Roberts (U.S.A.) discussed the interaction of the fuel with the can and the dimensional stability of fuel elements and fuel assemblies as a whole; these are the most important characteristics of the behavior of fuel elements in zircalloy cans which determine the estimation of the operating lifetime of the fuel elements and are responsible for an appreciable decrease in electrical energy production. In the U.S.A. restrictions on the operating conditions in order to prevent damage caused by the interaction of the fuel with the can mean a loss of up to 6% of the power, which is equivalent to an annual loss of 100 million dollars and by 1985 these losses will have grown to 400 million dollars. A research program has been drawn up to increase the efficiency of fuel elements in zirconium cans and implementation of this program will make it possible by 1980 to considerably reduce damage to fuel elements from fuel–can interaction. This is being

Translated from Atomnaya Énergiya, Vol. 45, No. 6, pp. 466-468, December, 1978.

 0038-531X/78/4506-1204$07.50

done by increasing the grain size in pelleted oxide fuel in order to cut down the yield of gaseous fission products and to produce the necessary texture of the metal on the inner surface of the can so as to increase the threshold stress for crack formation. It is planned to completely eliminate this form of damage by 1985 by creating a barrier on the inner surface of the can (either in the form of an electroplated copper coating 5-10 μ thick or in the form of a layer of pure zirconium produced by joint extrusion).

Ten papers were devoted to the study of various aspects of the interaction of fuel with the can. This effect is being considered as the main cause of local rupture of fuel cans during service. In the opinion of most researchers, rupture occurs by the mechanism of corrosion-induced cracking under stress in the presence of iodine (fission product). Iodine corrosion-induced cracking develops only under the partial condensation of iodine. Corrosion-induced cracking occurs when a threshold iodine concentration ($\sim 10^{-6}$ g/cm^2 at 400°C) is surpassed and the stress, growing under the effect of irradiation and cold working, exceeds a threshold value. The sensitivity of the material to iodine corrosion-induced cracking depends on the texture, the most disadvantageous being a texture with the normals of the (0002) plane making an angle of ± 50-70° to the radial direction. The presence of a hydride layer on the can surface prevented or slowed down iodine corrosion-induced cracking. Moreover, B. Cox (Canada) showed that the formation of cracks along radially oriented hydrides can stimulate the first stage of iodine corrosion-induced cracking. According to the data of N. Stele (Federal German Republic), iodine corrosion-induced cracking speeds up appreciably when a certain threshold of linear energy release is surpassed. On the basis of research on the effect of various fission products on the rupture of zircalloy cans, W. Grabb (U.S.A.) came to the conclusion that only iodine causes corrosion-induced cracking to develop whereas the presence of cadmium results in embrittlement.

In nuclear power reactors zircalloy suffers uniform corrosion with the formation of a thin oxide film (in PWR), accelerated corrosion (oxide film thickness of up to 100 μ), and local corrosion with the formation of bulges of up to 300-500 μ (in BWR). According to the data of K. Widem and L. Lunde (Norway), the increase in the oxidation rate at focal points is the result of the oxide film cracking at grain boundaries and is reduced by the addition of chromium to the alloys. Studies performed on the SGHWR (Gt. Britain) established that local acceleration of the oxidation of zircalloy cans is not accompanied by increased hydrogen absorption and is observed at a neutron flux density above $1 \cdot 10^{13}$ neutrons/cm$^2 \cdot$ sec. Such acceleration is promoted by perturbations in the coolant flow, an unrecrystallized structure of the metal, and the existence of a galvanic pair consisting of zircalloy and austenitic stainless steel (the greatest bulges in the oxide film are observed near stainless steel spacer grids).

The dimensional stability of fuel cans and assemblies was discussed in seven papers. It was noted that the diameter and length of fuel elements may change during service and bending which occurs changes the clearance of fuel assemblies. Changes in the linear dimensions (diameter and length) of the fuel cans were caused by the total effect of creep and radiation-induced growth. Radiation-induced growth does not depend on external stresses and is determined by the type of alloy, its structural state and texture, and by the irradiation conditions (fluence and temperature).

R. Murgatroyd and S. Mepforn (Great Britain) discovered that the radiation-induced growth of recrystallized Zircalloy 2 is characterized by rapid attainment of the stage of saturation (at a fluence of $2 \cdot 10^{20}$ neutrons/cm^2) whereas in the cold-worked alloy it continues uninterruptedly as the fluence increases. A temporary interruption of the irradiation may lead to a partial relaxation of the radiation-induced growth. A change in the diameter of the cans is described well by the empirical relation $\Delta d/d = -K\Phi^{0.85}\sigma t^{0.65}$, where t is the time, Φ is the fast neutron flux, σ is the stress, and K is a coefficient allowing for the degree of recrystallization of the alloy and the texture.

S. Buckley et al., (Great Britain) presented the results of investigations on the mechanism of radiation-induced growth and the effect of alloying on it. In the experiments radiation damage was imitated directly in an electron microscope.

According to the data of J. Roberts (U.S.A.) in a PWR the bending suffered by fuel elements with zircalloy cans increases with the burn-up but stabilizes at burn-ups above 15,000 MW$\cdot$day/ton U. A practical problem confronting researchers is that of reducing the changes caused in the clearance of the fuel assembly by the fuel cans bending. Alloys with a higher creep resistance, in particular, are being used for this purpose. In BWR the bending of fuel elements is insignificant and the reduction in the clearance does not exceed 17%.

More than a third of the papers read were devoted to nuclear reactor safety and reliability and, in connection with this, to the behavior of fuel cans under the conditions of hypothetical emergency situations due to the loss of cooling agent (LOCA) or inadequate cooling (occurrence of film boiling). P. Hoffman (Federal

Republic of Germany) showed that under the conditions of LOCA fuel cans may experience brittle fracture at a temperature of less than 850°C as the result of the development of iodine corrosion-induced cracking and a decrease in ductility. At a higher temperature the presence of iodine (up to 10 mg/cm^3) does not affect the strain behavior of the cans. The character and the tangential strain depend on the temperature range and the temperature gradient on the can perimeter: With small gradients the tangential strain is considerable whereas with low gradients it is very small.

As established by R. Chapman (U.S.A.) a high heating rate (~30°C/sec) and a high temperature gradient on the can perimeter lead to a considerable localization of the strain and the formation of bulges. In the opinion of most researchers LOCA conditions are best reproduced by using simulators with internal heaters. Heating by the passage of a current causes increased tangential strain. Changes in the diametral gap along the can perimeter as well as differences in the cooling efficiency of various segments of the surface determine the character of the strain behavior and rupture. Irradiation has little effect on the tangential strain and the rupturing pressure of cans under high-temperature unsteady heating.

High-temperature heating with LOCA is accompanied by appreciable oxidation of the can. Subsequent emergency cooling may result in high stresses and brittle fracture. Under the conditions of film boiling the can may be pressed to the fuel rod, thus facilitating the development of diffusion interaction which, in turn, leads to further penetration of oxygen in quantities comparable to those occurring in the case of corrosion and affects the strain behavior of the can and the creep resistance.

Major attention is being paid to the estimation of the allowable embrittlement in the case of emergency situations with high-temperature heating. A paper by A. Zawadzki (Canada) showed that the present criterion elaborated for oxygen embrittlement on the basis of isothermal experiments (oxidation of under 17% of the can thickness and maximum heating temperature of 1477°K) is extremely cautious and it is, therefore, proposed to take an allowable oxygen content of 0.7 wt. % at half the can thickness. A similar conclusion was advanced by N. Chang et al., (U.S.A.) because of the conditions of thermal shock during emergency cooling. Several quantitative criteria are proposed for establishing the allowable oxygen content, e.g., the value of the dynamic fracture toughness, the thickness of the layer with a β-phase structure, etc. The use of all of these criteria, however, requires further research.

Great interest was aroused by the paper given by F. Erbacher et al., (Federal Republic of Germany) on the results of studies on the strain behavior of simulators of fuel assemblies under LOCA conditions, with an analysis of the character of the interaction, the dimensional stability, and the variations in the clearance.

Four U. S. papers and one Canadian paper considered the use of mathematical modeling to study the strain behavior of cans under steady-state and emergency conditions as well as to assess the kinetics of can oxidation under interaction with UO_2 and the oxygen distribution over the can thickness under various cooling conditions.

During the conference the Kroll memorial medal was ceremoniously presented to the eminent U. S. scientist, B. Lastman, who read a review paper "Zirconium technology. Twenty years of development."

The next, fifth conference is to be held in Boston, Mass., in 1980.

ALL-UNION SEMINAR ON THE PROCESSING TECHNOLOGY FOR ORES, AND RARE, DISPERSED, AND RADIOACTIVE ELEMENTS

V. A. Pchelkin and É. A. Semenova

The seminar was held in Moscow in May and June, 1978, with the participation of specialists of organizations and enterprises of the Ministries of Nonferrous and Ferrous Metallurgies, Geology, and the Chemical Industry, the Ministries of Institutes of Higher Education of the USSR, and the Academy of Sciences of the USSR.

The introductory address to the participants of the seminar was delivered by Academician B. N. Laskorin. He dealt with the development of work on the comprehensive utilization of processed raw material through the creation and introduction of technological schemes for the extraction of nonferrous, rare, disperse, and radioactive elements (molybdenum, copper, vanadium, zirconium, gold, rare-earth metals, strontium, fertilizers, and feed phosphates). He also spoke of the modernization of production through the introduction of new types of materials, equipment, and designs, of the widespread introduction of autoclave leaching, nonfiltration sorption methods, membrane technology, and the creation of new ion-exchange resins and flocculants, new equipment, and improvement of environmental protection.

The first plenary meeting heard five review papers. A paper by I. P. Smirnov and S. A. Pirkovskii was devoted to the application in autoclave technology of horizontal four-chamber autoclaves with mechanical mixers and vertical autoclaves with pneumatic pulp mixing. Alloyed steels and commercial titanium were recommended as structural materials.

Sorption methods of separating valuable accompanying elements during ore processing (paper by B. N. Laskorin and L. I. Vodolazov) facilitate the direct extraction of dissolved components from pulp and any density and guarantee the requisite degree of concentration and purification. As a result of the introduction of these methods in industry the productivity of plants was increased 1.5-3 times, the extraction of useful components rose by 5-10%, many technical operations harmful to the health were eliminated, and a continuous technology was created, ensuring total, comprehensive automation by the simplest, accessible control and inspection means.

Processes based on the application of selective membranes provide capabilities for purifying, separating, concentrating, and neutralizing various technological solutions and effluents, for intensifying leaching, oxidation, reduction, and winning of metals, and for separating and enriching gaseous mixtures (paper by N. M. Smirnova). In combination with other methods they make it possible to utilize valuable components, to reuse them, and to obviate the discharge of chemical reagents into the environment.

In a report on further perfection of pulp separation, washing of precipitates and clarification of solutions in hydrometallurgy the main attention was on the application of polyacrylamide and other types of flocculants as well as the development of new means and methods of intensifying these processes (paper by I. A. Yakubovich). There is particular interest in flotation-flocculation clarification of solutions as well as apparatus used for this purpose, fluidized-bed apparatus operating in a system of liquid and disperse solid particles. The extensive use of filter baffle plates based on synthetic materials has opened up prospects for improving the qualitative and quantitative indices of the separating processes.

Particular consideration was given to the use of incombustible solvents in extraction processes (paper by D. I. Skorovarov et al.). The use of tetrachloroethylene as a solvent for extracting agents in the flow sheets for extractive purification and recovery of some nonferrous and rare metals showed that the flow sheets developed have advantages over those using kerosene (a higher maximum extractant capacity, increased efficiency of extractive recovery, etc.). Oxy-oximes and aryl sulfonates were recommended for the extraction of copper, cobalt, and nickel, di(2-ethylhexyl) phosphoric acid was suggested for the extraction of indium and the iodine form of tributyl phosphate, for thallium. Recommendations were made about the extraction of gold

Translated from Atomnaya Énergiya, Vol. 45, No. 6, pp. 468-469, December, 1978.

0038-531X/78/4506-1207$07.50 © 1979 Plenum Publishing Corporation

from spent electrolytes by using trialkylamines and mixtures of them with neutral organophosphorus compounds of petroleum sulfoxides. It was pointed out that lead could be extracted from solutions from the processing of cassiterite ores by using solutions of tributyl phosphate, trialkyl benzyl ammonium chloride, and trialkylamine and that metals tending to form isopoly or heteropoly compounds (molybdenum and tungsten) could be extracted with trialkyl amines. Trialkyl amine and tributyl phosphate were recommended for the extraction of vanadium.

Liquid extraction with organic solvents was recognized to be an effective method of processing lean phosphorites, making it possible to obtain both pure phosphoric acid and commercial salts and high-grade fertilizers. The process is extremely promising because of its use of inexpensive, easily available, commercially produced solvents and because of its efficiency. The seminar heard a report on an extraction technology for processing lean phosphorites, making it possible to recover and utilize such useful components as fluorine, rare-earth elements, uranium, strontium, and scandium.

Methods have been developed for obtaining rare-earth alloying elements based on silicon for modifying cast irons and steels. A carbon-thermal method of obtaining alloying elements has been mastered on the pilot plant scale. Beforehand, the oxides are briquetted or molded with carbon. The continuous, slag-free process is carried out in standard ferroalloy furnaces. The recovery of the rare-earth metals in the alloying element is 95%. The composition of the alloying element is 30-60% rare-earth metals, 50-60% silicon, and the remainder is iron. The wide range of rare-earth metal content and the insignificant inclusions of foreign metals makes an almost universal and technological alloying element for adding to steel and case iron. An aluminum-thermal method of obtaining alloying elements has been introduced on a commercial scale. Rare-earth oxides are used for the reduction, which is effected by the aluminum. The charge contains ferrosilicon, calcium oxide, and fluorspar. The process is carried out periodically in electric steel-making furnaces. The direct recovery of the rare-earth metals in the alloying element reaches 65-70%. The composition of the alloying element is 30-40% rare-earth metals, 5-8% aluminum, 50-55% silicon, and the remainder is iron. It was noted at the seminar that an alloying element containing magnesium is especially promising for the modification of cast iron.

Beryllium alloys have been created with an enhanced set of mechanical and technological parameters in comparison with the standard grades. Microalloying with magnesium has made it possible to substantially improve the properties not only of extensively used highly alloyed grades of beryllium bronze with a beryllium content of 1.8-2.1%, but has also proved effective in alloys with a reduced beryllium content (to 1.6-1.8%).

The introduction of hydrometallurgical processes on a commercial scale was described by representatives of the Dnepropetrovsk Metallurgical Institute, the Zaporozhets Industrial Institute, and the Zaporozhets Machine-Building Institute ("On the application of rare-earth metals for the modification of cast irons and steels to obtain improved quality"), the Chelyabinsk Electrometallurgical Combine ("On the development of a technology for obtaining ferroalloys with rare-earth metals in industrial vacuum furnaces"), the All-Union Scientific-Research Institute for Chemical Engineering (VNIIKhT) ("On the use of an induction furnace with a cold crucible for obtaining homogeneous alloys from components with widely differing physical properties").

Great interest among the seminar participants was aroused by papers (V. P. Shulik, V. V. Orlov, E. L. Fenokhin et al.,) on the introduction of such methods and means of intensifying processes in hydrometallurgy and pyrometallurgy as optimized technical designs for ore plots, crushing mills, up-to-date grinding mills, cascade-type pulverizers, and the designs of a parametric series of leaching, sorption, and desorption apparatuses of the SNK, PIK, IPK, and USI.

It was pointed out at the seminar that considerable work has been done on the computation of the maximum allowable discharges of noxious substances into the atmosphere, on the decontamination and utilization of gaseous and liquid discharges, on the optimization of methods of determining toxic substances in the atmosphere, on the creation of new methods of analytical control for determining tantalum, niobium, individual rare-earth elements, low concentrations of rare and dispersed elements in minerals, extractants in mineral fertilizers, in effluents, as well as on the optimization of schemes for monitoring technological processes (paper by Yu. K. Kvaratshkeli, N. N. Tokarev, et al.).

The recommendations of the seminar reflected suggestions for improvements in the technology of processing the ores of rare, dispersed, and radioactive elements.

PROBLEMS OF FUEL UTILIZATION IN THE POWER INDUSTRY

B. E. Novikov

As a result of the predominant role of large atomic power plants, operating in the basic mode, in providing energy for the European part of the USSR the considerable daily fluctuations in the loads of the energy systems should be covered through reconstruction of existing highly-maneuverable, fossil-fueled energy units and construction of new ones.

The enhanced role of coal as a fuel for energy production gives rise to major problems. The principal reserves of coal and lignite are situated in the eastern regions of our country. A program of building large fuel and energy complexes in the eastern regions of the country will be carried out in order to reduce the cost of transporting fuel and energy from the East to the West.

The solution of these problems should be directed at the development of new methods of burning and treatment of solid fuel in order to reduce the metal content of boiler units, increasing fuel economy, and cutting down harmful discharges into the atmosphere.

These problems were the subject of the All-Union Meeting "New Methods of Fuel Utilization in the Power Industry" which met in Moscow on May 29 and 30, 1978, under the auspices of the Science Council of the Central Design Board at the Ministry of the Power Industry of the USSR and the G. M. Krzhizhanovskii Power Engineering Institute (ÉNIN). The more than 120 specialists from 47 organizations who attended heard and discussed 33 papers.

The review papers at the meeting were devoted to promising methods of burning solid fuel, the mechanisms by which noxious discharges are formed during combustion of organic fuel and, environmental protection.

The other papers could be arbitrarily divided into three groups.

Vortex Furnaces. The papers in this section of the meeting were devoted to the experience gained with the combustion of peat, pulverized lignite, and shale in vortex furnaces at a comparatively low temperature (the temperature at the combustion center is reduced by 100-200°C). This makes it possible to considerably cut down the slagging of the furnace and convective heating surfaces as well as to reduce the formation of nitrogen and sulfur oxides. At the present time furnaces of this type are used with boilers with a capacity of up to 500 tons/h. Some papers considered the use of a high-temperature furnace process in a special vortex chamber. It was pointed out that it would be possible to build powerful steam generators of only half the height for furnaces of this type.

"Fluidized-Bed" Combustion of Fuel. Work has recently been stepped up considerably on the development of steam generators for the fluidized-bed combustion of pulverized coal. Thus, a fluidized-bed boiler with a capacity of 10 tons of steam/h has been put into service. Design work is under way on powerful steam generators of this type.

The combustion of fuel in a fluidized bed appreciably intensifies heat exchange, significantly reduces the formation of nitrogen oxides, and allows the discharges of sulfur compounds to be cut by 90% in comparison with combustion in a chamber. Such steam generators have much smaller overall dimensions and, therefore, are cheaper.

Treatment and Gasification of Fuel Burners. At the present time work on the comprehensive use of fuel with thermal improvement of the fuel is of significance. A paper presented by ÉNIN gave the results of pilot-plant operations on the comprehensive treatment of Kansk–Achinsk coal, as well as shale. Interest has been aroused by a method being developed at the Institute of Combustible Minerals for the thermal processing of moist Siberian coal into heating coal with a heat of combustion of 7000 kcal/kg.

Translated from Atomnaya Énergiya, Vol. 45, No. 6, pp. 469-470, December, 1978.

0038-531X/78/4506-1209$07.50

Extensive work is being done on the development of various methods of gasifying coal. Note should be taken of promising development; work on processes with plasma gasification of coal (ÉNIN paper) and coal gasification in a fluidized-bed reactor with heat supplied to the reaction zone from a high-temperature external source of heat, viz., a furnace chamber or, in the future, a nuclear reactor.

A noteworthy paper was one on the development of gas burners operating on the principle of two-front combustion of gases with an extremely low heat of combustion. These burners ensure stable combustion of large quantities of low-calorie gas, which had not been used previously as a fuel and which contaminated the atmosphere.

In assessing the work of the meeting, one must point out that many important and interesting results were reported, results which will make it possible to develop and extend investigations on new methods of fuel utilization and will facilitate the introduction of these methods into the power industry.

INTERNATIONAL MEETING ON FAST-ATOM INJECTORS FOR THERMONUCLEAR FACILITIES

N. N. Semashko

The meeting, which was held at the Culham Laboratory (Great Britain) in June, 1978, was attended by some 50 persons; they heard and discussed more than 40 papers on the creation of powerful modern injectors and the trends in their development. The Soviet delegation presented papers on ion sources, the design principles of their electric supply and protection systems, and the design of the injector for the T-10M tokamak.

Ion Sources. At the present time there are four main types of high-current ion sources. Two of them make use of a discharge in a magnetic field (these are the so-called duopigatrons and the periplasmatrons) and the other two, outside a magnetic field (sources without an external magnetic field and with a peripheral magnetic field) (Table 1).

Ion Emitters. In the gas-discharge chambers of all types of sources a discharge is ignited, forming a plasma with a large area of ion emission (up to several hundred square centimeters) and a high degree of uniformity over the emission surface (no more than 10%).

The main problem in constructing gas-discharge ion emitters is that of developing a cathode with a long lifetime, increasing the energy efficiency of discharge, and attaining maximum proton component content in the extracted beam. The cathode still remains one of the weakest spots since its lifetime is limited. A pin-shaped tungsten cathode in sources without an external magnetic field, e.g., has a lifetime of 1000-2000 h. A search is under way for new types of cathodes; in particular, studies are being made of a hollow cathode of lanthanum hexaboride. The latter is considered to be a promising type.

Much attention is being paid to increasing the energy efficiency of the discharge or, in other words, to reducing the power lost in the discharge to obtain one ampere of extracted beam. In most modern sources the discharge efficiency lies within the range 0.5-1.5 A/kW. In the latest designs this figure has been raised to 3-4 A/kW, mainly by creating a so-called magnetic wall in the construction of the gas-discharge chamber. The magnetic wall was proposed in 1973 and displayed its positive qualities in the duopigatron. It helped improve the uniformity of ion emission. The sense of this wall consists in the following. A magnetic field is organized near the walls of the discharge chamber, this field is produced by a large number of permanent magnets which constitute a multipole magnetic system with alternating polarity. The magnetic field strength quickly falls off with distance into the chamber so that the main volume of the gas-discharge plasma, including the surface of ion emission lies outside the magnetic field. The magnetic wall substantially reduces the ion stream on it and thus increases the energy efficiency of the discharge. This wall has been developed in designs of a source without an external magnetic field.

Intense research is being done on ways of increasing the proton component content in the gas-discharge plasma and thus in the extracted beam as well. In particular, the use of a magnetic wall increases the proton component yield to a certain extent.

Translated from Atomnaya Énergiya, Vol. 45, No. 6, pp. 470-472, December, 1978.

 0038-531X/78/4506-1210$07.50

TABLE 1. Modern High-Current Sources

Source	Kind of particles	Beam current, A	Energy, keV	Pulse duration, sec	Gas eff., %	Energy eff., A/kW	Proton component fraction, %
Duopigatron, Oak Ridge, U.S.A.	H, D	70	45	0,2	50	2	80
	H*	100	80	0,02			
JAERI, Japan	H, D	35	75	0,01			
Periplasmatron, Fontenay-aux-Roses, France	H	35	30		50	2	70
	H*	60	30				
Without external magnetic field, Berkeley, U.S.A.	D	80	20	0,02	50	0,7	70
	D	15	120	0,5			
	D*	65	120	0,03			
I. V. Kurchatov Atomic Energy Institute	H, D	35	25	0,02			
	H	100	25	0,01			
	H	20	10	0,3			
With peripheral magnetic field, Calem, Gt. Britain	H	30	30	0,05	50	2—4	70
	H	50	25	0,01			
	H*	60	80	0,5			

*In development stage.

The gas efficiency of sources of modern design reaches 40-50% and for the time being does not need to be increased since use is made of a neutralizer which abuts directly on the source and utilizes the gas leaving the source. Particular attention is attracted by the problem of impurities which the source introduces and which may enter the thermonuclear apparatus. The trend has been to construct the sources' insulators from ceramic materials with a hard vacuum seal: by metal—ceramic soldering or, failing this, by a threaded seal. The effect of the material of the cathode and the ion-optical electrodes has not been studied adequately.

Ion-Optical System. An intense, weakly divergent ion beam is formed with the aid of a multiple-aperture ion-optical system, extracting ions from a large-area plasma emitter with a moderate current density (< 0.5 A/cm^2). Special attention has been devoted recently to calculations and experimental investigations on a two-stage system to obtain shaped ion streams with an energy of up to 120 keV.

In the multiple-aperture ion-optical system it is essential to shape each individual elementary beam in the set from which the complete ion beam is formed. Some discrepancy is observed: The minimum divergence of the first reaches ±0.5° whereas that of the second is no less than ±1°. Evidently, this is due to the non-uniformity of the plasma concentration on the emission surface, inaccuracy in the preparation of the electrodes, etc. The characteristics of ion-optical systems with slit and cylindrical apertures were discussed in detail at the meeting.

The formation of plasma in the neutralizer and its effect on the beam divergence are related directly to the ion-optical system shaping the beam and producing a minimum angle of divergence. The problems now being studied intensively include the formation of a reverse meniscus in the ion-optical system and its effect on the production of secondary particles, the interaction of elementary beams (strip or cylindrical), and the formation of static fields in the plasma of the neutralizer and their effect on the dynamics of the primary beam.

Much attention was devoted to the discussion of systems of the power supply to an ion-optical source and protection for it during breakdown. It is assumed that a power of no more than 5 J should be released in the electrode during breakdown. The ion source, therefore, should be isolated from the power supplies by passive power-limiting devices.

A considerable role in preventing breakdowns in the transient stage of the formation of an ion beam is played by the proper synchronization of pulses of discharge and high voltage.

The power supply accounts for about 60% of the cost of the injector and, therefore, careful attention must be paid to its design. Thus far no optimal supplies which would be sufficiently reliable in operation have been developed. This problem, as well as the development of a control system for a large number of ion sources, requires further research.

TABLE 2. Characteristics of High-Power Injection Systems of Large Apparatuses

Facility	Power, MW	Energy, keV	No. of injectors	No. of pulse sources in injector	Current of one source, A	Pulse duration, sec	Type of source
TFTR	20	120	4—6	3	70	0,5	Without external magnetic field
MFTF	24	20	—	24	80	0,01	Same
	18	80	—	24	80	0,5	"
D III	20	80	6	2	70	0,5	"
PLT	4	40	4	1	60	0,3	Duopigatron
PDX	10	40	6	1	80	0,3	"
DITE	1	30	2	2	30	0,1	With peripheral magnetic field
T-10M	4,5	40/80	2	3	35	1,5	Duopigatron
JT-60	20	75	14	2	35	Up to 10	Periplasmatron
TFR	4	30	2	5	14	0,05	
JET	25	80/160	—	—	—	—	

Elements of the Injector Channel. The efficiency of transport of streams of ions and atoms in the injector channel depends on the vacuum conditions. The large gas flows and the maximum reduction of the entry of impurities into the thermonuclear apparatus led to the development of cryogenic equipment with a high pumping speed.

A noteworthy aspect is the creation of current collectors for ionic and atomic beams with a high specific power (5-15 kW/cm^2). At the present stage, with a pulse of up to 0.5 sec in the current collectors the heat is carried off in the interval between pulses. The planes of the collectors are inclined at small angles to the beam axis, thus reducing the specific power.

A high energy efficiency in the injector could be attained by developing reliable systems for recuperating the energy of the ionic beams. These systems can also be used in current collectors to reduce the specific power. Several systems of energy recuperation are being analyzed. The main trend is towards retardation of the ionic beam in the main channel of the injector without magnetic deflection. Consideration is also being given to a system in which the stream of ions is divided into several beams with subsequent retardation of these beams.

Particular attention is being paid to the construction of an atom guide, a channel joining the vacuum chamber of the injector to the chamber of the thermonuclear apparatus. During a pulse here the pressure is observed to rise and this results in a drop in the power of the injected beam. Methods are being developed for solving this problem by raising the pumping speed, choosing an appropriate material for the channel wall, the channel design, etc.

The diagnostics of high-power particle streams has for some time now been based on contactless methods, optical methods of determining the position of the beam and measurement of its characteristics: The component composition and the angular divergence. The former is done with photodiodes and the latter, by measuring the Doppler shift of the H_α and H_β lines and from their broadening.

Injectors. Several high-power injectors are now being designed for large thermonuclear apparatuses (Table 2). All of them are based on the recharging of positive hydrogen (deuterium) ions with an energy not exceeding 120 keV. Test stands have been built, or soon will be, in some laboratories for model experiments. Apparatuses of the next generation and reactors will require an injector power of hundreds of megawatts and an atomic energy far exceeding 200 keV (especially for open traps). At such an energy the efficiency of the positive-ion cycle is low and studies are being conducted on injection systems based on a negative-ion cycle with a potential high energy efficiency.

The meeting was on a very high level. The environment created by the organizers, workers of the Culham Laboratory, was conducive to a fruitful discussion and exchange of views on all problems of present-day injectors.

SOVIET – ITALIAN SEMINAR ON PLASMA RESEARCH IN TOKAMAKS

L. G. Golubchikov

The seminar, which was held in Frascati, Italy, from June 19 to 23, 1978, discussed the results of research and development on the Soviet tokamaks T-10, T-4, TM-3, and T-7 and the Italian tokamak FT. The sessions were held in a new building which houses the FT device so that during breaks it was possible to go to the control room and to observe the characteristics of the latest discharges on the display screen.

The FT is a medium-sized tokamak ($R = 83$ cm, $a = 21$ cm) with a strong toroidal field ($H = 100$ kOe) and with power supply from a 120-MW pulse-excited generator. The apparatus is equipped with an up-to-date diagnostic system and an automatic data-collecting system and is designed to operate at a pulse repetition rate of 1 pulse every 10 min. Experiments are being conducted with liquid-nitrogen-cooled toroidal coils at a toroidal field of up to 65 kOe. The maximum discharge current I_{pl} attained is 440 kA, but it has hitherto not been possible to obtain conditions without current cutoff, which occurs 20-25 msec after the beginning of the pulse.

The apparatus has a stainless steel sylphon liner and a molybdenum diaphragm which can be replaced through a vacuum lock without disturbance to the vacuum conditions. The initial vacuum in the chamber in the heated state is $2 \cdot 10^{-8}$ mm Hg and $2 \cdot 10^{-9}$ mm Hg under operating conditions. Induction heating to 300°C is employed to keep the liner walls free of water. The high initial vacuum does not guarantee a low level of oxygen in the discharge but does guarantee a low rate of oxide formation on the walls. Additional purification by means of a low-temperature conditioning discharge with a current of 3-4 kA with a field of 1 kOe allowed the plasma density to be raised to 10^{14} cm^{-3} and permitted a quite low value of Z_{eff} to be obtained. It should be noted that the discharges are not sufficiently reproducible, especially in respect of such parameters as intensity and time variation of the signal of low-energy x rays. For a typical discharge in the FT with $H = 60$ kOe and $I_{pl} = 406$ kA ($q \simeq 3.5$) the parameters obtained were $n_e(r) \simeq 1.7 \cdot 10^{14} (1 - r^2/a^2)$ cm^{-3}, $T_e(r) \simeq (1 - r^2/a^2)^2 \cdot 10^3$ eV, $T_i(0) \simeq 600$ eV, $\tau_E \simeq 10$ msec, and $Z_{eff} \simeq 2$. The profile of the electron temperature T_e is typical of discharges with predominant light impurities.

Once the program of research on Joule heating is carried out, experiments on the auxiliary heating of the plasma at the frequency of lower hybrid resonance are planned to begin at the end of 1979. In the first stage the power of rf heating will be 0.5 MW and if this is successful, it will be possible to raise it to 1 MW.

In Frascati the members of the delegation became acquainted with the laboratory engaged in development of superconducting magnetic systems. The plans of the laboratory have now been switched to the creation of a superconducting system for the tokamak. The principal problems at the present time are those of developing superconducting materials for the realization of strong magnetic fields in large-scale installations and investigating a circulating method of cooling superconducting magnetic systems. The laboratory workers have produced a small batch of wire based on NbAl with a critical current of 60 A in a field of 64 kG and 20 A at 110 kG. Research has shown that such a wire retains its properties under a specific elongation of 0.4-0.5%, i.e., double that for niobium–tin superconductors.

After the seminar, the delegation visited the Plasma Physics Laboratory at the University of Milan where the "Tor" tokamak is being aligned ($R = 55$ cm, $a = 14.5$ cm, $H = 10$ kOe). The device was designed and built at the Culham Laboratory (Great Britain). The first experiments with a discharge have been carried out and adjustments are being made to the magnetic fields. The device is being set up for training students specializing in plasma physics. It is planned to conduct experiments in 1979 with microwave plasma heating at the frequency of electron cyclotron resonance with the aid of gyrotrons manufactured by Varian (power 100 kW, wavelength ~1 cm).

Translated from Atomnaya Énergiya, Vol. 45, No. 6, pp. 472-473, December, 1978.

0038-531X/78/4506-1213 $07.50

MEETING OF IAEA EXPERTS OF PREVENTION OF OCEAN POLLUTION

L. I. Gedeonov and V. M. Flegontov

Experts of the International Atomic Energy Agency met in Vienna, Austria, in February and March, 1978, to discuss the responsibility of the Agency in accordance with the convention on the prevention of ocean pollution by the dumping of wastes and other materials. This meeting was preceded by the following circumstances.

A convention on the prevention of ocean pollution by the disposal of radioactive wastes and other radioactive materials was drawn up in London in November, 1972. This convention went into effect in the second half of 1975. The Soviet Union ratified the document on December 15, 1975.

In accordance with appendices to the convention, the IAEA drew up a document presenting the concept of radioactive wastes with a high specific activity which are not permitted for ocean disposal and prepared a recommendation concerning the issuance of permits for and the performance of operations of waste disposal in the ocean.

The definition states that radioactive wastes or other materials with a high specific activity in packed form: for α emitters with a half-life of more than 50 years with a concentration above 10 Ci/ton; for β emitters (excluding tritium) with a concentration above 10^3 Ci/ton; for ^{90}Sr and ^{137}Cs with a concentration above 10^2 Ci/ton; and for tritium with a concentration above 10^6 Ci/ton.

The USA dumped radioactive wastes (in packed form) in the ocean up until 1965, after which it stopped the practice as economically unsound; the members of the European Economic Community still continue such dumping. By the end of 1974 β-active substances with activity of 175 kCi were dumped in containers on the ocean bed in the northeastern part of the Atlantic in the region bounded by the coordinates 35-50° latitude North and 10-25° longitude West. Since 1977 the operations of radioactive waste disposal in the ocean have proceeded in accordance with the above-mentioned definition and recommendations.

At the same time as these documents were adopted, the first consultative meeting of the contracting parties entrusted the IAEA with making further improvements in the definition and recommendations, including: the qualitative and quantitative definition of what a high-activity waste is; the strategy of isolation of wastes and their confinement in containers; a review of the oceanographic model which constituted the basis for the documents; prohibition of dumping in depths of less than 4 km; the disposal of liquid and unpacked, low-activity wastes; the conception of minimization of the level of radioactivity; a limitation on the number of sites for waste dumping; and development of a special standard container.

The IAEA later set up working groups, convened meetings of experts, and reviewed the oceanographic and radiological basis of the definition and recommendations. It was recognized that the Webb–Morley oceanographic model [2] adopted earlier oversimplifies the actual processes in the ocean and is not appropriate for calculations of concentrations of impurities for long periods of time. The experts recommended the more complete model of Sheperd [3] for the assessment of long-term nonlocal dispersion. The radiological basis of the temporary definition and recommendations was criticized. The opinion was expressed, in particular, that the radiological safety of man and of ecological systems is determined to a great degree by the rate at which radioactive substances are dumped into the ocean. The specific activity of the substances dumped is supposedly of lesser importance.

Finally, the IAEA considered the prepared review of the document, defining radioactive wastes with a high specific activity, and of the recommendations. For this purpose the eighth meeting of experts was convened in Vienna in February and March, 1978, with specialists from 23 countries and several international organizations invited.

As a basis for the work of the meeting, the IAEA Secretariat prepared a document containing proposed amendments and revisions to the text adopted earlier for the definition and the recommendations. In particu-

Translated from Atomnaya Énergiya, Vol. 45, No. 6, pp. 473-474, December, 1978.

 0038-531X/78/4506-1214 $07.50

lar, it was proposed that ocean disposal will be prohibited in the case of radioactive wastes containing α emitters with more than 10^{-2} Ci/ton of container dumped, β and γ emitters with more than 1 Ci/ton of container, and tritium with more than 10^5 Ci/ton. These values of the specific activity are 1/1000 of those adopted in the existing definition.

As a result of a thorough analysis of the problem, the experts proposed a ban on the ocean disposal, in packed form, of wastes with a high specific activity, containing radioactive substances in excess of the following limits: α emitters, 1 Ci/ton, but ^{226}Ra or the equivalent ^{210}Po, no more than 10^{-1} Ci/ton; α and β emitters with half-lives of more than 6 months (excluding tritium) or a mixture of β and γ emitters of unknown composition, no more than 10^2 Ci/ton; and tritium in β and γ emitters with half-lives of less than 6 months, no more than 10^6 Ci/ton. These concentrations should be considered to be averages for the total weight of the containers, not higher than 1000 tons.

This definition is ten times as stringent as the current one. A stricter wording of the existing recommendations was also worked out. In particular, the depth of the dumping site should on average be greater than 4 km, although there might be submarine hills of up to 400 m at that site. Preservation of the oceanic resources is listed among the goals which it is proposed to achieve, following the convention. Attention was drawn to the need to strive for long-term isolation and confinement of the wastes inside their jackets after dumping to the sea bed, etc. The recommendations exclude the dumping of liquid radioactive wastes.

The recommendations of the meeting of experts were used by the IAEA Secretariat to draw up a draft of the definition and recommendations which is to go through all the necessary levels until it is adopted by the contracting parties to the London convention.

It is to be expected that the international cooperation in the preservation of natural resources and, especially, the oceans will be fruitful and will make it possible to successfully resolve the ecological problems with account for the latest scientific advances.

LITERATURE CITED

1. J. Oliver, in: Proc. of European Nucl. Conf., Paris, Pergamon Press, Oxford (1975), Vol. 8, p. 355.
2. G. Webb and F. Morley, A Model for the Evaluation of the Deep Ocean Disposal of Radioactive Waste, National Radiological Protection Board Report NRPB-R 14, Harwell, U.K., June (1973).
3. J. Sheperd, A Simple Model for the Dispersion of Radioactive Waste Dumped on the Deep Sea Bed, Fisheries Research Tech. Report 29, Lowestoft, U.K. (1976).

THIRD INTERNATIONAL CONFERENCE ON COLLECTIVE METHODS OF ACCELERATION

V. P. Sarantsev

The program of the conference, which was held in Los Angeles in May, 1978, covered the main areas of research on collective methods of acceleration: Acceleration of ions in direct electron beams and electron rings, self-acceleration of ions in structures, and obtaining high-power ion beams and ways of accelerating them. The leading scientific centers engaged in work on these subjects took part in the conference. Upon comparing the program of this conference with the preceding one, we see that the specific weight of work on obtaining and accelerating ions has increased substantially over the past 2 years.

Electron-Ring Accelerators. The main effort at the present time is directed at constructing and starting up so-called prototype accelerators, facilities which in respect of their parameters can already be regarded as accelerators for nuclear physics, but the degree of development of the individual units does not allow them to be considered as working accelerators. Such facilities are being built at the Joint Institute for Nuclear Research (JINR) at Dubna, Garching (Federal Republic of Germany), and the University of Maryland (USA). The greatest success has been achieved at Dubna where various ions have been accelerated to an energy ~ 2 MeV/nucleon in the KUTI facility (collective heavy-ion accelerator). The intensity of light ions was $6 \cdot 10^{11}$ and that of heavy ions was $2 \cdot 10^{11}$ per acceleration cycle.

Great interest was aroused by experimental research on the dynamics of ion acceleration in a collective accelerator. The criterion of acceleration efficiency is the yield of the nuclear reaction with accelerated nitrogen ions as a function of the ion load in the ring. With a small load the rate of acceleration of the electron ring by the external field exceeds the maximum allowable value from the point of view of ion confinement, there are no accelerated ions, and the nuclear reaction yield is zero. When the load of ions in the ring is increased the ions begin to be confined, the acceleration process takes place normally, and the reaction yield rises. With a further increase in the load, the ion energy diminishes and the reaction yield falls off. Finally, when the ion energy drops below a threshold corresponding to an ion energy of 0.5 MeV/nucleon, the reaction yielded disappears.

The Pustarex electron-ring accelerator being built at Garching is a combination of two earlier experimental facilities in the Federal Republic of Germany. One of them is closely related to the "classical" type on which experiments were performed in Karlsruhe and the other is the Schuko compressor. Pustarex is an electron-ring accelerator in which during the compression process the ring is introduced into the accelerating system. Because of some technical difficulties, particularly the inadequate resistance of the conducting-layer to Foucault-current heating, the accelerator is now operating with an epoxy-resin chamber with no conducting layer. The main element in reducing the impedance, therefore, is a "squirrel cage." As a result, at the present time the electron ring is brought to the accelerating section with $3 \cdot 10^{12}$ particles and the main program of the Pustarex group for the immediate future consists of research on ways of screening the squirrel cage in order to increase the number of electrons to $6 \cdot 10^{12}$ after compression.

While pulsed magnetic fields are employed in KUTI and Pustarex to compress the electron ring, a team of physicists at the University of Maryland is experimenting with compression of an electron ring in a static magnetic field (UMERA). Retardation and arrest are fundamental for the latter facility. The parameters of the arrested ring are still far from those expected ($N_e = (1\text{-}4) \cdot 10^{12}$, $R = 5.5$ cm, $\Delta R = 1$ cm, $\Delta Z = 10\text{-}20$ cm, and accelerating force ~ 0.5 MeV/m).

Ion Acceleration in Intense Relativistic Electron Beams (IREB). In recent years there has been a significant change in the approach to collective acceleration of ions in direct IREB: In addition to research on the effect construction has begun of facilities with controlled motion of the ionization front.

The Sandia Laboratories (USA) are putting into operation a facility which, according to plans, is to demonstrate control of the propagation of an IREB front by pre-ionization of the accelerating channel with

Translated from Atomnaya Énergiya, Vol. 45, No. 6, pp. 474-476, December, 1978.

0038-531X/78/4506-1216$07.50

laser light. An electron beam with an energy of 600 keV, current 20 kA in a pulse, and duration 10 nsec is injected into a power $P \sim 5 \cdot 10^6$ W with a pulse duration of ~1 nsec which has been prepared ensures motion of the ionization front in the drift chamber at a given velocity (the required synchronization accuracy ~0.01 nsec). Experiments have begun on control of the motion and shape of the ionization front. New, encouraging results have been obtained in experiments on the passage of IREB in vacuum channels with dielectric walls.

The transport of IREB in such channels is of great interest for some applications. Moreover, with such transport ions are observed to be accelerated to an energy considerably exceeding the energy of the electron beam. The experiments were performed at the P. N. Lebedev Institute of Physics of the Academy of Sciences of the USSR (FIAN) and laboratories in the USA at an electron beam energy of 70 keV-1.5 MeV and a current of 10-70 kA. The tubes, made of various organic and inorganic materials, had a length of 5-40 cm and an internal diameter of 20-100 mm.

Generation of Ion Beams. In the area of generation of high-intensity ion beams, the main effort has been to raise the efficiency as well as to increase the density of the ion current. The U. S. Naval Research Laboratory has developed a reflex tetrode which is more efficient than the triodes hitherto used. In the reflex triode the anode is situated between two cathodes. The role of the second cathode is frequently played by a virtual cathode. Electrons emitted from the cathode penetrate the anode, losing part of their energy in the process, and are reflected from the second cathode without reaching it. They oscillate, repeatedly penetrating the anode and gradually losing energy. Ions move to the cathode in both directions and pass right through them.

The idea of reflex tetrodes consists in one-sided generation of an ion beam. For this purpose the anode is made as a double anode, one made of metallized Mylar and the other of a thicker polyethylene film. The metallized Mylar is the initial ion (proton) source and, therefore, a unidirectional stream of protons is formed, moving from the second anode to the virtual cathode (80-90% of the total ion current).

In the last three or four years Lewis diodes have been employed for the production of high-power ion beams; a characteristic feature of these diodes is that their anode consists of a dielectric insert with an aperture (most frequently, of polyethylene). The energy of the accelerated ions in such a diode can exceed the electron energy by a factor of 10-20. The pulse duration is several nanoseconds. At Cornell University (USA) diodes with magnetic insulation are used in the generation of ions. In these diodes the current of the extracted ion beam was 50% of the electron current with a pulse duration of 100 nsec. A magnetic lens was used to increase the density of the ion current in the beams. Experiments showed that even with a single lens the energy density in a neutralized ion beam can be increased roughly eightfold.

The construction of an ion gun with a spherical electrode configuration and magnetic focusing makes it possible to obtain a beam compaction factor of 50 at the focus; for a beam with an energy of 500 keV at the focal point the current density is 1000 A/cm^2.

The U.S. Naval Research Laboratory has performed experiments on the production of intense proton rings for obtaining a configuration with a rotated magnetic field. The Gamble II accelerator, operating on a reflex triode, has been used for these purposes. A hollow proton beam with a current of 200 kA, an energy of 1.2 MeV, and a pulse duration of 50 nsec is injected into a magnetic system with a length of 5 m. The magnetic field has a corkscrew configuration and ensures the possibility of compressions. The large radius of the ring after compression is 10 cm and the number of protons in the ring is $5 \cdot 10^{16}$. Calculations show that the magnetic field changes sign when the number of protons is $\sim 10^{17}$. It is proposed to reach this value by changing over to a low-impedance coaxial tetrode, which will increase the proton current to 500 kA.

In recent years much attention has been paid to ion-accelerating systems. It is of interest to study systems of autoresonance acceleration of ions (Osteen Co., USA). In this case use is made of the characteristic cyclotron mode arising in IREB propagating in a longitudinal magnetic field or in a resonator system. This mode in fact represents a wave of charge density and can be employed to accelerate protons and other ions. In principle, the mechanism of acceleration in this case is similar to ordinary resonance in linear accelerators. Control of the phase velocity of the accelerating mode, which is necessary in order to synchronize it with the motion of the ions, is achieved through spatial adiabatic variation of the magnetic guide field. The phase velocity varies in inverse proportion to the magnetic field.

After several years of preliminary theoretical investigations, the Osteen Co. decided to develop and construct a large experimental apparatus for research on the autoresonance ion acceleration system with the parameters:

Magnetic field, kG	25
Frequency of cyclotron mode, mHz	250
Wave amplitude, kV	250
Electrons:	
energy, MeV	3
current, kA	30
pulse duration, nsec	200
Ions:	
energy, MeV	30
current, A	30
Length of autoresonance accelerator, m	4

Magnetic lens configurations are also used effectively to accelerate ions (Cornell). As a neutralized, cold, hollow electron beam passes through the lens configuration the electron density increases at the outside radii of the tube. The density reaches $3 \cdot 10^{11}$ cm^{-3}. Acceleration as well as focusing is achieved because of such separation. A system under consideration and study is PULSELAC, consisting of eight lens-type accelerating modules which are capable of accelerating protons to 10 MeV and $^{20}N_e$ to 447 MeV.

Thus, work has started in many centers in the world on the creation of accelerators which would operate on the collective principle and would have a substantially high efficiency.

BOOK REVIEWS

M. Kh. Ibragimov, V. I. Subbotin,
V. P. Bobkov, G. I. Sabelev,
and G. S. Taranov
STRUCTURE OF TURBULENT FLOW AND THE HEAT EXCHANGE MECHANISM IN CHANNELS*

Reviewed by Yu. Klimov

The monograph under review expounds, analyzes, and generalizes numerous experimental and theoretical papers on the study of the turbulent flow of an incompressible fluid with constant properties in channels. A considerable number of the studies were carried out by the authors over a period of many years as applied to concrete problems of domestic power reactor construction. This enhances the practical importance of the material presented in the monograph. The monographs hitherto published on heat transfer contain material that is roughly 10 years old and concern turbulence to a lesser degree than follows from the importance of this topic for the thermal physics of power reactor engineering.

The monograph presents new information obtained by Soviet and foreign researchers in recent years. Thus, a gap is filled in the literature on an important chapter of reactor science and technology, turbulent heat transfer during the flow of fluids in channels.

The first chapter of the book presents the main methods of theoretical description of turbulent flow and heat exchange in channels. Chapter 2 deals with the physical features and the essence of the various characteristics of flows, viz., local, temporal, and spatial, as well as the spectra of the processes of turbulence and diffusion. In Chap. 3 the authors consider problems concerning the structure of turbulence, viz., the energy balance, the viscous sublayers, the flow core, the transition region, the statistical characteristics, and the anisotropy of momentum transfer. Chapter 4 is devoted to the mechanism of heat transfer in channels and the distinctive features of processes of turbulence, the "energy" balance of temperature pulsation, the structure of the temperature field in a nonisothermal flow, and the relations between the velocity and temperature pulsations. The last, fifth chapter, describes the hydrodynamics and heat exchange channels, including the inlet portions, and channels with rough walls.

In respect to character and treatment of the material, the book gravitates toward fundamental publications. The authors avoid narrow practicalness, striving to encompass particular cases with typical generalizations.

It should be noted that the authors of this monograph have for a long time successfully pursued research on heat exchange in nuclear reactors. The book can be considered as a distinctive account of the work done.

*Atomizdat, Moscow (1978).

Translated from Atomnaya Énergiya, Vol. 45, No. 6, p. 476, December, 1978.

0038-531X/78/4506-1219$07.50

Z. A. Al'bikov, A. I. Veretennikov,
and O. V. Kozlov

DETECTORS OF PULSED IONIZING RADIATION*

Reviewed by E. A. Kramer-Ageev

The monograph under review systematizes information on the development and use of analog detectors for high-intensity pulsed radiation. In detecting radiation from accelerators and pulsed reactors the reseacher devising the complex of recording apparatus is confronted with specific questions which do not arise under the conditions of static sources of ionizing radiation. The complexity of the detector construction increases many-fold when the apparatus is to be used to determine not only the dose, particle transport, or neutron fluence but also the shape of the pulse.

The authors of the monograph devote their main attention to the development and application of charge, scintillation, and semiconductor detectors.

In describing charge detectors the book gives the dependence of the sensitivity on the photon energy, estimates the limits of signal linearity, presents the pulse characteristics of the detectors, and makes practical recommendations concerning the use of the detectors.

The monograph generalizes and compares the characteristics of domestic and foreign (commercial and experimental) photoelectric detectors and scintillators. For radiometry of high-intensity radiation in short pulses the authors recommend the use of high-current phototubes (up to 18 A) of special designs, permitting a resolving time $\sim 10^{-9}$ sec to be obtained.

Interesting material is given in a chapter on semiconductor detectors for pulsed radiation. Ordinary semiconductor detectors are not suitable for high-intensity pulsed radiation owing to their low radiation resistance. The authors, therefore, draw the reader's attention to silicon detectors with an elongated depletion zone. The carrier drift velocity depends little on the electric field strength at high values of the latter and this makes it possible to maintain a constant resolving time for high-intensity pulses of radiation. Relations are given between the sensitivity of semiconductor detectors and the energy of photons and neutrons. The relation for the sensitivity of semiconductor detectors to neutrons, however, should have been made more exact, especially in the case of a semiconductor detector without a radiator in the low-energy range. Less attention has been devoted to calorimetric methods. In fact, the authors confined themselves to pyroelectric detectors, although the thermal-effect signal is difficult to separate from the photoconductivity current. Calorimeters of the ballometric type proved to be outside the field of view.

Of considerable interest are detectors with a logarithmic sensitivity which have unquestionable advantages in studies on the shape of radiation pulses containing slow components.

The monograph presents the material clearly and will be a useful guide in the development of pulsed radiation detectors.

In conclusion, one could point out some shortcomings of a methodological character: The monograph lacks recommendations as to the use of detectors in fields of an unknown spectral composition since their response frequently depends on the energy of the particles.

*Atomizdat, Moscow (1978).

Translated from Atomnaya Énergiya, Vol. 45, No. 6, p. 477, December, 1978.

 0038-531X/78/4506-1220$07.50

Yu. V. Gott

INTERACTION OF PARTICLES WITH MATTER IN PLASMA RESEARCH*

Reviewed by A. I. Akhiezer

In the past two decades effects associated with the interaction of particles with an energy of 50-100 keV/nucleon with matter have taken on great importance. Suffice it to mention the method of fabricating semiconductor devices by using initial semiconducting materials with ions of various masses, the use of recharging targets in the diagnostics of laboratory and cosmic plasma, research on the composition and structure of the surface of solids by the ion-scattering technique, etc. Particular mention should be made of the radiation resistance of the first vacuum wall of a thermonuclear reactor.

A natural consequence of practical inquiries was the appearance of a large number of experimental and theoretical papers devoted to the study of energy losses, scattering, ranges, and changes in the charge state of particles interacting with matter. It has now become necessary to generalize and systematize the data obtained. The publication of the monograph under review is very timely since it makes a successful attempt to resolve the problem posed.

The monograph considers effects which occur during the interaction of nonrelativistic ions with solid (amorphous) and gaseous substances and are of interest to the physics of high-temperature plasma.

The monograph consists of eight chapters and an appendix. The main emphasis in Chap. 1, which is devoted to the energy losses of particles in elastic collisions, is on methods of calculating atomic potentials and the energy of the interaction potential particles. The authors give approximate analytic solutions obtained for the Hartree–Fock–Slater equation by Slater, Gombas and Sondy, Clementi and Raymond. The coefficients necessary for calculating the wave functions of atoms from uranium hydrogen to uranium are given in a table which also shows the energy levels of atoms in the ground state. The Thomas–Fermi method for finding the potential of an atom is described and numerous approximate solutions of the Thomas–Fermi equation are given. The last section of this chapter is devoted to calculations of the effective scattering cross section and energy losses in elastic collisions.

Chapter 2 discusses topics associated with inelastic collisions. The authors expound the theory given by O. B. Firsov for energy transfer in collisions of low-energy particles, consider a modified Firsov theory which permits a qualitative description of the nonmonotonic dependence of the energy losses on the atomic numbers of the colliding particles, the polarization losses, retardation of particles in plasma, and the statistical spread of energy losses by particles in matter, and compare the theory with experiment. It follows from the materials in this chapter that at the present time the theory provides only a qualitative description of the energy losses of slow ions.

Experimental data about the energy losses of particles in different targets are given in Chap. 3. The simple empirical formula presented by the authors for the calculation of energy losses by hydrogen ions in various substances is valid for protons with an energy for 1 keV to 10 MeV and makes it possible in some cases to predict the energy losses of elements for which there are no experimental data at present.

Multiple scattering of low-energy particles in matter is discussed in Chap. 4. The authors give the results of analytic solution of kinetic equations describing the motion of particles in matter for different interaction potentials between particles. It is pointed out that the theory satisfactorily describes the experimental data. The final section of the chapter presents the solution found by O. B. Firsov to the problem of reproducing the interaction potential of particles from the angular distribution after single collision with the atoms of a target and gives the solution of the problem for particles which have undergone multiple scattering.

*Atomizdat, Moscow (1978).

Translated from Atomnaya Énergiya, Vol. 45, No. 6, pp. 477-478, December, 1978.

0038-531X/78/4506-1221 $07.50

The ranges and the variance of the ranges of particles in matter comprise the topic of Chap. 5. The data show that theoretical calculations of ranges (incorporating the empirical formula given in Chap. 3 for energy losses) are in satisfactory agreement with experimental results. A large quantity of experimental material on the ranges of various ions in substances is presented.

Chapter 6 describes experimental methods of determining the energy losses and ranges of particles in matter, the preparation of ultrathin layers of various substances used as a target, and determination of the thickness of these layers. The authors consider the physical properties of thin layers of substances (density, homogeneity, structure, oxidizability, optical properties) and their effect on the accuracy with which energy losses and ranges are determined.

Chapter 7 describes effects which accompany the bombardment of a solid with streams of atomic particles and neutrons and which play a large role in the radiation-induced damage to the walls of a thermonuclear reactor. Radiation materials science as applied to the problem of controlled thermonuclear fusion is a rapidly advancing area of science and engineering and this chapter is essentially an introduction to problems which are of interest to physics at this time.

The last chapter describes methods of diagnostics of laboratory and cosmic plasma. In particular, the authors consider a method of measuring the energy distribution in a stream of fast neutral particles in a thin solid target and subsequent analysis by the energy of the ions emerging from the target. This method is extremely promising for measuring the energy of ions in plasma with thermonuclear parameters since as the particle energy increases, so does the efficiency of the method. Moreover, the instruments used for the ionization of atoms of a solid target are much simpler in design and operation than the instruments with a gas target that are now in use. Various electrostatic analyzers for experimental physics are described in this chapter.

The Appendix gives data about such physical characteristics of the elements ranging from hydrogen to uranium as the atomic number, atomic mass, density, number of particles per unit volume under normal conditions, the electron velocity and energy on the Fermi surface, the work function, and the effective mass of an electron in the solid substance.

The monograph makes extensive use of results obtained by the authors. This includes experimental data on the slowing down and scattering of hydrogen ions in various substances as well as calculations of the scattering and range of low-energy ions in matter, the development of methods of fabricating ultrathin targets, construction of analyzers of atomic particles, and measurement of the energy spectra of ions in plasma in different thermonuclear devices.

The book was written by experimental physicists and, therefore, much attention has been devoted in it to experimental topics, nuances of the laboratory "cuisine," and it is hoped that this will be useful to the reader.

The book contains extensive reference material (34 tables, 381 figures, 563 references) of great interest to specialists engaged in work not only on the physics of plasmas and controlled-thermonuclear fusion but also working on nuclear physics.

A. D. Frank-Kamenetskii

MODELING NEUTRON TRAJECTORIES IN MONTE CARLO CALCULATIONS OF REACTORS *

Reviewed by L. V. Tochenyi

A variety of numerical and analytical methods and modifications of them, making it possible to obtain correct estimates of various parameters in an acceptable time, have recently been applied to reactor calculations. As a rule, the speed of calculation or the required volume of information is achieved as the result of simplifications in the description of the geometry of the model or the energy relations. Such simplifications are useful in exploratory, optimization work, but approximate methods are often powerless in calculations of complex constructions consisting of diverse media with possible cavities. Further difficulties arise when the object of the calculations cannot be described within the framework of traditional geometry of network methods.

The most effective result in solving such complex problems is demonstrated by the Monte Carlo method, especially on computers of the newest generation. A quite extensive library of programs satisfying all the growing needs of the users in now available for calculations. The progress made in the development of algorithms based on the Monte Carlo method is apparent.

The general idea of probability methods has been expounded in special monographs. The specific features of the application of these methods in calculations of nuclear reactors are analyzed in the book under review, very likely for the first time, in the domestic literature. Numerous publications have been scattered in periodicals, preprints, and reports and, therefore, the attempt made by A. D. Frank-Kamenetskii to systematize the extensive material is very timely.

The timeliness of the book manifests itself in several aspects. First, the author makes a detailed (and at the same time, brief) analysis of the distinctive physical features of reactor calculations and presents the methods now in use to describe the fundamental relations. Second, he considers domestic and foreign advances in developing Monte Carlo methods and thus leads the reader up to the concepts and ideas of recent years. In reading the book one feels the desire of the author to execute algorithms on a computer: He discusses the possible models of calculation, gives variants of FORTRAN programs, analyzes their details, etc.

The book would have gained much practical value, however, had the author given a brief review of the best known reactor programs with a description of the geometric modules, the parameters calculated, the characteristic computing times, and predictions as to their further development. Nevertheless, let us note that this is a useful book which will assist engineers and designers in understanding the physical ideas and mathematical concepts incorporated into the programs with Monte Carlo algorithms. These methods will undoubtedly be used with increasing success in computational studies on nuclear reactors.

*Atomizdat, Moscow (1978).

Translated from Atomnaya Énergiya, Vol. 45, No. 6, pp. 478-479, December, 1978.

0038-531X/78/4506-1223 $07.50

V. I. Davydov (editor), M. N. Gamrekeli,

and P. G. Dobrygin

THERMAL PROCESSES AND APPARATUS FOR OBTAINING OXIDES OF RARE AND RADIOACTIVE METALS*

Reviewed by I. G. Slepchenko

The book is devoted to the production of oxides of rare and radioactive metals by thermal methods and the choice of the drying and calcining equipment. It consists of five chapters, contains 114 illustrations, and a list of references at the end of each chapter (319 items), all of which enable the book to be used as a reference book.

Oxides of rare and radioactive metals are employed extensively in technology (electronics, nuclear power, new materials, and other branches). Technological schemes for obtaining these metals in the form of pure salts and in the form of oxides are being improved constantly. They changed substantially in connection with the mastery and introduction of sorption, extraction, and thermal processes. The thermal processes and technology for the production of oxides from compounds of rare and radioactive metals are extremely complex stages during which the purity of the end products must be preserved. With many examples the authors show the distinctive features of the technology for obtaining individual and mixed oxides of metals, considering the processes of drying and calcining the salts successively (Chap. 1).

Chapter 2 is devoted to the theoretical foundations of heat and mass transfer in processes of drying and thermal decomposition under different conditions. Notwithstanding the fact that there is an extensive literature on this subject, the authors deemed it necessary to give information which is indispensable in the analysis of complex irreversible processes. Thus, in the thermal decomposition of a uranyl nitrate solution to metal oxides, heat and mass transfer takes place in several stages: heating of particles (drops) to a temperature at which dehydration occurs; diffusion of vapor from the surface of the particle into the gaseous phase; thermal decomposition of the nitrate compounds; and diffusion of gas from the surface of the particles into the gaseous phase.

The mechanism of thermal formation of oxides from various compounds can be understood only with an evaluation of both heat and mass transfer and the kinetics of the chemical reactions. If internal diffusion constitutes the determining stage, the transfer rate decreases and it is difficult to achieve complete decomposition.

A product with particular physicochemical properties can be obtained in one stage in spray dryers, in an air-fluidized bed, and in flame and plasmochemical reactors. To preserve the uniformity of heat transfer in a fluidized bed the authors propose to distribute the temperature in the spray with allowance for other factors, which may determine the stability of the process (Chap. 2).

The kinetics of thermal processes for producing oxides (Chap. 3) is described very briefly. It is pointed out that there are few data on the kinetics and the information in the literature requires systematization.

The principal designs and calculation of apparatuses used to obtain oxides of rare and radioactive metals are given in Chap. 4. The choice of apparatus is determined by the scale of the production, the purity requirements on the product, the minimum losses and the special conditions of the production (toxicity of the product, radioactivity, nuclear safety, etc.). Moreover, the authors of the book recommend that the apparatus for a concrete process of oxide production be chosen by evaluating favorable conditions for effecting heat transfer and the rates of the chemical reactions.

The authors consider processes of drying moist materials in periodically and continuously operating apparatuses. It is shown that screw-conveyor apparatuses have an advantage over tubular apparatuses since

*Atomizdat, Moscow (1977).

Translated from Atomnaya Énergiya, Vol. 45, No. 6, p. 479, December, 1978.

 0038-531X/78/4506-1224 $07.50

hermetic sealing is simplified and the conditions for mixing solid products are improved. At the same time, rotary furnaces remain the fundamental apparatuses for drying and calcining ores and concentrates.

The authors correctly point out that the development of new processes and apparatuses is aimed at utilization of moving media, an elevated temperature, and automation. Examples are given of calculations for many types of apparatus employing fluidized and vibrofluidized beds, a spray dryer, and flame and plasma reactors.

The material of Chap. 5 of the book could become a separate book. In its present size the chapter is a logical extension of the description of the so-called ancillary equipment: feeders and dispensers for solid and liquid materials, heating devices, and gas scrubbers. In the absence of the characteristics of the ancillary equipment it is not possible to present processes realized.

The book is characterized by purposefulness and practicality.

ERRATA

In the article by I. E. Nakhutin et al., "Catalytic reduction of ruthenium tetroxide" (Vol. 45, No, 2, 1978) line 9 from the top on p. 786 should read: "We use the equation of [2]."

In the article by A. G. Bonch-Osmolovskii et al., (Vol. 45, No. 5, 1978) line 3 from the top on p. 30 should read: "Beam current, A...100."

INDEX

SOVIET ATOMIC ENERGY

Volumes 44-45, 1978

SOVIET ATOMIC ENERGY

Volumes 44-45, 1978

(A translation of Atomnaya Énergiya)

L

R

S

SOVIET ATOMIC ENERGY
Volumes 44-45, 1978
(A translation of Atomnaya Énergiya)

Volume 44, Number 1 January, 1978

Volume 44, Number 2 February, 1978

Engl./Russ.

Volume 44, Number 3 March, 1978

Volume 44, Number 4 April, 1978

Volume 44, Number 5 May, 1978

Volume 44, Number 6 June, 1978

Volume 45, Number 1 July, 1978

Volume 45, Number 2 August, 1978

Volume 45, Number 3 September, 1978

Volume 45, Number 4 October, 1978

Volume 45, Number 5 November, 1978

Volume 45, Number 6 December, 1978

BOOK REVIEWS

NEW RUSSIAN JOURNALS

IN ENGLISH TRANSLATION

BIOLOGY BULLETIN

Izvestiya Akademii Nauk SSSR, Seriya Biologicheskaya

The biological proceedings of the Academy of Sciences of the USSR, this prestigious new bimonthly presents the work of the leading academicians on every aspect of the life sciences—from micro- and molecular biology to zoology, physiology, and space medicine.

Volume 5, 1978 (6 issues) $175.00

SOVIET JOURNAL OF MARINE BIOLOGY

Biologiya Morya

Devoted solely to research on marine organisms and their activity, practical considerations for their preservation, and reproduction of the biological resources of the seas and oceans.

Volume 4, 1978 (6 issues) $95.00

WATER RESOURCES

Vodnye Resursy

Evaluates the water resources of specific geographical areas throughout the world and reviews regularities of water resources formation as well as scientific principles of their optimal use.

Volume 5, 1978 (6 issues) $190.00

HUMAN PHYSIOLOGY

Fiziologiya Cheloveka

A new, innovative journal concerned *exclusively* with theoretical and applied aspects of the expanding field of human physiology.

Volume 4, 1978 (6 issues) $175.00

SOVIET JOURNAL OF BIOORGANIC CHEMISTRY

Bioorganicheskaya Khimiya

Features articles on isolation and purification of naturally occurring, biologically active compounds; the establishment of their structure, methods of synthesis, and determination of the relation between structure and biological function.

Volume 4, 1978 (12 issues) $225.00

SOVIET JOURNAL OF COORDINATION CHEMISTRY

Koordinatsionnaya Khimiya

Describes the achievements of modern theoretical and applied coordination chemistry. Topics include the synthesis and properties of new coordination compounds; reactions involving intraspheral substitution and transformation of ligands; complexes with polyfunctional and macromolecular ligands; complexing in solutions; and kinetics and mechanisms of reactions involving the participation of coordination compounds.

Volume 4, 1978 (12 issues) $235.00

THE SOVIET JOURNAL OF GLASS PHYSICS AND CHEMISTRY

Fizika i Khimiya Stekla

Devoted to current theoretical and applied research on three interlinked problems in glass technology; the nature of the chemical bonds in a vitrifying melt and in glass; the structure-statistical principle; and the macroscopic properties of glass.

Volume 4, 1978 (6 issues) $125.00

LITHUANIAN MATHEMATICAL JOURNAL

Litovskii Matematicheskii Sbornik

An international medium for the rapid publication of the latest developments in mathematics, this quarterly keeps western scientists abreast of both practical and theoretical configurations. Among the many areas reported on in depth are the generalized Green's function, the Monte Carlo method, the "innovation theorem," and the Martingale problem.

Volume 18, 1978 (4 issues) $150.00

PROGRAMMING AND COMPUTER SOFTWARE

Programmirovanie

Reports on current progress in programming and the use of computers. Topics covered include logical problems of programming; applied theory of algorithms; control of computational processes; program organization; programming methods connected with the idiosyncracies of input languages, hardware, and problem classes; parallel programming; operating systems; programming systems; programmer aids; software systems; data-control systems; IO systems; and subroutine libraries.

Volume 4, 1978 (6 issues) $95.00

SOVIET MICROELECTRONICS

Mikroelektronika

Reports on the latest advances in solutions of fundamental problems of microelectronics. Discusses new physical principles, materials, and methods for creating components, especially in large systems.

Volume 7, 1978 (6 issues) $135.00

Send for Your Free Examination Copy

PLENUM PUBLISHING CORPORATION, 227 West 17th Street, New York, N.Y. 10011
In United Kingdom: Black Arrow House, 2 Chandos Road, London NW10 6NR, England
Prices slightly higher outside the U.S. Prices subject to change without notice.